Structural and functional integration within the primate masticatory system during development

DISSERTATION

To Fulfill the Requirements for the

Degree of „doctor rerum naturalium“

(Dr. rer. nat.)

Submitted to the Council of the Faculty of
Biological Sciences of the
Friedrich Schiller University Jena by

Edwin Dickinson

Born on January 20th, 1992 in Southampton, United Kingdom.

Date and Place of Defence: Friedrich-Schiller-Universität Jena, January 7th 2019.

Zugl.: Dissertation, Friedrich-Schiller-Universität Jena, 2019.

List of dissertation reviewers:

PD Dr. Kornelius Kupczik, Max Planck Institute for Evolutionary Anthropology, Leipzig, Germany.

Prof. Dr. Martin Fischer, Friedrich-Schiller-Universität Jena, Germany.

Prof. Callum Ross, University of Chicago, USA.

ABSTRACT

The masticatory apparatus combines an array of soft- and hard-tissue structures which collectively fulfil a range of dietary and social roles. The following thesis explores developmental changes to several key components of this system – including the adductor musculature, craniomandibular form, and the lever-arm mechanics of the masticatory apparatus – within a model primate species (*Macaca fascicularis*). In so doing, these studies provides an insight into ontogenetic scaling patterns within the masticatory system, and how differences in masticatory anatomy within this species during development may be observed to affect measures of overall masticatory function.

In study 1, significant changes were observed in both architectural and biomechanical properties during development. Fiber lengths, muscle mass and physiologic cross-sectional area (PCSA) all scaled with positive allometry relative to both jaw length and condyle-molar length during development. Temporomandibular joint (TMJ) height also scaled with positive allometry against both measurements of mandibular length, while jaw length and condyle-molar length were themselves observed to scale with positive allometry relative to basicranial length.

Study 2 introduces a technique for the non-destructive determination of architectural variables. To assess the accuracy of this process, digitally reconstructed data were compared to dissection-derived findings from the contralateral musculature. Strong agreement between methodologies was observed for both components of the masseter complex; however, the more complex temporalis muscle diverged in the measurement of muscle fiber lengths (and consequently, PCSA). This may be corrected in future studies by the division of more complex muscles into distinct subunits.

In study 3, the functional impact of these developmental changes was measured using a series of biomechanical models, simulating masticatory motions within individuals of different ages. Older, larger-bodied individuals demonstrated increases in both bite force and gape potential. As such, adults of both sexes display an improved ability to consume larger and more mechanically resistant food items, mirroring observed behavioural shifts within this species towards the consumption of larger and more mechanically resistant foods with increasing age. Developmental changes in muscle size and jaw length were observed to contribute most significantly to age-related differences in bite force and gape, respectively.

These findings demonstrate that changes in masticatory anatomy occur alongside developmental shifts in dietary ecology towards an increase in the consumption of larger and more mechanically resistant foods, and an increase in the prevalence of wide-gape display behaviours. The anatomical configuration of the primate masticatory system is therefore observed to closely reflect its dietary and social niche, adapting during life to meet changing functional demands. Future studies will continue to quantify ontogenetic, dimorphic, and interspecific differences in the primate face, and explore the relationship between masticatory form and function from an evolutionary perspective.

ZUSAMMENFASSUNG

Der Kauapparat besteht aus verschiedenen weichen und harten Gewebestrukturen, deren Zusammenspiel für die Nahrungsaufnahme und Sozialverhalten eines Tieres von Bedeutung ist. Die vorliegende Dissertation beschäftigt sich mit den Veränderungen in Form und Funktion während der Ontogenese mehrerer Schlüsselkomponenten dieses Systems bei einer Modellprimatenspezies, dem Javaneraffe oder auch Langschwanzmakak (*Macaca fascicularis*). Untersucht werden die Adduktorenmuskulatur, der knöcherne Schädel inkl. Unterkiefer sowie die Hebelarmmechanik des Kauapparates. Die drei Studien, die dieser Dissertation zugrunde liegen, geben dabei Einblick in das ontogenetische Skalierungsmuster innerhalb des Kausystems und zeigen, wie sich Unterschiede in der Kauanatomie innerhalb dieser Spezies während der Entwicklung auf deren Kaufunktion auswirken.

In Studie 1 wurden signifikante Veränderungen sowohl in den muskelarchitektonischen als auch in den biomechanischen Eigenschaften des Schädels während seiner Entwicklung festgestellt. Die Faserlängen, Muskelmassen und physiologische Querschnittsflächen skalierten positiv-allometrisch, bezogen sowohl auf die Kieferlänge als auch auf die Länge zwischen dem *Condylus mandibularis* und dem Backenzahn während der Entwicklung. Die Höhe des Kiefergelenks skalierte ebenfalls mit positiver Allometrie bezogen auf beide Längenmessungen des Unterkiefers. Kieferlänge und Distanz Condylus-Backenzahn skalierten mit positiver Allometrie bezogen auf die Basicraniallänge.

Studie 2 stellt eine Methode zur zerstörungsfreien Bestimmung von muskelarchitektonischen Variablen vor. Um die Genauigkeit dieses Verfahrens zu beurteilen, wurden digital rekonstruierte Daten mit anatomischen Kaumuskelpräparaten aus der kontralateralen Muskulatur eines Makakenkopfes verglichen. Eine hohe Übereinstimmung zwischen den Methoden wurde für beide Bestandteile des Masseter-Komplexes festgestellt. Allerdings überbewertete der Algorithmus die Messung der Muskelfaserlängen in dem komplexeren M. temporalis, was zu einer Überschätzung des physiologischen Querschnitts führte. Daher ist zu empfehlen, dass dieser Ansatz entsprechend den Anforderungen komplexer Muskelstrukturen für weiterr Studien angepaßt werden sollte

Der funktionelle Einfluss dieser Entwicklungsveränderungen wurde mithilfe einer Reihe biomechanischer Modelle in Studie 3 untersucht, wobei die Kaubewegungen in Individuen unterschiedlichen Alters simuliert worden sind. Ältere Individuen mit größerer Körpermasse zeigten sowohl eine Zunahme der Beisskraft als auch der Fähigkeit, den Kiefer weiter zu öffnen. Somit weisen erwachsene Makaken beider Geschlechter eine verbesserte Fähigkeit auf, größere und mechanisch widerstandsfähigere Nahrungsmittel zu fressen. Diese morphologischen Erkenntnisse bestätigen somit Verhaltensbeobachtungen zur Nahrungsaufnahme innerhalb dieser Spezies, die belegen, dass es eine Verschiebung des Nahrungsspektrums hin zu größeren und mechanisch widerstandsfähigen Nahrungsmitteln mit zunehmendem Alter gibt. Es wurde zudem festgestellt, dass in erster Linie die Zunahme der Muskelgröße und der Kieferlänge für die altersbedingten Unterschiede in der Beisskraft und dem Kieferöffnungswinkel verantwortlich ist.

Zusammengefasst zeigen die vorliegenden Ergebnisse, dass die entwicklungsbedingten Veränderungen in der Kauanatomie bei *M. fascicularis* neben der Auswirkung auf die Ernährungsökologie auch mit Veränderungen im Sozialverhalten (z.B. agonistisches Verhalten) in einhergehen. Es lässt sich daher schlussfolgern, dass die anatomische Anordnung des Kausystems der Primaten die Zuordnung sowohl zu einer ökologischen als auch sozialen Nische genau widerspiegelt

und sich der Kauapparat während der Ontogenese an die sich ändernden Funktionsanforderungen anpasst. Weiterführende Studien werden sich mit der ontogenetischen, sexualdimorphen und interspezifischen Variabilität bei weiteren Primatenarten beschäftigen, wobei die Beziehung zwischen Kauform und Funktion auch aus einer evolutionären Perspektive, d.h. unter Einbeziehung von Fossilien, untersuchen werden wird.

ACKNOWLEDGEMENTS

I would like to thank PD Dr. Kornelius Kupczik for providing me with the opportunity to conduct this research and produce this doctoral thesis under his guidance at the Max Planck Weizmann Center for Integrative Archaeology and Anthropology (Max Planck Institute for Evolutionary Anthropology) in Leipzig. I would also like to thank Dr. Laura Fitton (Hull York Medical School, York, United Kingdom) for her support, advice, and supervision throughout the duration of this project, and Prof. Dr. Martin S. Fischer for his useful comments and guidance on this project. I am similarly grateful to Prof. Paul O'Higgins (Hull York Medical School, York) and Prof. Fred Spoor (University College London, London) for making the sample available for use.

I would also specifically like to thank several individuals for their invaluable contributions to this project: David Plotzki and Sue Taft for help with µCT scanning; Vivian Allen, John Hutchinson, and Andrew Cuff for assistance with biomechanical model construction; Heiko Stark for his assistance with digital fascicle reconstruction; and Callum Ross and Courtney Orsbon for their advice on contrast-enhanced staining protocols.

I would also like to thank my friends and colleagues at both the Max Planck Institute for Evolutionary Anthropology in Leipzig and Hull York Medical School in York. Their support and guidance has been invaluable to me, and I am deeply grateful.

Finally, I would like to thank the Max Planck Society for financial support of this work. Their contributions are further acknowledged within all publications resulting from this project.

TABLE OF CONTENTS

Abstract 1

Zusammenfassung 2

Acknowledgements 4

1 Introduction 6

List of Publications 25

2 Ontogenetic changes to muscle architectural properties within the jaw-adductor musculature of *Macaca fascicularis* 26

3 Non-destructive determination of muscle architectural variables through the use of DiceCT 59

4 Modelling developmental changes in masticatory function within *Macaca fascicularis* 75

5 Discussion 102

6 Conclusions 114

7 Literature Cited 117

Supplementary Material 129

Declaration of Honour 131

Curriculum Vitae 132

1. INTRODUCTION

The masticatory apparatus comprises a complex and highly-integrated suite of soft- and hard-tissue structures (including the cranium and mandible, the dentition, and the muscles of mastication) which collectively perform a diverse array of biological functions relating to the jaw. Within primates, such tasks include the oral processing of food items, inter-individual communication and display, and predation defence (Hiiemae, 1984; Conroy, 1990; Troisi *et al.,* 1990; Plavcan and van Schaik, 1992; Fleagle, 1998). As the structure and configuration of elements within the masticatory complex are related to their functional capabilities, differences in craniofacial anatomy relate to variation in overall masticatory performance, determining critical parameters such as bite force potential and maximal attainable gape (Turnbull, 1970; Taylor and Vinyard, 2009; Santana *et al., 2*010; Hylander, 2013). Such differences might reflect differing uses of the masticatory apparatus due to differences in dietary composition, food processing strategies, or social behaviours.

During development, significant hard-tissue changes are known to occur within the craniofacial region of primates, which serve to reconfigure spatial relationships between components of the masticatory apparatus. These changes occur predominantly in the viscerocranium, which displays significantly greater postnatal growth than the neurocranium[1] (Schultz, 1960; Freedman, 1962; Cochard, 1985). The greatest changes are observed in the rostrum, which begins increasing in length and breadth during early postnatal life (Corner and Richtsmeier, 1991) through anterior projection from the zygomatic region, coupled with downward rotation of the premaxilla (Richtsmeier *et al.,* 1993). Significant changes are also noted in the mandible, which increases in length and breadth as well as robustness throughout ontogeny (Taylor, 2002) in association with the eruption of the permanent dentition and the extension of the postcanine tooth row; and in the zygomatic arches, which display consistent lateral migration throughout ontogeny resulting in an overall increase in bizygomatic breadth (Cochard, 1985). However, little is known about associated changes to soft-tissue structures of the craniofacial region during growth.

The following thesis will examine how growth and development impact upon the jaw-adductor musculature and related biomechanical variables within a primate species, and explore how such changes affect functional performance across a wide range of masticatory parameters. Throughout this study, a developmental sequence of specimens of the crab-eating macaque (also known as the long-tailed macaque) *Macaca fascicularis* will be used as a model taxon (Figure 1). A generalist feeder with a core subsistence strategy of selective frugivory and granivory (Wheatley, 1980; Corlett

[1] Within the context of these studies, the term 'neurocranium' is used within the anatomical-structural sense to refer to the portion of the skull that houses the brain. It is used in contrast to the 'viscerocranium', which represents the mandible and facial skeleton.

and Lucas, 1990; Lucas and Corlett, 1991), this species has been extensively utilized as a model taxon for analyses of the primate masticatory apparatus (e.g. Hylander, 1979; Bouvier and Hylander, 1981; Dechow and Carlson, 1990; Hiiemae et al., 1995; Wall, 1999). Further, observational data suggest that within *M. fascicularis*, dietary composition and the use of the masticatory apparatus in social display differs between juvenile and adult individuals (van Schaik and Noordwijk, 1986; Troisi *et al.,* 1990; Deputte, 1994).

Figure 1. Adult female *M. fascicularis* feeding on small seeds. Photo: André Ueberbach.

Dietary and social ecology of M. fascicularis

As noted above, the core dietary components of *M. fascicularis* are fruits and seeds. These foodstuffs are heavily supplemented, however, by the opportunistic exploitation of crustaceans and other invertebrates, fungi, leaves, and other plant matter (Wheatley, 1980; Corlett and Lucas, 1990; Lucas and Corlett, 1991; Yeager, 1996; Son, 2003). Behavioural observations also report significant shifts in dietary ecology during development. A long-term study of Indonesian *M. fascicularis* populations by van Schaik and Noordwijk (1986) reports that infants and juveniles exploit significantly more small (<10mm) fruits than adult conspecifics, and relatively fewer medium-sized (10-20mm) and large (>20mm) food items. Further, younger individuals, particularly infants, avoided the consumption of fruits with hard pericarps, and consumed relatively fewer fruits with mechanically challenging rinds (van Schaik and Noorwijk, 1986). However, adults regularly exploited such fruits, with adult males consuming twice as many mechanically hard fruits as soft fruits over the study period (van Schaik and Noordwijk, 1986).

In addition to changes in diet during development, the social role of the masticatory apparatus has also been observed to evolve throughout life. Social display practices are prevalent within *Macaca*,

with wide-gape canine baring (or 'yawning') displays being frequently employed as a measure by which hierarchical order is asserted and maintained (Altmann, 1967; Troisi *et al.,* 1990; Thierry, 2004; Soltis, 2004). The frequency with which such behaviours are performed appears strongly correlated with age in *M. fascicularis*, undergoing an almost fourfold increase in frequency between sub-adulthood and adulthood in both males and females (Deputte, 1994). Within each age group, males demonstrated these postures more frequently than equivalently-aged females; though adult female yawning frequency was still greater than that of juvenile males (Deputte, 1994).

Developmental differences reported in both dietary and social ecology within *M. fascicularis* therefore impact the use of the jaw throughout ontogeny, with older individuals consuming larger and more mechanically-challenging foodstuffs while also experiencing social pressures towards maximizing gape potential for social display behaviours. The study of this species therefore enables analyses of how anatomical components of the masticatory apparatus may adapt during development to reflect functional differences in the use of the masticatory apparatus throughout ontogeny.

Rationale for the study

Quantifying changes in the musculoskeletal anatomy of the masticatory system during ontogeny allows us to analyze how components of the masticatory system scale during development. The impact of these anatomical changes upon key parameters of masticatory performance can then be assessed. By combining these data with behavioural observations of shifts in dietary and social ecology within this species during development, we may begin to explore how competing ecological pressures imposed by dietary and social shifts throughout ontogeny collectively impact upon the developing primate jaw.

In combination, the studies presented in this thesis therefore provide both crucial data on the developing masticatory apparatus within primates, while allowing us to explore the extent which developmental differences in dietary and social ecology reflect functional constraints imposed by the soft- and hard-tissue anatomy of the masticatory complex. Such data have important implications for our understanding of developmental integration within the primate masticatory apparatus.

The biomechanics of mastication

Force transmission through the masticatory apparatus

Craniofacial form plays a critical role in the functional performance of the masticatory system. While the forces required to manipulate the jaw during masticatory behaviours are intrinsically generated within the muscles of mastication, the efficiency with which these forces are transmitted through the

masticatory apparatus to the terminal dental element (or bitepoint) is dependent upon the spatial configuration of the muscle relative to the temporomandibular joint (TMJ) and the bitepoint in question (Greaves, 1978; Greaves, 1983). By altering the relative positions of these components, masticatory forces can be transferred with increased or decreased efficiency.

This configuration can be divided into two distinct components: the relationship between each muscle of mastication and the TMJ (referred to as the lever arm, or 'in-lever' of the system), and that between the TMJ and the terminal bitepoint (the load arm, or 'out-lever') (Greaves, 1978; Spencer 1999). The ratio between these two lengths is known as mechanical advantage, and expresses the efficiency with which a muscle's intrinsic force can be transmitted to a specific bitepoint (Radinsky, 1981; Greaves, 1983; Greaves, 1985; Dechow and Carlson, 1990; Smith, 1993). For a given muscle, an increase in relative lever arm length – achieved either by reconfiguring the muscle's position relative to the temporomandibular joint, or by decreasing load arm length by moving the bitepoint closer to the TMJ – improves mechanical advantage (and thus the efficiency of force transfer). As such, each muscle possesses a unique mechanical advantage for different bitepoint along the dental row; whilst for a given bitepoint, each of the jaw-adductors may present a different degree of mechanical efficiency.

Adaptations towards maximizing biomechanical efficiency can be readily observed on an interspecific level. Within cercopithecines, Singleton (2005) reports that durophagous mangabeys (represented by both *Cercocebus* and *Lophocebus*) demonstrate shorter palates, more posteriorly located molar bitepoints, and elongated muscle lever arms relative to *Papio*. This biomechanical configuration improves the mechanical advantage of their jaw adductors at postcanine bitepoints, an adaptation which may reflect their highly mechanically challenging diet. Similarly, within colobines, species which specialize in seed predation and habitually exploit unripe fruits with mechanically resistant pericarps (such as *Presbytis runicunda* and *Trachypithecus phayrei*) possess an increased mechanical advantage relative to taxa who subsist on less challenging food items (Koyabu and Endo, 2010). The same trend can be observed within Phyllostomidae (leaf-nosed bats), with species which specialize in the consumption of mechanically challenging fruits demonstrating a reduction in rostrum length, which serves to reduce relative load-arm lengths and thus improve bite force potential (Santana *et al., 2*012; Dumont *et al., 2*014).

During ontogeny, however, major changes in craniofacial configuration are known to occur – potentially impacting the spatial relationship between components of the masticatory complex and altering mechanical efficiency. It is generally hypothesized that, within primates, younger individuals would demonstrate higher mechanical advantages. Two reasons underpin this assumption. Firstly, as the muscles of mastication increase in size and force generation potential during growth (Cachel

1984; Herring and Wineski, 1986; Weijs *et al.,* 1987), younger individuals experience a relative disadvantage in bite force potential. An increase in mechanical advantage would enable juveniles to partially compensate for their smaller and weaker musculature through increased efficiency of force transmission through the masticatory apparatus (Santana *et al., 2*012; Fitton *et al., 2*015). The second factor relates to patterns of craniofacial growth within the primate order. As the rostrum and mandible undergo significant elongation in many taxa during development (Cochard, 1985; Corner and Richtsmeier, 1991; Taylor, 2002), load arm lengths within the masticatory system may consequently increase – decreasing mechanical advantage.

A number of studies have sought to evaluate this hypothesis through quantifying the effects of growth and development upon mechanical efficiency both within primates and across the mammalian order, with no consensus findings on the scaling of mechanical advantage during ontogeny. Within papionins, load-arm lengths were observed to remain consistent throughout development within 7 of 9 taxa; however, two species (*Cercocebus torquatus* and *Papio anubis*) displayed a steady elongation of this distance due to an anterior migration of the molar during development (Singleton, 2015). Lever-arm lengths of the temporalis and deep masseter also remained similar throughout growth across all taxa; though within superficial masseter, lever arms demonstrate a trend towards increasing mechanical efficiency within older individuals (Singleton, 2015).

Quantification of the mechanical advantage of jaw-adductors within *M. fascicularis* during development, meanwhile, highlights differences in biomechanical trends between bitepoints. The mechanical advantage of both temporalis and masseter were reported to remain consistent between juvenile and adult individuals at the incisors. Meanwhile, significant differences were observed between age groups for a molar bitepoint (measured at the most posterior molar cusp) (Dechow and Carlson 1990: Table 5), in which adult females presented the most mechanically advantageous configuration; followed by adult males, and finally juveniles. This trend likely represents the effects of the dental eruption sequence, in which posteriorly-positioned permanent molars (M2 and M3) exist closer to the TMJ and therefore possess a more advantageous configuration.

Studies of Carnivoran taxa also indicate high degrees of variation in biomechanical efficiency during growth. In an analysis of *Crocuta crocuta*, the mechanical advantage of the temporalis was observed to increase in a consistent manner through ontogeny, reaching its apex at around 22 months of age (Tanner *et al.*, 2010). However, no clear pattern of ontogenetic change could be observed in the mechanical advantage of the masseter (Tanner *et al.*, 2010). Within the coyote (*Canis latrans*), ontogenetic trends in mechanical advantage did not follow a traditional growth pattern; instead representing two distinct clusters that differentiated juveniles possessing decicuous dental elements

from older juveniles and adult individuals (La Croix *et al., 2*011). Across the youngest group, pups as young as two weeks of age demonstrated commensurate mechanical advantages to those aged 10-14 weeks. However, all individuals aged 21 weeks and above demonstrated similar mechanical efficiency which, in all cases, exceeded that of the younger group. Interestingly, the period of transition (14-21 weeks) between these two groups defines the age range in which the deciduous postcanine teeth typically undergo replacement (La Croix *et al., 2*011). Collectively, such studies show that the effects of ontogeny upon masticatory efficiency may vary significantly between taxa, and even between muscles within a single species.

Biomechanical effects upon jaw gape

In addition to modulating force transmission, biomechanical properties of the masticatory also influence jaw excursion potential, or gape. Gape is a critical variable in the context of dietary ecology – dictating the maximum size of potential food items that can be orally ingested. By increasing gape potential, larger food items may be incorporated into the diet; whilst an increase in gape potential further enables medium- or large- sized food items to be placed more posteriorly along the dental row to improve leverage during feeding (Taylor *et al., 2*015). Wide jaw gapes also form a critical component of certain specialized feeding strategies, such as tree-gouging (Taylor and Vinyard, 2004; Taylor *et al., 2*009). Maximizing jaw gape is also important within a social context, as wide-gape jaw postures occupy a crucial role for many primate taxa as a means of social display (Altmann 1967; Troisi et al., 1990; Hylander 2013; Terhune *et al., 2*015). A high volume of species, particularly among the Cercopithecidae, display both strict social hierarchies and intensive degrees of male-male competition (Thierry, 2000; Soltis, 2004; Cords 2012). Within such societies, wide gape canine-baring jaw postures represent a crucial form of indirect conflict between agonistic parties, being frequently used as a means of intimidation and dominance assertion (Thierry, 2004; Soltis, 2004). High levels of male-male competition are further associated with an increase in canine dimorphism; an adaptation which itself also necessitates an increase in gape potential to facilitate functional clearance for the enlarged canines found in male individuals (Plavcan and van Schaik, 1992; Plavcan, 2001; Hylander 2013). Indeed, maximum gape potential has been demonstrate to correlate strongly with canine height across extant Catarrhines (Hylander, 2013).

From an anatomical perspective, the functional trade-off between optimization for maximizing bite force and maximizing gape potential can also be observed within the lever/load arm ratios of the masticatory apparatus. Though relative increases in lever arm lengths may increase mechanical advantage, a relatively shorter muscle lever arm will decrease muscle stretch per degree of jaw rotation, enabling a greater maximum attainable gape (Herring and Herring, 1974; Dechow and Carlson, 1990; Terhune *et al.,* 2015; Taylor *et al.,* 2018). This mirrors the phenomenon observed in

the architectural configuration of muscle fibers within the masticatory apparatus (discussed below), which similarly exhibit a structural dichotomy between adaptations for maximizing bite force and those which enhance gape potential.

In addition to the modification of lever-arm ratios, many other biomechanical factors also impact upon maximum gape potential. Increasing the length of the mandible generates absolutely wider gapes per degree of jaw rotation, by maximizing the distance between the temporomandibular joint and the bitepoint and thus creating a wider arc of rotation around the joint center (Smith 1981; Hylander, 2013). The effects of increasing mandibular length upon absolute gape are therefore magnified towards the anterior dentition (Figure 2). In a similar vein, the height of the mandibular condyle above the occlusal plane also impacts upon gape potential along the dental row. For a given jaw length, a lower height of the TMJ above the occlusal plane reduces the magnitude of muscle stretch for a given degree of jaw rotation by increasing the included angle at the TMJ between the origination-TMJ and TMJ-insertion muscle vectors (Herring and Herring, 1974). By minimizing this stretch per degree of angular rotation, muscles increase in their relative excursion potential and therefore permit the production of larger overall maximum gapes (Terhune et al., 2015).

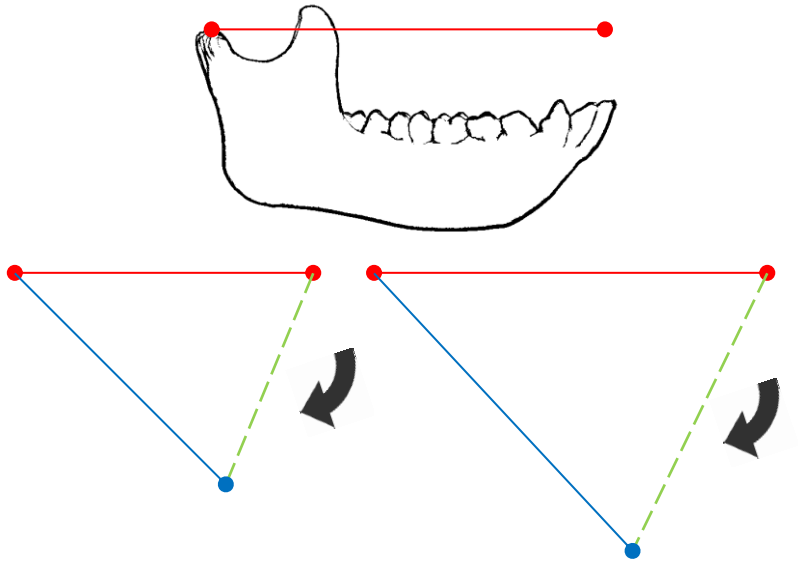

Figure 2. Schematic diagram highlighting the positive effect of increasing jaw length upon gape potential. As the length of the jaw (illustrated in red) increases, rotation of the jaw to an abducted position (e.g. a 45° gape, illustrated in blue) results in a larger absolute gape (dotted green line).

Within cercopithecines, a number of biomechanical adaptations towards gape maximization can be observed. Among these taxa, wide gape jaw postures are of particular importance within a social context; most notably within adult males, whose highly competitive social environment ascribes a key role to canine-baring (or 'yawning') displays as a means of asserting an individual's hierarchical

status and, ultimately, reproductive potential (Altmann 1967; Troisi *et al.,* 1990; Plavcan and van Schaik 1992; Plavcan, 2001; Hylander, 2013; Terhune *et al.,* 2015). Relative to female conspecifics, male *M. fascicularis* demonstrate both absolutely and relative longer mandibles; further, males possess mandibular condyles that sit significantly closer to the occlusal plane relative to both mandibular length and condyle-M1 length (Terhune *et al., 2*015). Males also demonstrate significantly greater anteroposterior curvature of the mandibular condyles relative to females, a trait which has been suggested to increase the potential for condylar rotation and facilitate larger overall gapes (Herring, 1972; Hiiemae and Kay, 1973; Wall, 1999; Terhune *et al., 2*015). These anatomical interpretations are supported by observational data reported by Deputte (1994), who notes that adult males practice wide-gape postures with significantly greater frequency than females within a social context. Wide-gape yawning displays also increase in frequency during development; with both sexes showing a fourfold increase in the frequency of such behaviours between sub-adulthood and adulthood (Deputte 1994).

Meanwhile, cercopithecines as a whole demonstrate a significant suite of biomechanical adaptations towards gape maximization relative to their sister-clade of colobines, who generally exhibit decreased smaller group sizes and diminished inter-male aggression and display relative to Cercopithecine taxa (Singleton 2015; Yeager and Fitzpatrick 1998; Sterck 2012). Such adaptations are present even among relatively durophagous cercopithecine taxa such as *Cercocebus torquatus* and *Lophocebus albigena*; suggesting that the biomechanical configuration of the masticatory apparatus within this subfamily places greater emphasis upon gape maximization than the mechanical efficiency of force transmission (Singleton, 2005).

Muscle architecture and its functional implications

The structure of skeletal muscle

The muscles of mastication are directly responsible for generating the forces necessary to move the jaw. As the structure of skeletal muscle is intimately related to a muscle's functional capabilities, the contractile properties of these muscles are dependent upon the intrinsic properties and internal configuration of their constituent components, as well as the overall volume of available muscle tissue (Huxley 1957, 1974; Gans and Bock 1965; Gans 1982; Lieber 1986).

The functional unit of force generation within a muscle is the sarcomere. Sarcomeres comprise overlapping actin and myosin filaments, which interact to produce muscle force (Gans 1965; Gordon *et al.,* 1966; Lieber *et al. ,* 1986). These filaments – sometimes referred to as 'thick' (myosin) and 'thin' (actin) filaments – are themselves hierarchically structured at the molecular level: for example, the actin filament is composed of a series of actin monomers arranged helically, alongside two

regulatory proteins (Lieber *et al.,* 1986; Lehman *et al., 2*009). Force is generated by a three-stage process of interaction between these two filament types. The heads of myosin filaments first attach to their actin counterparts via unique binding sites (which are blocked by tropomyosin when muscle is relaxed, but freed as the muscle undergoes contraction); undergo a power stroke; and finally detach (Huxley 1969). This process is then repeated along the sarcomere.

Muscle contraction induces the filaments of actin and myosin to slide past one another. As they do so, the degree of overlap between these filaments changes (Gordon et al., 1966). For a muscle to generate its maximum isometric force, the maximum degree of overlap between actin and myosin filaments is required (Gordon *et al.,* 1966; Lieber 2010; Lieber and Ward 2011; Azizi and Deslauriers 2014). This is known as attaining 'optimal sarcomere length'. In mammals this length is roughly 2.7 µm, and across all vertebrates generally falls within a range of 2.2-2.7 µm (Blemker and Saul 2012). Sarcomeres are serially arranged to form myofibrils, which are arranged in parallel to form muscle fibers (Lieber *et al.,* 1986). Fibers are the fundamental biological unit of muscles; representing multinucleated cells often many centimetres in length. Around 1,000 myofibrils are arranged in parallel in each adult muscle fiber, giving each fiber a diameter in the region of 50 µm; though in neonatal individuals, myofibril count can be reduced by as much as a factor of ten (Goldspink 1970). As fibers consist of sarcomeres arranges in series, 'optimal fiber length' is defined as the number of sarcomeres in a fiber multiplied by the 'optimal sarcomere length' (as defined above).

Several further layers of hierarchical structure exist within skeletal muscle, as schematically illustrated in Figure 3. Muscle fibers are each encased within a connective tissue (the endomysium), and arranged in bundles to form fascicles. These fascicles are themselves encased in another connective tissue (the perimysium), and collectively form a single muscle which is itself encased within a final layer of connective tissue (the epimysium).

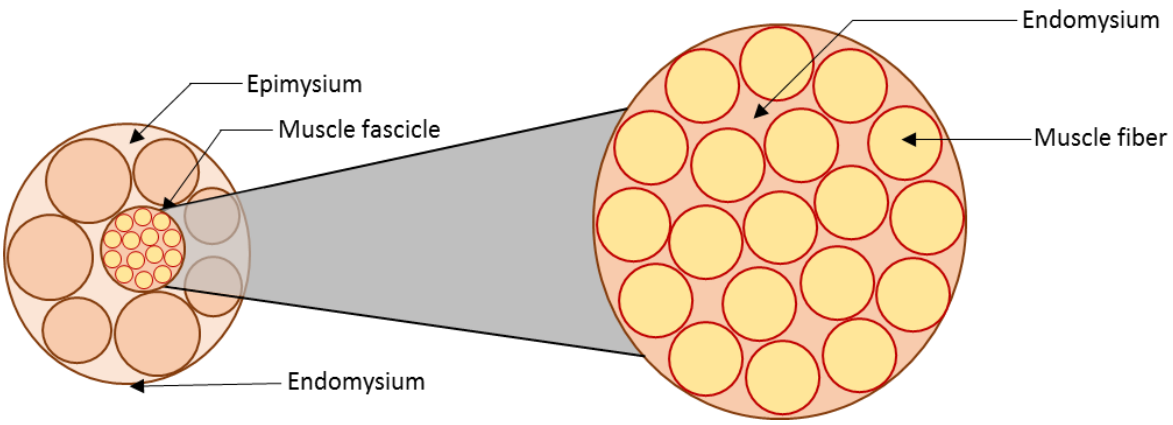

Figure 3. Diagrammatic illustration of the hierarchical nature of skeletal muscle.

Force generation within skeletal muscle

As described above, the maximum force a muscle fiber may generate is dependent upon the length of its constituent sarcomeres. At an optimal length, fibers may produce their maximal potential force; though as fibers are stretched beyond this length, the degree of overlap between actin and myosin filaments is reduced, and maximum tension likewise falls (Gordon *et al.,* 1966; Gans 1982). Should a sarcomere become stretched to the point where no overlapping filaments occur, no tension can be produced. However, this degree of stretching rarely occurs, due to accessory proteins (such as Titin) and the presence of connective tissues, which prohibit such extreme stretching (Lieber *et al.,* 1986; Lieber and Friden, 2000).

The arrangement of fibers within a muscle is a critical determinant of functional performance. The architectural configuration of muscle fibers serves to constrain functional parameters, and dictates the degree to which a muscle can be seen as optimized towards a specific contractile profile (Gans and Bock, 1965; Gans, 1982; Sacks and Roy, 1982). For example, total fiber lengths are proportionally related to a muscle's contractile velocity and maximal excursion (Bodine et al., 1982; Bang et al., 2006; Gokhin et al., 2009) and, within the jaw, strongly impact the maximal functional gape that can be attained by limiting the range of postures at which forces can be produced (Herring et al., 1979; Taylor and Vinyard 2004, 2009; Williams et al., 2009). Meanwhile, total fiber count, which reflects the cross-sectional area of a muscle, is proportionately related to the maximum contractile force that a muscle may generate (Gans 1982; Powell 1984).

The elongation of muscle fibers within the adductor musculature has been observed within a diverse array of primate species whose dietary or social ecologies require a high degree of excursion potential in order to maximize jaw gape. Within tree-gouging marmosets, whose feeding strategies involve anchoring the upper dentition into a tree and using the lower teeth to gouge holes through the bark (Coimbra-Filho and Mittermeier 1976, 1977), muscle fiber lengths within the jaw-adductor musculature are significantly longer than those found in non-gouging callitrichids such as tamarins (Taylor and Vinyard, 2004; Taylor *et al., 2*009, Eng et al., 2009). Similarly, fiber lengths within the adductor musculature have been experimentally shown to correlate strongly with maximum ingestive food size across a broad sample of strepsirrhines, highlighting the role of fiber architectural properties as a determinant of a species' dietary ecology (Perry *et al., 2*011). Functional specializations within fiber lengths have also been demonstrated within the postcranial musculature; *Galago senegalensis*, a habitual arboreal leaper, presents significantly longer muscles fibers within the epaxial musculature than the arboreal quadruped *Nycticebus coucang*, reflecting its requirement for the generation of relatively larger muscle excursions and higher whole-muscle contraction velocities (Huq *et al., 2*015).

An increase in fiber count and cross-sectional area has similarly been observed within taxa whose dietary ecology necessitates the production of high masticatory forces. For example, *Sapajus apella,* a species which habitually consumes more mechanically resistant food items than other Cebids, demonstrate a significant increase in masticatory force potential relative to their sister taxa (Taylor and Vinyard, 2009). Similarly, among Phyllostomid bats, species classified as exploiting a highly durophagous diet (such as hard-fruit specialists and carnivorous taxa) demonstrate an increase in the cross-sectional area of the temporalis muscle which enable them to produce greater maximum bite forces (Santana *et al., 2*010).

Due to the conflict between structural adaptations associated with maximizing gape and those which increase bite force potential, there exists a functional trade-off between these performance parameters within the architectural configuration of skeletal muscle (Gans and Bock, 1965; Gans, 1982; Lieber, 2002). For a given volume of muscle tissue, fiber lengths can be maximized by arranging muscle fibers in parallel, following the orientation of the axis of force generation (known as a parallel-fibered muscle). However, the number of fibers that can be accommodated within such a muscle is relatively low. By comparison, pinnate muscles (which feature a higher number of shorter muscle fibers oriented transversely to the axis of force generation) enable greater forces to be generated, at the cost of excursion potential and contractile velocity (Lieber *et al.,* 1986). The angle of pennation (θ) dictates the extent to which fiber orientation is offset from the axis of force generation. A higher angle of pennation, in which fibers are oriented more horizontally to this axis, decreases the efficiency of individual fibes as the vertical component of force generation for each fiber is reduced. However, this loss of individual fiber efficiency is more than accounted for by the increase in fiber count which is enabled; such that for a given volume of muscle, overall force production is increased by the adoption of a highly pinnate configuration (Gans 1982; Otten 1988).

The force generation potential of a muscle is typically expressed using the variable of physiologic cross-sectional area, or PCSA: a multi-variable product which combines the volume of available muscle tissue, the length of its constituent fibers, and their orientation. This measure has been demonstrated to be proportionally related to the maximum force a muscle may generate (Gans, 1982; Powell et al., 1984).

Developmental changes in muscle architectural properties

Quantifying variation in architectural properties during development is therefore critical to understanding ontogenetic changes in muscle function. Such data provide an important means of contextualizing observed differences in dietary or social behaviour during ontogeny. To date, developmental changes to architectural properties within the masticatory system are not reported

for any primate species. Similar data have been reported, however within other mammalian taxa, demonstrating that architectural properties of the adductor musculature may exhibit high degrees of developmental plasticity.

Between the ages of 4 and 20 weeks, the cross-sectional area of the adductor musculature increases fourfold within New Zealand rabbits *(Oryctolagus cuniculus)* (Weijs et al., 1987). Fiber lengths also increase during this period by around 15% (Weijs *et al.,* 1987). Meanwhile, an analysis of the masseter in the developing pig by Herring and Wineski (1986) reports a 300% increase in fiber lengths during postnatal development; whilst a study on the pterygoid complex in rats reports that the number of muscle fibers increases by 30% between birth and adulthood in the lateral pterygoid and doubles within the medial pterygoid (Rayne and Crawford, 1975).

More recently, a pair of feeding experiments have also demonstrated the effects of masticatory loading patterns upon architectural properties within the adductor musculature. Within developing rabbits, dietary divisions between a 'high load' test group (fed on food pellets and hay blocks) and an 'underuse' group (fed on ground food pellets) produced a 20% increase in masseter cross-sectional area over a three month period (Taylor *et al., 2*006). The findings of this study were later replicated by Ravosa *et al.,* (2010), who report a 15% increase in masseter size over a six-month study period. However, no changes to the lengths of constituent fibers were noted between feeding groups (Taylor *et al., 2*006).

These studies demonstrate the significant degree of developmental plasticity within architectural properties during ontogeny. Given the implied effect of such changes upon critical parameters of masticatory performance, such data underline the importance of understanding such changes within the developing primate masticatory apparatus.

Determining architectural variables within skeletal muscle

Architectural variables have been extensively collected within both mammalian and non-mammalian taxa for a diverse array of muscular elements across the body (*e.g.* Sacks and Roy, 1982; Anapol and Jungers, 1986; Lieber and Blevins, 1989; Friederich and Brand, 1990; Anapol and Barry, 1996; Murray et al., 2000; Payne et al., 2006; Oishi et al., 2008; Michilsens et al., 2009; Org an et al., 2009 ; Lamas *et al., 2*014; Perry et al., 2014; Terhune et al., 201 5; Ito and Endo, 2016; Ogihara et al., 2017; Taylor *et al., 2*018) through the means of gross dissection. Such studies have largely followed a similar methodological protocol, in which the skin and overlying musculature are first removed before the muscle is excised from its bony attachments. Isolated muscles are either immersed in water to directly determine muscle volume, or weighed to determine muscle mass (from which volume is then calculated, as mammalian muscle tissue presents a broadly consistent density of 1.056 g/cm^3).

Muscles are then typically sectioned, following the orientation of surface fascicles, at selected sampling sites to expose cross-sections at regions of interest through the muscle. The orientation of fascicles is then measured *in situ*. Fiber lengths may similarly be measured directly from the exposed cross-section (*e.g.* Anapol and Barry, 1996; Taylor et al., 2009; Lamas et al., 2014; Terhune et al., 2015), though many studies have alternatively employed a chemical digestion method in which muscles are immersed in an acidic solution to dissolve connective tissues, before fibers are manually separated under a microscope and measured independently (*e.g.* Perry and Wall, 2008; Organ et al., 2009; Hartstone-Rose et al., 2012; Perry et al., 2014).

Though such a technique is both popular and relatively time-efficient, it also carries a number of disadvantages. Gross dissection is inherently destructive to a specimen, and therefore irreversible. Further, as many studies rely upon sampling only a small number of total muscle fibers at select sampling sites, the determined architectural profiles may not necessarily be representative of the entire muscle as a whole. To overcome these shortfalls, new imaging modalities have recently begun to increase in popularity as a means of non-invasively visualizing muscular structures. Diffusion tensor magnetic resonance imaging (DTI), which tracks the diffusion of water molecules through skeletal tissues, has been successfully applied to visualize muscle volumes and approximate muscle fascicle orientations in the hindlimb musculature of humans, rabbits, rats, and mice (Damon et al., 2002; Heemskerk et al., 2005; Sinha et al., 2006; McMillan et al., 2011; Schenk et al., 2013). However, the clarity of contrast between tissues is relatively poor compared to other imaging techniques. By comparison, diffusible iodine-based contrast-enhanced computed tomography (diceCT) offers improved contrast between connective tissue and muscle. Contrast-enhanced μCT – which includes both iodine-based staining and the use of other staining agents, including phosphomolybdic acid, phosphotungstic acid, osmium tetroxide, and others – has been extensively used to visualize muscle volumes *in situ* (*e.g.* Jeffery et al., 2011; Tsai and Holliday, 2011; Cox and Jeffery, 2011; Cox et al., 2012; Hautier et al., 2012; Holliday et al., 2013; Baverstock et al., 2013; Gignac and Kley, 2014; Cox and Faulkes, 2014; Gignac et al., 2016), and recently has been shown to demonstrate the potential for digital reconstruction of muscle fascicular properties from which architectural variables can be derived (Kupczik *et al., 2*015; Dickinson *et al., 2*018). This latter publication (Chapter 3) represents the first publication to non-destructively determine muscle PCSA (through the digital reconstruction of muscle volume, muscle fiber lengths and muscle orientation) through the use of diceCT; as well as the first application of the diceCT toolkit to a primate species. Such a technique enables whole-muscle fascicle distributions to be visualized in three dimensions, substantially increasing the number of fascicles which can be analysed whilst producing digital datasets which may be more easily integrated into other mediums of musculoskeletal modelling (as demonstrated in Chapter 4).

Quantifying functional performance within the masticatory system

Both the internal structure and overall form of the masticatory musculature, as well as the biomechanical configuration of the craniofacial complex, are intrinsically related to the overall performance of the masticatory apparatus. Significant changes to both the soft- and hard-tissue components of this system have also been shown to occur as a product of ontogeny. To fully understand the relationships between form and function within the developing masticatory apparatus, however, we need a means of quantitatively analysing how anatomical changes to the soft- and hard-tissue anatomy of the masticatory complex impacts upon overall masticatory performance.

Historically, two-dimensional static models have been used to estimate muscle force products within musculoskeletal elements (e.g. Greaves, 1978; Throckmorton and Throckmorton, 1985; Sinclair an Alexander, 1987). Such analyses are capable of calculating the mechanical efficiency of a particular biomechanical configuration and, consequently, can produce estimates of overall force potential at bitepoints along the dental row for specified muscle force inputs. However, such models capture only a static condition for one precise configuration of the masticatory apparatus; further, they do not allow for three-dimensional joint moments to be computed.

By comparison, multibody dynamics analysis (MDA) represents a technique by which the functional impact of anatomical differences can be modelled in three dimensions across a wide range of jaw postures, as components of the system are manipulated into new configurations. A multibody system comprises a series of rigid anatomical bodies (representing hard-tissue anatomical structures) connected to and constrained by joint objects, and acted upon by active components (representing muscles) at specific nodes along their surface (Curtis *et al., 2*011). Activation of these muscular components (with a user-determined contractile force) produces motion in the recipient body and generates moments of force around the associated joint objects. The resultant forces of all active muscles are combined to produce an overall force around each joint, and ultimately generate whole-body movements which can be analyzed by the user and compared between models (Langenbach *et al., 2*002; Sellers and Crompton 2004; Curtis *et al., 2*010; Gröning *et al., 2*013; Watson *et al., 2*014).

Multibody models exist in one of two forms: forward and inverse dynamic models. Forward dynamics calculates the motion of rigid bodies based on an input of applied muscle forces, as described above. By contrast, inverse dynamics uses an input of body motions to calculate the muscle forces necessary to generate such movements. However, recent studies have observed that inverse dynamic solutions present a number of inherent problems, most notably that of indeterminacy (de Zee et al., 2007; Curtis *et al., 2*011). Given the high number of potential muscle force combinations that exist (even

within a simple model), many possible muscle recruitment patterns can produce the same body motions – making it impossible to determine the unique muscle recruitment solution that relates to the biological condition (Curtis *et a.* 2011). As a solution, many studies utilize optimization criteria to analyze this range of possible results, selecting those which minimise joint loads or muscle energy expenditure to represent the best approximation of the natural condition (Shi *et al., 2*012; Gröning *et al., 2*013).

Within an MDA model, muscles are represented by connective strands with attachments on two rigid bodies connected by a shared joint. These strands may either connect the points of origin and insertion directly (in a linear manner), or wrap around the external contours of objects along their path. Whole muscles are typically modelled by multiple strands, which represent different portions of the muscle body. This technique enables the modelling of changes in the orientation of a muscle's line of action along its length, and also allows for regional heterogeneity in muscle fiber architecture (i.e. changes in fiber length or pennation angle between anterior and posterior portions of a muscle) to be represented.

This latter element is particularly critical in the modelling of masticatory muscles, which have been demonstrated to show high degrees of regional heterogeneity in architectural properties. Within the superficial masseter of *M. fascicularis*, anterior fibers can grow up to 70% longer than fibers in the posterior portion of the muscle within adult males (Terhune *et al.,* 2015); whilst fiber lengths within the temporalis, meanwhile, can reach 10-20% greater lengths within the middle portion of the muscle (Terhune *et al., 2*015). Similar variation in architectural properties has been reported within other taxa. Elongation of muscle fibers within the anterior portion of superficial masseter has also been demonstrated within rats (Nordstrom and Yemm, 1972) and pigs (Herring *et al. ,* 1979). However, this trend is not universal: within both common marmosets (*Callithrix jacchus*) and cotton-top tamarins (*Saguinus oedipus*), no significant differences between anterior and posterior fibers within superficial masseter were identified by Taylor *et al.* (2009).

Previous MDA models of the masticatory complex

MDA modelling techniques have previously been employed to investigate functional performance within the masticatory complex of several taxa, including an adult male specimen of *M. fascicularis* (Curtis *et al., 2*008). For this specimen, the masseter complex, pterygoid complex, and temporalis were all modelled using architectural properties determined during dissection of the specimen, and bite force potential was assessed at bitepoints along the postcanine dental row through a 30° gape cycle at 5° increments (Curtis *et al., 2*008). At each gape angle, potential bite force increased for more posteriorly-positioned bitepoints (reflecting the shorter load arm length for these dental

elements); whilst overall bite force potential decreased towards wider gape angles, as muscle fibers moved beyond their optimal ranges for maximizing force production (Curtis *et al., 2*008: Fig. 3).

Other models have employed similar methodologies to explore bite force potential across different species. For the tegu *Tupinambis merianae*, a highly complex model featuring 116 muscle strands representing the collective muscles of mastication was created by Gröning *et al.* (2013). Bite force potential was measured at four bitepoints (ranging from the most proximal to most distal tooth within the dental row), and compared to *in vivo* bite force data collected from the same specimen. Bite forces were closely matched between the two datasets, demonstrating the ability of MDA modelling techniques to accurately reflect functional performance parameters when subject-specific architectural data are incorporated (Gröning *et al.*, 2013). Similarly, bite force estimates derived from a model of the masticatory system in European rabbits by Watson *et al.* (2014) closely matched bite force data collected *in vivo* from this species (albeit from different individuals). This model also incorporated *in vivo* kinematic data to better replicate the motion of the jaw during mastication, as opposed to modelling a simple hinge-rotation and anteroposterior translation motion path used in earlier studies (*e.g.* Curtis *et al., 2*008).

MDA models have also been constructed to model bite force potential within extinct taxa. For example, reconstruction of the masticatory complex within the carnivorous dinosaur *Tyrannosaurus rex* yielded a potential bite force of 35,000-57,000N at a posterior bitepoint, far exceeding the estimates for any previously modelled taxon (Bates and Falkingham, 2012). However, such models incorporate high degrees of uncertainty regarding both muscle size and architectural configuration. Within the above example, muscle volume was derived by digitally reconstructing three-dimensional volumes of hypothetical muscle objects; whilst muscle architectural data was initially derived from the muscles of an alligator (*Alligator missisippiensis*) and scaled to muscle volume (Bates and Falkingham, 2012). As the results of multibody dynamics simulations are highly sensitive to modelling parameters – particularly those relating to the soft-tissue parameters of muscle volume, fiber length, and tendon slack length – however, such reconstructions are unlikely to represent a good approximation of the biological condition.

Though masticatory performance has therefore been modelled within a diverse range of mammalian and non-mammalian species, currently these taxa have been represented by a single specimen. No interspecific or ontogenetic sequences of models within a single species have been analysed. The absence of these data precludes analyses of the effects of sexual dimorphism or growth and development upon overall masticatory performance. Within Chapter 4, I present a series of MDA models representing distinct developmental stages within *M. fascicularis*, which serve to quantify

specific variables of functional masticatory performance within a primate taxon during development for the first time.

Overview of the thesis

Project outline

Collectively, the constituent studies of this thesis aim to measure ontogenetic changes to the primate masticatory system during development, and quantify the functional impact of such changes upon overall masticatory performance. The masticatory system within individuals of different ages will be analysed at several hierarchical levels: from the micro-scale organization of individual muscle fascicles within the jaw-adductor musculature and its impact upon the contractile properties of these muscles, to developmental changes in craniofacial form and their effect upon the biomechanical efficiency of force transmission and gape generation within the masticatory apparatus.

The developmental sequence used throughout this thesis consists of 26 specimens of *Macaca fascicularis*, from a collection of *M. fascicularis* crania stored at Hull York Medical School, York, United Kingdom. These crania represent a full developmental sequence, from infant specimens with only deciduous teeth in occlusion to fully mature adult male and female specimens. In several analyses (see chapters 2 and 4), these specimens have been divided into three discrete age groups (infant, juvenile, and adult) on the basis of dental eruption patterns. Specimens prior to the eruption of the first permanent molar were designated as infants, and those possessing permanent molar teeth up to but not including the third permanent molar classified as juveniles. Adults were subsequently divided by sex on the basis of canine size; however, younger individuals were not sexually distinguished as differences were not consistently apparent. Of these 26 individuals, six were classified as infants, twelve as juveniles, and eight as adults (of which four were male and four female). No specimens presented recognisable soft or hard tissue pathologies.

By analysing masticatory form and performance across this developmental period, we may begin to relate anatomical variation between individuals of differing age categories to previously reported differences in dietary and social ecology between infant, juvenile, and adult individuals of *M. fascicularis* within wild populations. Integrating knowledge of anatomical changes during ontogeny will help us to better understand how masticatory capabilities interact with and restrict an individual's ecology, and improve interpretations of age-related differences in ecology within primate groups.

Aims and objectives of the study

Within chapter two, I quantify ontogenetic changes to masticatory muscle architecture and associated biomechanical variables across the full developmental sample, to address how growth and development impact upon soft- and hard-tissue components of the masticatory system. Data from the dissection of the specimens, which include muscle size, fiber lengths and pennation angles, and physiologic cross-sectional area, are presented for each individual within our sample. Simultaneously, I quantify developmental changes to biomechanical components of the masticatory system, including muscle lever-arm (or in-lever) lengths and TMJ height (the height of the temporomandibular joint above the occlusal plane). The scaling relationships of these variables are assessed against jaw length and condyle-molar length, two biomechanical proxies for load-arm (or out-lever) length which have been used in previous biomechanical studies (e.g. Perry *et al.,* 2011; Taylor and Vinyard 2013; Taylor *et al.,* 2015) to assess scaling relationships within the masticatory system. These data are subsequently analysed with reference to reported ecological differences between infant, juvenile and adult individuals of *M. fascicularis*, to better understand the external pressures acting upon the masticatory system during development and improve our interpretation of behavioural differences observed between age groups within wild populations.

Within chapter three, I apply high-resolution imaging modalities alongside a textural-recognition algorithm (Kupczik *et al.,* 2015) to explore new methods of quantifying muscle architectural properties within three dimensions. Using a diceCT protocol alongside traditional gross dissection, I evaluate the efficacy of this digital technique as a means of non-destructively determining architectural variables and digitally visualizing the internal structure of muscular components. Muscle volume, fiber lengths, pennation angle and PCSA are all determined using a fully-digital and wholly non-destructive workflow, and compared to the results derived from gross dissection of the contralateral muscles. This represented the first study to non-destructively determine muscle PCSA, and serves as a methodological benchmark which current researchers are now applying to their own datasets.

Finally, within chapter four, I combine the datasets and techniques explored within the preceding chapters with the aim of contextualizing form-function relationships within the developing masticatory apparatus, and quantifying how differences in craniofacial morphology and muscle properties between age groups affect masticatory function. Dissection data collected from representative individuals of each age category are incorporated with digital models of the cranium, mandible and muscle portions generated using diceCT to produce full three-dimensional models for the masticatory apparatus of *M. fascicularis* at differing stages of development. These models are then simplified and, through the use of Multibody Dynamics Analysis, measures of masticatory

performance such as bite force and maximum gape potential are compared between the infant, juvenile, adult female and adult male models. In order to compare feeding performance upon specific food items, performance data are collected for hypothetical food items of controlled sizes (1cm, 2cm, 3cm, 4cm and 5cm diameters) for each model. Finally, to explore how each parameter of the masticatory apparatus contributes to overall functional performance, a series of hypothetical models are created in which a juvenile is iteratively adapted towards an adult morphology. This final analysis makes it possible to analyse the contributions of each variable (e.g. muscle mass, muscle architecture, lever-arm length, jaw length) to overall performance, and in so doing greatly improves our understanding of how trends within each of these variables during development impacts upon masticatory function within *M. fascicularis*.

Together, these studies both provide an anatomical context to the ecological changes noted to occur during ontogeny within *M. fascicularis*, while addressing long-standing questions relating to the ontogeny of masticatory function within primates as a whole. By quantifying functional masticatory performance at each stage of development, we can explore the extent to which differences in diet and social behaviour within *M. fascicularis* during development are a product of functional constraints imposed by the soft- and hard-tissue anatomy of the masticatory complex. Further, the hypothetical models produced in chapter three allow us to analyse how changes to specific variables within the masticatory apparatus relate to functional performance, allowing us to better interpret variation (both ontogenetic and interspecific) within these features in other taxa through the lens of functional performance. As a result, these data have important implications not only for our understanding of dietary and social ecology within *M. fascicularis*, but also for our understanding of developmental integration and anatomical specializations within the primate jaw more broadly.

As this work is submitted as a cumulative thesis, each of the three chapters has been written to function as a standalone publication. Some redundant passages may thus occur.

LIST OF PUBLICATIONS WITHIN THIS THESIS

CHAPTER 2 (accepted, *American Journal of Physical Anthropology*): Dickinson E, Fitton LC, Kupczik K. 2018. Ontogenetic changes to muscle architectural properties within the jaw-adductor musculature of *Macaca fascicularis*.

Author contributions: ED, LF and KK conceived the study; ED dissected the specimens, recorded architectural and biomechanical data, performed all analyses, prepared the figures, and wrote the manuscript. LF and KK critically revised the manuscript and helped prepare the article for submission. Own contribution in total: 90%.

CHAPTER 3 (published, *The Anatomical Record*): Dickinson E, Stark H, Kupczik K. 2018. Non-destructive determination of muscle architectural variables through the use of DiceCT. The Anatomical Record 301: 363-377.

Author contributions: ED, HS and KK conceived the study; ED dissected and stained the specimen and processed the µCT data. HS and ED tested the sensitivity of reconstruction parameters. ED ran the analyses, prepared the figures, and wrote the manuscript. HS and KK critically reviewed the manuscript and helped prepare the article for submission. Own contribution in total: 90%.

CHAPTER 4 (in preparation): Dickinson E, Kupczik K, Fitton LC. Modelling developmental changes in masticatory function within *Macaca fascicularis*.

Author contributions: ED, KK and LF conceived the study. ED dissected and stained the specimens, constructed the MDA models, performed all analyses, prepared the figures and wrote the manuscript. KK and LF critically reviewed the manuscript and helped prepare the article for submission. Own contribution in total: 90%.

I have read the authors' contributions stated above and confirm their correctness.

_____ PD Dr. Kornelius Kupczik (Supervisor)

2. Ontogenetic changes to muscle architectural properties within the jaw-adductor musculature of *Macaca fascicularis*

Edwin Dickinson, Laura C. Fitton and Kornelius F. Kupczik

Accepted for publication in *American Journal of Physical Anthropology,* 19.05.2018

Abstract

Objectives. Changes to soft- and hard-tissue components of the masticatory complex during development can impact functional performance by altering muscle excursion potential, maximum muscle forces, and the efficiency of force transfer to specific bitepoints. Within *Macaca fascicularis*, older individuals exploit larger, more mechanically resistant food items and more frequently utilize wide-gape jaw postures. We therefore predict that key architectural and biomechanical variables will scale during ontogeny to maximize bite force and gape potential within older, larger-bodied individuals.

Materials & Methods. We analyzed 26 specimens of M. fascicularis, representing a full developmental spectrum. The temporalis, superficial masseter and deep masseter were dissected to determine muscle mass, fiber length, and physiologic cross-sectional area (PCSA). Lever-arm lengths were also measured for each muscle, alongside the height of the temporomandibular joint (TMJ) and basicranial length. These variables were scaled against two biomechanical variables (jaw length and condyle-molar length) to determine relative developmental changes within these parameters.

Results. During ontogeny,muscle mass, fiber length and PCSA scaled with positive allometry relative to jaw length and condyle-molar length within all muscles. TMJ height also scaled with positive allometry, while muscle lever arms scaled with isometry relative to jaw length and with positive allometry (temporalis) or isometry (superficial and deep masseter) relative to condyle-molar length.

Conclusion. Larger individuals demonstrate adaptations during development towards maximizing gape potential and bite force potential at both an anterior and posterior bitepoint. These data provide anatomical evidence to support field observations of dietary and behavioural differences between juvenile and adult M. fascicularis.

Introduction

Significant hard-tissue changes are known to occur within the primate craniofacial region during development. Muscle attachment sites are spatially reconfigured, the rostrum becomes increasingly prognathic, and deciduous dental elements are replaced by their permanent counterparts, extending the postcanine dental row (Cochard, 1985; Dechow and Carlson, 1990; Ravosa, 1991; Richtsmeier, Cheverud, Danahey, Corner and Lele, 1993; O'Higgins and Jones, 1998; Collard and O'Higgins, 2001; Bolter and Zihlman, 2003; Singleton, 2015). Collectively these changes serve to alter the biomechanical relationship between the muscles of mastication, the temporomandibular joint (TMJ), and the dentition (Hylander, 1985; Ravosa, 1996). During development, however, the masticatory musculature also undergoes significant changes in both size and internal configuration through alterations to the length, orientation and cross-sectional area of constituent muscle fibers (*e.g.* Rayne and Crawford, 1975; Weijs, Brugman and Klok, 1987; Pearson, 1990; Stewart and German, 1999; Lieber 2002). As the structure of skeletal muscle is integrally related to its functional capabilities (Gans and Bock, 1965; Gans, 1982; Lieber, 2002), such changes may impact the capacity to generate masticatory forces, as well as altering maximal excursion potential or gape (Bang *et al.,* 2006; Gokhin, Bang, Zhang, Chen, and Lieber*,* 2009). Studies exploring the effects of growth and development upon architectural parameters within the masticatory system have been performed on a range of mammalian taxa, including pigs (Herring and Wineski, 1986) and rabbits (Weijs *et al.,* 1987). However, despite the importance of understanding the development of the adductor musculature within primates as a means of contextualising observed differences in both dietary and social behaviours during ontogeny, such data are not reported for any primate species.

Detailing ontogenetic changes to both soft- and hard-tissue components of the masticatory apparatus is therefore necessary to better address questions regarding ecological and behavioural pressures acting upon the primate masticatory system during growth. For example, do developmental changes to the masticatory complex reflect changes in feeding performance necessary to enable dietary shifts between juvenile and adult populations? How do the unique social pressures placed upon the masticatory apparatus in many dimorphic primate taxa impact upon soft- and hard-tissue structures during development? To address such questions, this study analyses ontogenetic changes to the masticatory muscle architecture and associated biomechanical variables within a developmental sequence of a cercopithecoid primate (*Macaca fascicularis*), in order to explore the functional impact of developmental changes to the masticatory complex.

Behavioural observations suggest meaningful functional shifts in the use of the masticatory system within *M. fascicularis* during development. A long-term study of Indonesian *M. fascicularis* populations by van Schaik and Noordwijk (1986) reports variance in feeding strategies between adult and non-adult individuals. Infants and juveniles exploited significantly more small (<10mm) fruits than adult conspecifics, and relatively fewer medium-sized (10-20mm) and large (>20mm) fruits. Within adults, males consumed relatively more medium-sized and larger fruits than their female counterparts. Further, younger individuals, particularly infants, avoided the consumption of fruits with hard pericarps, and consumed relatively fewer fruits with mechanically challenging rinds (van Schaik and Noordwijk, 1986). However, adults regularly exploited such fruits, with adult males consuming twice as many mechanically hard fruits as soft fruits over the study period (van Schaik and Noordwijk, 1986).

In addition to changes in diet during development, the social role of the masticatory apparatus has also been observed to evolve throughout life. Within *Macaca*, wide-gape canine baring (or 'yawning')

displays are frequently employed as a measure by which hierarchical order is asserted and maintained (Altmann, 1967; Troisi, Aureli, Schino, Rinaldi and Angelis, 1990; Thierry, 2004; Soltis, 2004). Adaptations towards maximizing gape have been frequently discussed within adults – most notably adult males – of sexually dimorphic taxa (Herring and Herring, 1974; Smith, 1984; Hylander, 2013; Taylor *et al.,* 2018), and the frequency with which such behaviours are performed appears strongly correlated with age in *M. fascicularis,* undergoing an almost fourfold increase in frequency between sub-adulthood and adulthood in both males and females (Deputte, 1994). Within each age group, males demonstrated these postures more frequently than equivalently-aged females; though adult female yawning frequency was still greater than that of juvenile males (Deputte, 1994).

In addition to maximizing the efficacy of such display behaviours, adaptations towards increased gape within adults may also reflect an adaptive response to the increased size of the permanent canine, particularly within male individuals (Hylander 2013). Canine size has been demonstrated to correlate strongly with maximum gape potential across a range of catarrhine primates (Hylander and Vinyard, 2006; Hylander, 2009; Hylander, 2013), as an increase in gape may prove necessary to facilitate requisite canine clearance within the jaw. As increased canine size is itself interpreted to reflect a social adaptation towards the high incidence of both direct (through use as a weapon) and indirect (through social display) agonistic conflicts (Plavcan, van Schaik and Kappeler, 1995; Plavcan and van Schaik, 1997) between adult males, adaptations enhancing canine clearance would seem to further represent pressures imposed by the social ecology of a species upon masticatory function.

Such observations suggest that ontogenetic changes to soft- and hard-tissue structures to increase both bite force potential and maximum gape throughout development are necessary within *M. fascicularis* as part of the transition from juvenile to adult dietary and social ecologies. Older individuals exploit larger, harder food items, and require wide gapes as a means of social interaction and display (van Schaik and Noordwijk, 1986; Troisi *et al.,* 1990; Deputte, 1994). Previous studies have identified differences in muscle architectural properties and craniofacial form between adult male and female *M. fascicularis*, which relate to the ability of males to obtain wider gapes and generate higher bite forces (Terhune, Hylander, Vinyard and Taylor, 2015). Through quantifying such changes during growth within *M. fascicularis*, we may better understand how these dietary and social pressures impact upon the developing masticatory apparatus within a primate species.

Ontogenetic changes within the masticatory apparatus

A critical determinant of functional performance within the masticatory complex is the internal architecture of the jaw-adductor musculature (Gans and Bock, 1965; Gans, 1982; Otten, 1988; Lieber and Friden, 2000; Lieber, 2002), which may influence both dietary and social ecology by constraining functional parameters (Lieber and Friden, 2000; Taylor and Vinyard, 2009; Taylor, Eng, Anapol and Vinyard, 2009). For example, as muscle fibers consist of serially arranged sarcomeres, total fiber lengths are proportionally related to a muscle's contractile velocity and maximal excursion (Bodine *et al.,* 1982; Bang *et al.,* 2006; Gokhin *et al.,* 2009) and strongly impact the maximal functional gape that can be attained by limiting the range of postures at which forces can be produced (Herring, Grimm and Grimm 1979; Taylor and Vinyard 2004, 2009; Williams, Peiffer and Ford, 2009). Meanwhile, the multi-variable product of physiologic cross-sectional area (PCSA) has been demonstrated to be proportionally related to the maximum force a muscle may generate (Gans, 1982; Powell, Roy, Kanim, Bello and Edgerton, 1984). Consequently, within the context of diet, architectural properties of the chewing muscles contribute (alongside other factors) to the upper limits of bite force that can

be generated (Turnbull, 1970; Taylor and Vinyard, 2009; Santana, Dumont and Davis, 2010) and the maximum food item size that can be ingested (Taylor *et al., 2*009; Perry, Hartstone-Rose and Wall, 2011; Hartstone-Rose, Perry and Morrow, 2012), while these internal properties also impact social behaviours by dictating the maximum attainable gape for an individual during canine-baring displays (Terhune *et al.,* 2015).

There exists a paucity of data on the masticatory musculature of immature primate specimens. Muscle mass within the jaw-adductors of anthropoids has been shown to scale with positive allometry during development (Cachel, 1984). However, to address the functional impact of ontogeny upon parameters of masticatory performance such as gape and bite force, architectural data reflecting simultaneous changes to fiber lengths and configuration are necessary. Such data have to this point only been reported during growth in non-primate taxa, but indicate the potential for significant changes to muscle fiber properties during ontogeny. Fiber lengths have been shown to increase by 300% during postnatal development within the developing pig masseter (Herring and Wineski, 1986), and by 15% within the New Zealand rabbit between the ages of 4 and 20 weeks (Weijs *et al.,* 1987). Weijs *et al.* (1987) also recorded a fourfold increase in PCSA in the developing rabbit during this developmental period. Such studies demonstrate the significant degree of developmental plasticity within architectural properties during ontogeny, and underline the importance of understanding such changes within the developing primate masticatory apparatus.

By contrast, the bony apparatus of the masticatory system has been analysed in detail both within cercopithecines and more broadly within primates during growth (*e.g.* Dechow and Carlson, 1990; Corner and Richtsmeier, 1991; Richtsmeier *et al.*, 1993; Mitteroecker, Gunz, Bernhard, Schaefer and Bookstein, 2004). Craniometric data collected on developmental sequences of *M. fascicularis* (Ravosa, 1991) and *C. torquatus* (O'Higgins and Jones, 1998) highlight that males and females share a strongly similar developmental trajectory for much of the juvenile period, though males demonstrate both time and rate hypermorphosis (Ravosa, 1991). However, divergences are reported in the face during the latter stages of development, occurring roughly coincident with the eruption of the permanent canine. These are interpreted as reflecting specific adaptations towards accommodating characteristics of the enlarged permanent canine in males, and increasing maximum gape potential during agonistic displays (Ravosa, 1991). Indeed, gape maximization has been suggested to experience particularly strong positive selection within adult male macaques and other cercopithecines (Hylander, 2013; Terhune *et al.*, 2015; Taylor *et al.,* 2018), due to the high social importance of yawning behaviours as a means of hierarchical assertion.

The biomechanical impact of ontogenetic changes in craniofacial form has also been analysed within the cercopithecine clade (Singleton, 2015). Within papionins (including *Macaca*), the distance between the temporomandibular joint (TMJ) and distalmost molar tooth were observed to remain consistent throughout development within seven of the nine studied taxa; however, two species (*C. torquatus* and *P. anubis*) displayed a steady elongation of this distance due to an anterior migration of the molar during development (Singleton, 2015). The relative positions of both temporalis and deep masseter to the TMJ also remained similar throughout growth, though superficial masseter was observed to consistently migrate in an anterior direction during development. Quantification of developmental changes to the mechanical advantage of jaw-adductors within *M. fascicularis* (Dechow and Carlson, 1990) also showed that this ratio remains relatively conserved during growth. Equal values were reported in juvenile and adult macaques for both temporalis and masseter at the incisors, though differences were observed between age groups during molar biting (measured at the

most posterior molar cusp) (Dechow and Carlson, 1990: Table 5). At this bitepoint, adult females presented the most mechanically advantageous configuration, followed by adult males, and finally juveniles.

Taken together, these data suggest that by maintaining relatively consistent lever and load-arm distances, overall masticatory efficiency remains generally stable during development. However, the lateral migration of muscle attachments relative to the TMJ during growth (Singleton, 2015) suggests that overall muscle size (and consequently, PCSA) likely increases substantively during this period; resulting in absolutely higher potential force within older/larger individuals. This interpretation is supported by data presented by Dechow and Carlson (1990), in which peak stimulated forces within the jaw adductors of *M. fascicularis* were reported to increase significantly during development. At an incisor bitepoint, peak forces increased from 70N in juveniles to 133N and 151N in adult females and males respectively, while at a molar bitepoint forces increased from 140N in juveniles to 286N in adult females and 369N in adult males. Such an increase in bite force potential may be necessary to enable the more mechanically resistant diet observed in adults (van Schaik and Noordwijk, 1986), and may also prove important during aggressive inter-individual conflicts (Soltis, 2004).

Scaling of muscle architectural properties

Despite an absence of data on juvenile individuals, architectural features of the primate masticatory musculature have been widely assessed within adult specimens. Several recent studies have sought to quantify how architectural properties scale against key biomechanical variables such as jaw length and condyle-molar length across a diversity of primate groups, including hominoids (Taylor and Vinyard, 2013), strepsirrhines (Perry *et al.,* 2011), and platyrrhines (Taylor, Yuan, Ross and Vinyard, 2015). These studies report no consensus scaling relationship for key architectural variables. Within hominoids, both muscle mass and PCSA are reported to scale with positive allometry relative to jaw length and condyle-M1 length in both the masseter and temporalis (Taylor and Vinyard, 2013), improving relative force production capabilities. Within strepsirrhines, the architectural variables of muscle mass, fiber length, and PCSA scale close to isometry relative to the same measures, though include the possibility of both slight negative and slight positive allometry for several variables (Perry *et al.,* 2011). Finally, within platyrrhines muscle mass, fiber lengths, and PCSA all scale with negative allometry relative to both jaw length, and condyle-M1 length (Taylor *et al.,* 2015).

In addition to interspecific studies of muscle architectural variation, the impact of sexual dimorphism upon masticatory muscle architecture has also been previously analysed. Within the temporalis of adult *M. fascicularis*, males possess significantly longer muscle fibers and significantly greater PCSAs relative to both jaw length and condyle-molar distance compared to females (Terhune *et al.,* 2015). No significant differences in superficial masseter PCSA were reported, while fiber lengths were significantly longer in males for the anterior, but not posterior, portion of this muscle (Terhune *et al.,* 2015). A bony analysis also demonstrated significantly longer mandibles and more curved mandibular condyles within the adult males of this species (Terhune *et al.*, 2015). These findings were interpreted to reflect adaptations towards facilitating wide-gape jaw postures within male individuals. This is supported by measures of maximal attainable jaw gape collected in anaesthetized adult *M. fascicularis* by Hylander (2013), which highlights a significant disparity in maximum jaw gape potential: with males capable of maintaining jaw gapes up to 74° compared to a maximum gape angle of 55° in females. When scaled to jaw length, males maintain a significant advantage in relative gape potential compared to females (Hylander, 2013).

Within sooty mangabeys (*Cercocebus atys*), a specialised durophagous feeder also within the cercopithecoid clade, adult males have similarly been reported to possess relatively longer muscle fibers than females within superficial masseter, most notably in the anterior portion (Taylor *et al.,* 2018). However, relative differences were not observed in other jaw adductors, or within other architectural variables such as PCSA, demonstrating that the extent of sexual dimorphism reported for architectural variables in *M. fascicularis* by Terhune *et al. (*2015) is not universal within cercopithecine primates, even among otherwise strongly dimorphic taxa.

Hypothesis and predictions

The functional demands placed upon the masticatory apparatus appear to shift significantly throughout the developmental trajectory of *M. fascicularis*. Compared to smaller-bodied juveniles, adults feed more extensively upon larger and more mechanically-resistant food items (van Schaik and Noordwijk, 1986); further, their social ecology places strong pressures on attaining wide maximum gapes for agonistic display behaviours, which serve a key role in establishing and maintaining hierarchies (Troisi *et al.,* 1990; Deputte, 1994; Soltis, 2004). Such social pressures are particularly strong within adult males, who occupy an intensely competitive social environment in which direct and indirect agonistic conflicts with other males are common (Altmann, 1967; Thierry 2004; Soltis, 2004). Contrastingly, as the adductor musculature is predicted to be much smaller and less powerful within juveniles (Cachel, 1984; Singleton, 2015), pressures placed upon the masticatory complex within these individuals may be more strongly related towards maximizing mechanical efficiency (Fitton *et al.,* 2015).

In this study we address the hypothesis that architectural and biomechanical variables within *M. fascicularis* scale during ontogeny so as to maximize masticatory forces and (particularly) jaw gapes within larger, adult individuals. To test this hypothesis, we put forward a series of predictions regarding the scaling of muscle architectural variables and associated biomechanical proxies during development in this species.

Prediction 1. Muscle fiber lengths will scale with positive allometry relative to jaw length and condyle-molar length. Adult *M. fascicularis* (of both sexes) consume both medium-sized and large food items with greater frequency than infants or juveniles (van Schaik and Noordwijk, 1986). Adult individuals, particularly adult males, also possess larger canines which necessitate increased canine clearance (Plavcan and van Schaik, 1997; Hylander and Vinyard, 2006; Hylander *et al.*, 2009) and more frequently engage in social displays of the canine dentition as a means of establishing social dominance (Deputte, 1994). Each of these factors requires adaptations within the masticatory apparatus towards gape maximization. The elongation of the jaw during development (Cochard, 1985; Richtsmeier *et al.,* 1993), and within adult males relative to females (Hylander, 2013; Terhune *et al.*, 2015), represents one mode by which gape potential is improved, through enabling a greater absolute increase in gape per degree of jaw rotation. However, as canine height has been shown to scale with positive allometry relative to jaw length within Old-World monkeys, including within the cercopithecine subfamily (Ravosa, 1991), we predict that fiber lengths will also scale with positive allometry relative to jaw length to ensure requisite canine clearance within adult individuals, and to maximize the impact of canine-baring social displays by increasing maximum gape potential. We further predict that fiber lengths will scale with positive allometry relative to condyle-molar length, to better enable the ingestion of larger food items at the posterior dentition. Such a trend would mirror interspecific scaling patterns of fiber lengths within the adductor musculature of Old-World

monkeys demonstrated by Taylor, Yuan, Ross and Vinyard (2013), who report that fiber lengths within temporalis and superficial masseter scale with positive allometry relative to both jaw length and condyle-M1 distance. Within adults, meanwhile, we predict that adult males will possess absolutely and relatively longer muscle fibers than females (as demonstrated by Terhune *et al.,* 2015), reflecting the increased importance of gape maximization within mature males for social display during agonistic conflicts and the greater size of their canine dentition.

Prediction 2. Muscle mass and PCSA will scale with positive allometry relative to jaw length and condyle-molar length. Adult *M. fascicularis* are further reported to consume a greater frequency of mechanically challenging food items than juvenile conspecifics occupying the same environment (van Schaik and Noordwijk, 1986). Adaptations towards maximizing gape include the elongation of muscle fibers (Prediction 1), which would detract from the optimization of the jaw-adductor muscles towards force production (Gans and Bock, 1965; Gans, 1982; van Eijden, Korfage and Brugman, 1997). However, a previous study exploring this potential trade-off within *Sapajus apella* reports the presence of additional muscle mass as a means of overcoming the decreased efficiency in force generation associated with longer muscle fibers (Taylor and Vinyard, 2009); with the net effect of S. *apella* being able to produce both wider jaw gapes and greater forces. Terhune *et al.* (2015) similarly show that, within *M. fascicularis*, adult males demonstrate increased muscle mass and PCSA in addition to longer muscle fibers relative to females, particularly within the temporalis.

We therefore predict that muscle mass and PCSA will both scale with positive allometry during development, while adult males will demonstrate increased muscle mass and PCSA relative to females. An increase in muscle mass would enable larger individuals to overcome the theoretical trade-off between gape and force production (Gans, 1982; Taylor and Vinyard, 2009). Meanwhile, a positively allometric scaling of PCSA would enable larger individuals to better exploit more mechanically challenging foods which other, smaller members of the group may be prohibited from consuming by their more gracile masticatory musculature. This predicted scaling pattern would also support data presented by Taylor *et al.* (2013), who report that PCSA scales with positive allometry relative to both jaw length and condyle-M1 length within Old World monkeys, and data presented by Dechow and Carlson (1990) on the scaling of maximum bite force within *Macaca* during ontogeny .

Prediction 3. TMJ height will scale with negative allometry relative to jaw length. For a given jaw length, a lower height of the TMJ above the occlusal plane reduces the extent of muscle stretch for a given degree of jaw rotation by increasing the included angle at the TMJ between the origination-TMJ and TMJ-insertion muscle vectors (Herring and Herring, 1974). By minimizing stretch per degree of angular rotation, individuals are capable of producing larger overall maximum gapes (Terhune *et al.*, 2015). Therefore, the height of the temporomandibular joint (TMJ) relative to the occlusal plane is predicted to scale with negative allometry relative to jaw length during development. Meanwhile, TMJ height is predicted to be decreased within adult males relative to females, so as to improve relative gape potential within adult males and maximize the efficacy of agonistic canine-baring displays.

Prediction 4. Muscle lever arms will scale with negative allometry relative to jaw length and condyle-molar length, and with isometry relative to basicranial length. The lever-arm lengths of the jaw-adductors relative to their load arms reflect the mechanical advantage of these muscles (Radinsky, 1981; Greaves, 1983, 1985). A relatively shorter muscle lever-arm will decrease muscle stretch per degree of jaw rotation, enabling a greater maximum attainable gape; a trait that is

advantageous within adults both at the anterior teeth (for social display) and the posterior dentition (for feeding). Whilst a trade-off of this configuration would be a decline in the mechanical advantage of these muscles (a potential problem given the increased dietary hardness in adults (van Schaik and Noordwijk, 1986)), projected simultaneous increases in relative mass and PCSA (see Prediction 2) may circumvent any loss in biting force due to shorter muscle lever arms. We therefore predict that lever arms will be relatively longer in younger, smaller-bodied individuals, maximizing mechanical advantage within their smaller jaw adductors, and scale with negative allometry during development so as to maximize gape within larger adults. Similarly, we predict that adult males will possess relatively shorter lever arms than females, so as to maximize gape potential within mature male individuals.

We also assess the scaling relationship between lever-arm lengths and basicranial length during ontogeny. Unlike mandibular proxies, the length of the basicranium does not reflect the load-arm of the masticatory system, and is reported to scale with negative allometry relative to load-arm length within cercopithecines (Ravosa, 1991). We therefore predict that lever-arm lengths will scale with isometry relative to basicranial length during ontogeny.

Prediction 5. Jaw length and condyle-molar length will scale with positive allometry relative to basicranial length. An increase in jaw length enables wider absolute gapes per degree of jaw rotation by maximizing the distance between the TMJ and the dentition, thus creating a wider arc of rotation around the joint center (Williams *et al., 2*009; Terhune *et al.,* 2015). Increasing the distance from the TMJ to a given bitepoint, however, also decreases mechanical advantage (Radinsky, 1981; Greaves, 1983, 1985). Given the combined dietary and social pressures upon gape maximization within adult *M. fascicularis,* particularly among adult males, we predict that relative jaw lengths will increase during development such that maximum gape potential is increased within older individuals; while among adults, males will possess longer jaws than females (as previously reported by Terhune *et al.* (2015)). The associated decline in the mechanical efficiency of force transfer is hypothesized to be counterbalanced by an increase in muscle mass and PCSA (see Prediction 2).

Materials and Methods

Sample

The sample comprised 26 heads of *Macaca fascicularis* representing a full developmental spectrum from infants to fully mature adults. All specimens were acquired from Hull York Medical School, University of York, England from a colony previously used in dental caries experiments unrelated to the current study (Smith and Beighton 1986, 1987). The diet provided to these specimens is unknown. Classification into the categories of infant, juvenile, and adult was based on dental eruption patterns, with specimens prior to the eruption of the first permanent molar designated as infants, and those possessing permanent molar teeth up to but not including the third permanent molar classified as juveniles; the full molar eruption sequence data for each individual is presented in Table S1. Adults were subsequently divided by sex on the basis of canine size; however, younger individuals were not sexually distinguished as differences were not consistently apparent. Of these 26 individuals, six were classified as infants, twelve as juveniles, and eight as adults (of which four were male and four female). No specimens presented recognisable soft or hard tissue pathologies (one specimen previously designated for this study was removed from the sample as cranial pathologies were recognised during the dissection process). Prior to dissection, the specimens had been fixed using a formaldehyde solution and stored in 70% ethanol, before being transferred into

vacuum-sealed packages for long-term preservation. The concentration of formaldehyde used during fixation is unknown, as the specimens were fixed prior to our acquisition of the tissue. However, inspection of this tissue leads us to believe that a relatively high concentration was used. Consequently, we employ a lower specific density when estimating the volume of our tissue of 1.055g/cm3, in line with results published for 37% formaldehyde-fixed tissue by Ward and Lieber (2005).

Data collection

Muscle architecture

Architectural measurements from the superficial masseter, deep masseter, and temporalis muscles were collected from each of the 26 individuals. For each specimen, the skin, any overlying musculature, and fascia were removed. The configuration of each muscle in situ was noted prior to their removal. The superficial masseter and deep masseter were initially removed to expose the lateral surface of the ascending ramus and the lateral tendon of temporalis. Once the temporalis had been freed from its cranial attachments, a section of the mandibular ramus and posterior corpus was removed using an Emax Evolution mechanical micro-saw (Nakanishi Inc., Tochigi, Japan), the anterior border of which extended forward to incorporate the tendinous insertions of the temporalis muscle. This section and the attached temporalis were removed to enable observation of the intact medial insertions of temporalis in situ prior to harvesting. The temporalis was then freed from its mandibular attachments. The anterior portion of temporalis has previously been described as a distinct muscle whose deeper fibers are inseparable from those of the anterior boundary of temporalis, and which shares a common tendon (Ross, 1995). However, given the extent of interdigitation between these portions of temporalis and their unified insertion, this portion was considered here to be part of the temporalis muscle. Following removal, all muscles were blotted dry, trimmed of any excess connective tissues, and weighed to the nearest 0.0001g using a Kern analytical balance (Kern & Sohn, Balingen, Germany).

Fiber lengths were measured immediately post-weighing, following protocols outlined by Anapol and Barry (1996) and by Taylor *et al.* (2009). Superficial masseter and temporalis were sectioned along their lengths, following the orientation of visible surface fascicles, to produce anterior, middle, and posterior portions (Figure 1). Deep masseter was bisected following the orientation of superficial fascicles to expose the interior surface of the muscle's midline. Five fibers from each of the exposed surface of posterior temporalis, anterior temporalis, posterior superficial masseter, anterior superficial masseter, and deep masseter portions were measured at approximately evenly spaced intervals along each section. Fiber length (Lf) was measured as the linear distance between a single fiber's proximal and distal points of termination (Figure 1).

Twenty-three of the twenty-six specimens had been fixed with the incisors in occlusion, while three adult male individuals were fixed with jaws open to angles between 45-50°. In order to correct fiber length measurements within these three specimens, a correction curve was calculated using fiber architectural data derived from adult *M. fascicularis* specimens presented by Taylor *et al.* (2014). They report that when stretched to a maximum gape (approximately 74°; Hylander, 2013), masseter fiber lengths were increased by 74% and temporalis fiber lengths by 44%. At the gapes found within our specimens, fiber lengths were therefore projected to be elongated by 45-50% in masseter and 27-30% in temporalis. Though some small deviations may occur as a result of this correction method, these are not expected to meaningfully affect the results from these specimens.

The perpendicular distance between the distal termination of the fiber and the muscle's central myotendinous junction was also measured for the calculation of PCSA (Figure 1). Both measurements were taken under a magnifying lens, using digital callipers accurate to the nearest 0.01mm.

PCSA (cm^2) was calculated using the formula:

$$\frac{muscle\ mass\ (g) \times \cos(\theta)}{fiber\ length\ (cm) \times 1.055\ (g/cm^3)}$$

in which θ represents the angle of pennation and 1.055 g/cm^3 represents the density of formaldehyde-fixed mammalian muscle tissue (Ward and Lieber, 2005).

Biomechanical variables

Prior to dissection, microCT scans were collected for each specimen, and reconstructed using average isometric voxel sizes of 0.1 x 0.1 x 0.1 mm. The resultant datasets were segmented to produce separate volumes for the cranium and mandible using Avizo 8.0 (FEI, Thermo Fisher Scientific). Generated three-dimensional surfaces of these bony elements were used to place relevant landmarks. In total, 12 landmarks were placed describing the left and right mandibular condyles, the most posterior molar tooth in the dental row, the mandibular first incisor, the inion and basion on the base of the cranium, and origination and insertion points for each of temporalis, superficial masseter, and deep masseter through the centre of the muscle (Table 1). To ensure accurate placement of our muscle landmarks, photographs acquired during the dissection process were used as a reference. The use of single landmarks to represent a muscle's origination and insertion, though a simplification, provides a good approximation of muscle orientation and lever-arm lengths and has been commonly utilized to assess mechanical leverage within the masticatory apparatus (*e.g.* Dechow and Carlson, 1990; Koyabu and Endo, 2010; Hartstone-Rose *et al., 2*012).

Jaw lengths were calculated as the horizontal distance from the right temporomandibular joint to the right I_1. Similarly, condyle-molar lengths were calculated as the horizontal distance from the right temporomandibular joint to the most posterior molar tooth within the dental row (Figure 2). This posterior molar tooth ranged from the dP_4 in infant specimens to the M_3 in adults. Use of the posterior-most molar accords with previous biomechanical studies within *Macaca* (e.g Dechow and Carlson, 1990); moreover, the M_3 displays high degrees of dental wear within adult cercopithecines, reflecting a high frequency of masticatory loading and the larger magnitudes of bite force generated at this bitepoint (Gantt, 1979). In each instance, measurements were made to a central point upon the occlusal surface of the tooth. TMJ height was measured as the vertical distance from the occlusal surface of the most posterior molar tooth to the centre of the right mandibular condyle (Figure 2). Basicranial length was measured as the horizontal distance from the inion to the basion (van Minh, Mouri and Hamada, 2015). Finally, muscle moment arm lengths were calculated as the perpendicular distance from the TMJ to the muscle's line of action through the centre of each muscle (Figure 2).

Data analysis

To evaluate our scaling predictions, we employed a series of reduced major axis (type-II) regressions analysing each architectural or bony measure against the relevant biomechanical variable. This method is specifically designed to handle error in both x and y variables (Sokal and Rohlf, 1995), and has been previously used in similar studies evaluating the scaling relationships of muscle architectural variables against biomechanical proxies or body mass (*e.g.* Perry and Wall, 2008; Perry

et al., 2011; Taylor *et al.,* 2013). Both x and y variables were log-transformed prior to analysis. Further, multi-dimensional variables were converted into muscle mass$^{1/3}$ and PCSA$^{1/2}$ respectively prior to transformation, to ensure that slopes reflecting isometry were normalized to 1 across all variables. All statistical analyses were performed using PAST (v3.14), and graphs produced using the *R* package ggplot2 (Wickham, 2009).

Results

Anatomy of adductor musculature within *Macaca fascicularis*

The morphology of the masticatory musculature within macaques has been previously described (*e.g.* Hartman and Strauss, 1933; Schumacher, 1961; Schwartz and Huelke, 1963; Zielinski, 1965), though much of the literature to data has been focused upon *Macaca mulatta*. However, there appear to be few significant differences in anatomical configuration between these sister taxa. Across specimens, the superficial masseter originated from the anterior 50-80% of the inferior surface of the zygomatic arch. The orientation of superficial fascicles followed an inferior-posterior direction, towards the muscle's insertion on the lateral gonial angle of the mandible. Internally, a central aponeurosis was found to divide bipennate fibers in all specimens. Immediately deep to the superficial masseter, but separated by a fascial layer, lay the deep masseter. This portion originated from the inferior and medial surfaces of the posterior third to two-thirds of the zygomatic arch – such that the anterior border of deep masseter upon the zygomatic arch could be found deep to the posterior border of superficial masseter. Fascicles of this muscle followed an inferior-anterior orientation to insert on the lateral surface of the ascending ramus of the mandible. A distinct depression or groove was found to outline the anterior, posterior, and (particularly) inferior borders of the muscle's insertion site. The fascial distinction between deep and superficial portions of the masseter was clearest in adult individuals and least defined in infants, where interdigitation of fascicles between layers was common.

Temporalis originated from the lateral wall of the cranial vault, defined by the extent of the temporal fossa. Fascicles were arranged in a fan-like structure and thus differed greatly in orientation at their point of origin. In the anteriormost portion of temporalis, fibers assumed a distinctive inferior orientation; however, there was complete interdigitation between fascicles of this muscle portion and the posterior portion of temporalis. The fascicles of the temporalis converged to a single orientation before passing under the zygomatic arch. Two distinct tendinous insertions were present across specimens, as well as a number of broader surface attachment areas such as that which encompasses the anterior border of the coronoid process. The lateral tendinous head typically runs deep to the superficial masseter but anterior to the deep masseter (though in some individuals it was observed to pass anteriorly to both portions of the masseter complex), and inserts onto the lateral surface of the mandible at a height slightly beneath that of the dental row, and close to the angle at which the mandibular ramus and corpus meet. The insertion of the medial head was found on the lowest margins of the anterior surface of the ascending ramus, and on the superior surface of the mandible corpus immediately behind the postcanine dental row.

A schematic and photographic depiction of differences in muscle size and configuration between age groups is presented in Figure 3.

Scaling relationships of architectural variables

Statistics summarizing the scaling relationships of architectural variables are reported in Table 2. Fiber lengths within all three muscles (superficial masseter, deep masseter, and temporalis) scaled with positive allometry relative to condyle-molar length (Figure 4). Fiber lengths within superficial masseter and temporalis also scaled with positive allometry relative to jaw length (Table 2), whilst fiber lengths within deep masseter also tended towards positive allometry, but bootstrapped 95% confidence intervals could not rule out isometry. Within adults, males possess absolutely and relatively longer (when scaled against both jaw length and condyle-molar length) muscle fibers within all three muscles, with temporalis presenting the most dimorphic differences in fiber length, followed by superficial masseter, and finally deep masseter. Relative differences between sexes were greater when scaled against jaw length than condyle-molar length.

Muscle mass scaled with positive allometry relative to both jaw length and condyle-molar length across all muscles (Figure 5). Similarly, PCSA scaled with positive allometry relative to both jaw-length and condyle-length in each muscle (Figure 6). In terms of muscle mass, temporalis demonstrated the most strongly positive allometry, whilst in terms of PCSA, deep masseter was the most positively allometric muscle (Table 2). Both muscle mass and PCSA are absolutely and relatively increased within adult males relative to adult females. As with fiber length, temporalis shows the greatest pattern of dimorphism, followed by superficial masseter and finally deep masseter; while relative differences are more prominent when scaled against jaw length than condyle-molar length.

Prediction 1 (that fiber lengths would scale with positive allometry relative to both jaw length and condyle-molar length) was therefore supported, with the exception of deep masseter versus jaw length, which tended towards positive allometry but could not rule out isometry. Prediction 2 (that muscle mass and PCSA would scale with positive allometry relative to both jaw length and condyle-molar length) was also universally supported across all muscles. Our predictions that adult males would also display greater fiber lengths (Prediction 1), muscle mass and PCSA (Prediction 2) than females were also supported. Complete architectural data for each individual specimen is reported in Table S1.

Scaling relationships of biomechanical variables

Statistics summarizing the scaling relationships of biomechanical variables are reported in Table 3. TMJ height scaled with positive allometry relative to jaw length, and also relative to condyle-molar length, during development (Figure 7). Within adults, meanwhile, males possess absolutely greater TMJ heights, though males and females possess an almost identical ratio of TMJ height to both jaw length and condyle-molar length. Consequently, Prediction 3 (that TMJ height would scale with negative allometry relative to jaw length) was not supported.

Lever arms for all muscles scaled with approximate isometry relative to jaw length (Figure 8), with 95% confidence intervals that included the possibility for slight negative or slight positive allometry (Table 3). Meanwhile, lever arms lengths scaled with positive allometry relative to condyle-molar length within temporalis, and tended towards positive allometry (but with 95% confidence intervals that could not exclude isometry) within superficial and deep masseter (Figure 8). Consequently, Prediction 4 (that lever arms would scale with negative allometry during development) was not supported. Within adults, however, negative allometry within lever-arm lengths is observed: with

males possessing relatively shorter lever-arm lengths across all three muscles when scaled to both jaw length and condyle-molar length. This component of our prediction was therefore supported.

Lever arm lengths tended towards positive allometry relative to basicranial length during development (Figure 9), though 95% confidence intervals also included positive allometry (Table 3). Among the jaw adductors, lever-arm lengths within temporalis were most positively allometric, while superficial and deep masseter presented scaling patterns closer to isometry (Figure 9).

Finally, jaw length scaled with positive allometry relative to basicranial length (Figure 10), though 95% CIs could not exclude isometry (Table 3). Meanwhile, condyle-molar length scaled with isometry or slight negative allometry relative to basicranial length. As a result, Prediction 5 (that jaw length and condyle-molar length would scale with positive allometry relative to basicranial length) was only partially supported. Within adults, males possess both absolutely and relatively longer jaws (and condyle-molar lengths) relative to females, in line with our prediction.

Discussion

Scaling of muscle architectural variables during development

Our results indicate that fiber lengths scale with positive allometry during development relative to both jaw length and condyle-molar length, supporting Prediction 1 and suggesting that relative gape performance increases within *M. fascicularis* throughout development. An increase in feeding performance during development is additionally evidenced by the positively allometric scaling of PCSA across the adductor musculature (supporting Prediction 2), enabling larger individuals to produce greater masticatory forces and allowing more mechanically resistant food items to be consumed by older individuals. Within adults, males possessed both absolutely and relatively longer muscle fibers and relatively greater PCSAs than females across all muscles, when scaled to both jaw length and condyle-molar length, matching findings reported by Terhune *et al.* (2015).

As *M. fascicularis* demonstrates a shift in dietary ecology towards the exploitation of both larger and more mechanically-resistant foods with increasing age (van Schaik and Noordwijk, 1986), such adaptations may be a key means of supporting the more demanding dietary repertoire observed within adult individuals. Though the diet of *M. fascicularis* is less focused upon foods of extreme size and mechanical resistance than that of certain other cercopithecoid taxa (such as *C. atys*; McGraw, Vick and Daegling, 2011; Daegling *et al.,* 2011; Taylor *et al.,* 2018), the consumption by adults of both large and mechanically-challenging food items such as crustaceans has been documented (Son, 2003) alongside a core subsistence strategy of selective frugivory and granivory supplemented by the opportunistic exploitation of invertebrates and other plant matter (Wheatley, 1980; Corlett and Lucas, 1990; Lucas and Corlett, 1991; Yeager, 1996; Son, 2003). The increase in both gape potential and PCSA observed within adults – particularly adult males – might also prove important during periods of resource scarcity (initiated either by the seasonal absence of preferred foods or by broader environmental factors which restrict overall food item availability) by diversifying the range of exploitable foods. Indeed, dietary diversification may be particularly crucial for adult males given their increased body sizes (4.6-8.3kg) compared to females (2.2-5.7kg) (Fa, 1989: Table 2). The larger body size of males will likely increase their daily caloric requirements: in *Papio anubis*, which shows a similar level of dimorphism to *M. fascicularis* (in which adult males approach two times the weight of females), resting metabolic rate (RMR) is almost twice as high in adult males (798 kcal/day) than in females (434 kcal/day) (Leonard and Robertson, 1992: Table 5). Similar patterns are also observed

within dimorphic hominoids including *Pongo pygmaeus* and *Pan troglodytes* (Harvey and Clutton-Brock, 1985; Leonard and Robertson, 1992; Smith and Jungers, 1997). Given these presumably elevated caloric requirements and requisite feeding times, the increased muscle mass observed within adult males may also serve a secondary role in minimizing the accumulation of muscle fatigue within the masticatory apparatus during extended feeding bouts.

Beyond their impact upon feeding performance, architectural adaptations towards generating wide jaw gapes and high bite forces are also highly important within a social context. Increased relative fiber lengths allow functional clearance for the larger canines found in adult males (Plavcan and van Schaik, 1992; Plavcan, 2001), and enable wider maximum gapes to be attained during agonistic canine-baring jaw postures. The high incidence of aggressive conflicts between adult *M. fascicularis* individuals (Thierry, 2000; Thierry, Iwaniuk and Pellis, 2000; Soltis, 2004) might also contribute to the positive scaling of adductor PCSA during growth. Our results suggest that relative bite force potential at the anterior dentition increases throughout life within *Macaca*, a finding supported by bite force data collected by Dechow and Carlson (1990), and by data presented by Taylor *et al.* (2013) on the scaling of PCSA to jaw length and body size within Old World monkeys. Maximizing anterior bite force through increasing adductor PCSA may provide a crucial advantage during aggressive inter-male conflicts and, alongside increases in fiber length, might represent part of a suite of anatomical adaptations within the masticatory apparatus of *Macaca* towards a highly competitive social environment in which agonistic displays and physical conflicts play a key role in determining an individual's hierarchical status and, ultimately, reproductive potential.

By comparison to adductor muscle data reported within adult *M. fascicularis* by Terhune *et al.* (2015), we report significantly lower muscle masses and PCSA values (e.g. a mean adult male temporalis muscle mass of 23.1 g *vs* 53.4 g). This decrease in muscle mass (and consequently PCSA) likely reflects the effects of tissue shrinkage within our sample, which had been preserved in a high concentration formaldehyde solution prior to our acquisition of the specimens. However, the same patterns of architectural dimorphism are observed here as by Terhune *et al.* (2015). Further, measurements of fiber length appear closely comparable between the two datasets (*e.g.* mean fiber lengths of 15.7 mm vs 17.6 mm in superficial masseter, and 24.7 mm vs 26.3 mm within temporalis).

Scaling of biomechanical variables during development

Our results indicate that TMJ height scales with positive allometry relative to jaw length (and also to condyle-molar length), contrary to Prediction 3. As increasing relative TMJ height limits gape potential by increasing muscle stretch per degree of jaw rotation (Herring and Herring, 1974), older individuals do not show adaptations within the height of the mandibular condyle towards gape maximization. Within adults, males are reported to possess relatively reduced TMJ heights compared to females by Terhune *et al.* (2015), improving their gape potential. However, no differences in relative TMJ height between males and females were observed within our sample.

Our results also indicate that all muscle lever-arms scale with approximate isometry relative to jaw length, and with slight positive allometry or isometry relative to condyle-molar length and basicranial length. These findings largely correspond to previous work on changes to muscle leverage during ontogeny. Singleton (2015) reports that, during development, temporalis and deep masseter maintain a consistent position relative to the TMJ within papionins, whilst superficial masseter experiences a slight anterior migration throughout life to mitigate the loss of anterior bite forces associated with lengthening of the rostrum (Spencer, 1999; Greaves, 2012; Singleton, 2015). Though

changes to the lever-arm length of superficial masseter were not observed within our sample, other mechanisms appear to fulfil this role of circumventing losses to bite force potential. For example, the positively allometric scaling of adductor PCSA relative to jaw length and condyle-molar length during development would serve to increase bite force potential across the dentition, even as the jaw increases in length.

Within adults, however, negative allometry within lever-arm lengths is observed, with males possessing relatively shorter lever-arm lengths across all three muscles when scaled to both jaw length and condyle-molar length. As a reduction in lever-arm length reduces muscle stretch per degree of jaw rotation (thus enhancing gape potential), these differences may reflect the increased social pressures upon males towards gape maximization, to enhance the efficacy of wide-gape canine-baring displays within a social context (Altmann, 1967; Troisi *et al.,* 1990, Deputte, 1994; Soltis, 2004). Though reducing lever-arm lengths negatively impacts the mechanical advantage of the respective muscles, relative increases in both muscle mass and PCSA within adult males circumvent any loss in masticatory performance as a product of their altered biomechanical configuration.

Finally, we report that jaw length scales with positive allometry relative to basicranial length during development, while condyle-molar length scales with isometry (or slight negative allometry) relative to the basicranium. Within adults, meanwhile, males possess both absolutely and relatively longer jaws (and condyle-molar lengths) relative to females. As increasing mandibular length represents a key adaptation towards gape maximization (Williams *et al.,* 2009; Terhune *et al.,* 2015), our data suggest that older individuals – particularly adult males - display a jaw morphology better adapted to maximizing gape potential, even at the cost of mechanical advantage. These data further demonstrate the extent to which adaptations towards gape maximization can be observed within the adult male masticatory complex, further supporting observations by Taylor *et al.* (2018) regarding the extent to which male cercopithecines appear to prioritize gape performance as part of an intensively competitive social environment dominated by agonistic male-male encounters.

Our findings also correspond to data presented by Ravosa (1991) on the scaling of jaw length relative to basicranial length, in which a positively allometric relationship is also reported within both cercopithecines and colobines. That condyle-molar length scales with isometry (or slight negative allometry) relative to basicranial length, meanwhile, reflects the posterior migration of the most proximal bitepoint (from dP_4 in infants to M_1/M_2 in juveniles and M_3 within adults) during development. Older individuals offset the loss in postcanine mechanical advantage associated with the anterior elongation of the jaw by the eruption of more posteriorly-situated permanent molars, which present similar load-arm lengths to the most-proximally positioned teeth within infants and younger juveniles. As a result, the relationship between basicranial length and the distance from the TMJ to the most posterior tooth remains relatively consistent throughout life.

<u>Interpreting developmental changes to the masticatory complex</u>

It is noteworthy that while the scaling of architectural variables during development all corresponded to our predictions, our predictions relating to the biomechanical configuration of the adductor musculature were largely not upheld. Rather than demonstrating adaptations towards gape maximization within older individuals, muscle lever arm lengths scale with isometry relative to jaw length and tend towards positive allometry for a molar bitepoint. This may reflect the need for larger adults to retain high postcanine bite forces for feeding (and potentially high anterior bite forces for

antagonistic conflicts), rather than wholly optimizing the configuration of their masticatory system towards gape maximization.

The reduced magnitude of changes to muscle lever arms, compared to architectural properties of the adductor musculature, might also suggest that the biomechanical configuration of the masticatory musculature remains relatively conserved during development, a finding previously reported within papionins by Singleton (2015). The highly-integrated nature of the primate masticatory apparatus (*e.g.* Vinyard, Wall, Williams and Hylander, 2003; Ross, Iriarte-Diaz and Nunn, 2012; Terhune *et al.,* 2015) may support this interpretation, wherein the high complexity of the masticatory apparatus produces a many-to-one relationship between form and function such that many possible adaptations could incur the same functional effect (Wainwright, Alfaro, Bolnick and Hulsey, 2005; Terhune *et al.,* 2015). Within *M. fascicularis*, muscle architectural changes to PCSA and fiber lengths during ontogeny may circumvent the need for extreme changes to biomechanical features such as lever-arm lengths and TMJ height within the masticatory complex.

The complex and highly inter-related nature of the masticatory system also necessitates considerations of other variables not examined here but which may impact upon masticatory performance. For example, changes in muscle fiber phenotype during development may impact upon dietary ecology by altering the contractile capabilities of the adductor musculature. Sexually dimorphic differences in muscle fiber profile are reported in adult *P. anubis* by Wall *et al.* (2013) in which males possess a higher concentration of type-II fibers, enabling them to generate faster and more powerful bites. This same trend was reported by Maxwell *et al.* (1979) within *M. mulatta*, and a similar relationship within *M. fascicularis* was predicted by Terhune *et al.* (2015). Maxwell *et al.* (1979) further report that juvenile *M. mulatta* present a fiber profile more similar to adult males in having a higher proportion of type-II fibers in both the temporalis and masseter. However, as fiber phenotypes have been shown to vary drastically as a result of both ageing (Anapol and Herring, 2000; Korfage, van Wessel, Langenbach, Ay and van Eijden, 2006) and diet (Ravosa *et al.,* 2010) within other mammalian taxa, further quantification of such changes within the primate adductor musculature during development is necessary. Future studies should also endeavour to study the effects of ontogeny upon the efficacy of the dentition in promoting food breakdown. Though younger individuals appear to be at a relative disadvantage in force production, the increased sharpness of newly-erupted dental cusps in younger individuals may enable the equally successful processing of food items at lower masticatory forces (Popowics and Fortelius, 1997; Evans and Sanson, 1998; Lucas, 2004).

Conclusions

Our findings show that the masticatory apparatus within *M. fascicularis* demonstrates architectural and biomechanical adaptations during development towards maximizing gape potential, through the positive scaling of fiber lengths relative to both jaw length and condyle-molar length, and the positive scaling of jaw length relative to basicranial length. As a result, older and larger individuals possess a masticatory complex that would better enable the consumption of larger food items and allow the generation of wider jaw gapes at the anterior dentition. These findings support observational data reporting that older *M. fascicularis* feed more extensively on such food items (van Schaik and Noordwijk, 1986), while both adult males and females utilize wide-gape jaw postures more frequently within a social context than juvenile conspecifics (Deputte, 1994).

However, not all developmental changes observed within the masticatory apparatus impart a positive effect upon gape potential. During ontogeny, lever arm lengths scale isometrically relative to jaw length and tend towards positive allometry relative to condyle-molar length, such that biomechanical efficiency (in terms of maximizing force transmission) remains constant at the incisors during life and actually increases for the molar tooth, at the cost of potential gape. As PCSA also scales with positive allometry relative to both jaw length and condyle-molar length, this could reflect the need for adults to retain high bite forces at the posterior dentition for feeding (and potentially at the anterior dentition for defensive or aggressive purposes), which would preclude them from wholly optimizing the masticatory system towards gape maximization.

These data suggest that both dietary and social pressures may strongly influence developmental changes to the masticatory apparatus of *M. fascicularis*. Given the diversity of social and dietary niches found within the primate order, we suggest that the quantification of architectural changes within other primate taxa during development is necessary to better contextualize the data reported here. Further, analysing ontogenetic changes within other elements of the masticatory apparatus, such as muscle fiber type composition and changes in dental morphology, may improve our understanding of how growth and development impacts upon overall masticatory performance within primates.

Acknowledgements

We would like to thank two anonymous reviewers and the Associate Editor for their insightful comments during the review process. We are also grateful to a number of individuals for their help during the course of this study: Paul O'Higgins (Centre for Anatomical and Human Sciences, Hull York Medical School) and Fred Spoor (University College London) for making the collection available to use; Claire Terhune (University of Arkansas), for data used in the calculation of our fiber length correction factor; Martin Walters and Silke Brauer for easing access to and transportation of specimens; and Federico Becerra, for his input during discussions relating to the project. Financial support was provided by the Max Planck Society.

Literature Cited

Altmann S. 1967. The structure of primate social communication. In: Altmann S, editor. Social communication among primates. Chicago: University of Chicago Press. p 3325-3362.

Anapol F, and Barry K. 1996. Fiber architecture of the extensors of the hindlimb in semiterrestrial and arboreal guenons. Am J Phys Anthropol 99(3):429-447.

Anapol F, and Herring SW. 2000. Ontogeny of histochemical fiber types and muscle function in the masseter muscle of miniature swine. Am J Phys Anthropol 112(4):595-613.

Bang M-L, Li X, Littlefield R, Bremner S, Thor A, Knowlton KU, Lieber RL, and Chen J. 2006. Nebulin-deficient mice exhibit shorter thin filament lengths and reduced contractile function in skeletal muscle. The Journal of Cell Biology 173(6):905-916.

Bodine SC, Roy R, Meadows D, Zernicke R, Sacks R, Fournier M, and Edgerton V. 1982. Architectural, histochemical, and contractile characteristics of a unique biarticular muscle: the cat semitendinosus. Journal of Neurophysiology 48(1):192-201.

Bolter DR, and Zihlman AL. 2003. Morphometric analysis of growth and development in wild-collected vervet monkeys (Cercopithecus aethiops), with implications for growth patterns in Old World monkeys, apes and humans. Journal of Zoology 260(1):99-110.

Cachel S. 1984. Growth and allometry in primate masticatory muscles. Arch Oral Biol 29(4):287-293.

Cochard LR. 1985. Ontogenetic allometry of the skull and dentition of the rhesus monkey (Macaca mulatta). In: Jungers WL, editor. Size and scaling in primate biology. New York: Plenum Press. p 231-255.

Collard M, and O'Higgins P. 2001. Ontogeny and homoplasy in the papionin monkey face. Evolution & Development 3(5):322-331.

Corlett R, and Lucas P. 1990. Alternative seed-handling strategies in primates: seed-spitting by long-tailed macaques (Macaca fascicularis). Oecologia 82(2):166-171.

Corner BD, and Richtsmeier JT. 1991. Morphometric analysis of craniofacial growth in Cebus apella. Am J Phys Anthropol 84(3):323-342.

Daegling DJ, McGraw WS, Ungar PS, Pampush JD, Vick AE, and Bitty EA. 2011. Hard-object feeding in sooty mangabeys (Cercocebus atys) and interpretation of early hominin feeding ecology. PLoS One 6(8):e23095.

Dechow PC, and Carlson DS. 1990. Occlusal force and craniofacial biomechanics during growth in rhesus monkeys. Am J Phys Anthropol 83(2):219-237.

Deputte BL. 1994. Ethological study of yawning in primates. I. Quantitative analysis and study of causation in two species of Old World monkeys (Cercocebus albigena and Macaca fascicularis). Ethology 98(3-4):221-245.

Evans A, and Sanson G. 1998. The effect of tooth shape on the breakdown of insects. Journal of Zoology 246(4):391-400.

Fa JE. 1989. The genus Macaca: a review of taxonomy and evolution. Mammal Review 19(2):45-81.

Fitton LC, Dickinson E, Swan K, and Cobb S. 2015. Functional Integration During Development Within The Masticatory Apparatus. The FASEB Journal 29(1 Supplement):865.815.

Gans C. 1982. Fiber architecture and muscle function. Exercise and Sport Sciences Reviews 10(1):160-207.

Gans C, and Bock WJ. 1965. The functional significance of muscle architecture--a theoretical analysis. Ergebnisse der Anatomie und Entwicklungsgeschichte 38:115.

Gantt, DG. 1979. Patterns of dental wear and the role of the canine in Cercopithecinae. Am J Phys Anthropol 51(3):353-359.

Gokhin DS, Bang M-L, Zhang J, Chen J, and Lieber RL. 2009. Reduced thin filament length in nebulin-knockout skeletal muscle alters isometric contractile properties. American Journal of Physiology-Cell Physiology 296(5):C1123-C1132.

Greaves WS. 1983. A functional analysis of carnassial biting. Biol J Linn Soc 20: 353–363.

Greaves WS. 1985. The mammalian postorbital bar as a torsion-resisting helical strut. J Zool 207: 125–136.

Greaves WS. 2012. The Mammalian Jaw: A Mechanical Analysis. Cambridge: Cambridge University Press.

Hartman CG, and Strauss WL. 1933. The anatomy of the rhesus monkey (Macaca mulatta). Baltimore: The Williams & Wilkins Company.

Hartstone-Rose A, Perry JM, and Morrow CJ. 2012. Bite force estimation and the fiber architecture of felid masticatory muscles. Anat Rec 295(8):1336-1351.

Harvey PH, and Clutton-Brock TH. 1985. Life history variation in primates. Evolution 39(3):559-581.

Herring SW, and Herring SE. 1974. The superficial masseter and gape in mammals. The American Naturalist 108(962):561-576.

Herring SW, and Wineski LE. 1986. Development of the masseter muscle and oral behavior in the pig. Journal of Experimental Zoology Part A: Ecological Genetics and Physiology 237(2):191-207.

Herring SW, Grimm AF, and Grimm BR. 1979. Functional heterogeneity in a multipinnate muscle. Developmental Dynamics 154(4): 563-575.

Hylander WL. 1985. Mandibular function and biomechanical stress and scaling. American Zoologist 25(2):315-330.

Hylander WL. 2009. The functional significance of canine height reduction in early hominins. Am J Phys Anthropol Suppl 48:154.

Hylander WL. 2013. Functional links between canine height and jaw gape in catarrhines with special reference to early hominins. Am J Phys Anthropol 150(2):247-259.

Hylander WL, and Vinyard CJ. 2006. The evolutionary significance of canine reduction in hominins: functional links between jaw mechanics and canine size. Am J Phys Anthropol Suppl 42:107.

Korfage J, Van Wessel T, Langenbach G, Ay F, and Van Eijden T. 2006. Postnatal transitions in myosin heavy chain isoforms of the rabbit superficial masseter and digastric muscle. Journal of Anatomy 208(6):743-751.

Koyabu DB, and Endo H. 2010. Craniodental mechanics and diet in Asian colobines: morphological evidence of mature seed predation and sclerocarpy. Am J Phys Anthropol 142(1): 137-48.

Leonard WR, and Robertson ML. 1992. Nutritional Requirements and Human Evolution: A Bioenergetics Model. American Journal of Human Biology 4:179-195.

Lieber RL. 2002. Skeletal muscle structure, function, and plasticity. Philadelphia: Lippincott Williams & Wilkins.

Lieber RL, and Friden J. 2000. Functional and clinical significance of skeletal muscle architecture. Muscle & Nerve 23(11):1647-1666.

Lucas P, and Corlett R. 1991. Relationship between the diet of Macaca fascicularis and forest phenology. Folia Primatologica 57(4):201-215.

Lucas PW. 2004. Dental functional morphology: how teeth work. Cambridge: Cambridge University Press.

Maxwell LC, Carlson DS, McNamara JA, and Faulkner JA. 1979. Histochemical characteristics of the masseter and temporalis muscles of the rhesus monkey (Macaca mulatta). Anat Rec 193(3):389-401.

McGraw WS, Vick AE, and Daegling DJ. 2011. Sex and age differences in the diet and ingestive behaviors of sooty mangabeys (Cercocebus atys) in the Tai Forest, Ivory Coast. Am J Phys Anthropol 144(1):140-153.

Mitteroecker P, Gunz P, Bernhard M, Schaefer K, and Bookstein FL. 2004. Comparison of cranial ontogenetic trajectories among great apes and humans. Journal of Human Evolution 46(6):679-698.

O'Higgins P, and Jones N. 1998. Facial growth in Cercocebus torquatus: an application of three-dimensional geometric morphometric techniques to the study of morphological variation. Journal of Anatomy 193(2):251-272.

Otten E. 1988. Concepts and models of functional architecture in skeletal muscle. Exercise and Sport Sciences Reviews 16(1):89-138.

Pearson AM. 1990. Muscle growth and exercise. Critical Reviews in Food Science and Nutrition 29(3):167-196.

Perry JM, Hartstone-Rose A, and Wall CE. 2011. The jaw adductors of strepsirrhines in relation to body size, diet, and ingested food size. Anat Rec 294(4):712-728.

Perry JM, and Wall CE. 2008. Scaling of the chewing muscles in prosimians. In: Vinyard CJ, Ravosa MJ, Wall CE, editors. Primate craniofacial function and biology. New York: Springer. p 217-240.

Plavcan JM. 2001. Sexual dimorphism in primate evolution. Am J Phys Anthropol 116(S33):25-53.

Plavcan JM, and van Schaik CP. 1992. Intrasexual competition and canine dimorphism in anthropoid primates. Am J Phys Anthropol 87(4):461-477.

Plavcan JM, van Schaik CP. 1997 Interpreting hominid behavior on the basis of sexual dimorphism. J Hum Evol 32:345–374.

Plavcan JM, van Schaik CP, Kappeler PM. 1995. Competition, coalitions and canine size in primates. J Hum Evol 28:245–276.

Popowics TE, and Fortelius M. 1997. On the cutting edge: tooth blade sharpness in herbivorous and faunivorous mammals. Annales Zoologici Fennici 34:73-88.

Powell PL, Roy RR, Kanim P, Bello MA, and Edgerton VR. 1984. Predictability of skeletal muscle tension from architectural determinations in guinea pig hindlimbs. Journal of Applied Physiology 57(6):1715-1721.

Radinsky LB. 1981. Evolution of skull shape in carnivores I: Representative modern carnivores. Biol J Linn Soc 15:369–388.

Ravosa MJ. 1991. The ontogeny of cranial sexual dimorphism in two Old World monkeys: Macaca fascicularis (Cercopithecinae) and Nasalis larvatus (Colobinae). International Journal of Primatology 12(4):403.

Ravosa MJ. 1996. Jaw morphology and function in living and fossil Old World monkeys. International Journal of Primatology 17(6):909-932.

Ravosa MJ, Ning J, Costley D, Daniel A, Stock S, and Stack M. 2010. Masticatory biomechanics and masseter fiber-type plasticity. Journal of Musculoskeletal Neuronal Interactions 10(1):46-55.

Rayne J, and Crawford G. 1975. Increase in fibre numbers of the rat pterygoid muscles during postnatal growth. Journal of Anatomy 119(2):347.

Richtsmeier JT, Cheverud J, Danahey S, Corner B, and Lele S. 1993. Sexual dimorphism of ontogeny in the crab-eating macaque (Macaca fascicularis). J Hum Evol 25(1):1-30.

Ross CF. 1995. Muscular and osseous anatomy of the primate anterior temporal fossa and the functions of the postorbital septum. Am J Phys Anthropol 98(3):275-306.

Ross CF, Iriarte-Diaz J, and Nunn CL. 2012. Innovative Approaches to the Relationship Between Diet and Mandibular Morphology in Primates. International Journal of Primatology 33(3):632-660.

Santana SE, Dumont ER, and Davis JL. 2010. Mechanics of bite force production and its relationship to diet in bats. Functional Ecology 24(4):776-784.

Schumacher GH. 1961. Funktionelle morphologie der kaumuskulatur. Jena: G. Fischer.

Schwartz DJ, and Huelke DF. 1963. Morphology of the head and neck of the macaque monkey: the muscles of mastication and the mandibular division of the trigeminal nerve. Journal of Dental Research 42(5):1222-1233.

Singleton M. 2015. Functional geometric morphometric analysis of masticatory system ontogeny in papionin primates. Anat Rec 298(1):48-63.

Smith K, and Beighton D. 1986. The effects of the availability of diet on the levels of exoglycosidases in the supragingival plaque of macaque monkeys. Journal of Dental Research 65(11):1349-1352.

Smith K, and Beighton D. 1987. Proteolytic activities in the supragingival plaque of monkeys (Macaca fascicularis). Archives of Oral Biology 32(7):473-476.

Smith R. 1984. Comparative functional morphology of maximum mandibular opening (gape) in primates. In: Chivers DJ, Wood B, Bilsborough A, editors. Food acquisition and processing in primates. New York: Plenum Press. p 231-255.

Smith RJ, and Jungers WL. 1997. Body mass in comparative primatology. J Hum Evol 32(6):523-559.

Sokal R, and Rohlf F. 1995. Biometry. New York: WH Freeman.

Soltis J. 2004. Mating Systems. In: Thierry B, Singh M, and Kaumanns W, editors. Macaque societies: a model for the study of social organization. Cambridge: Cambridge University Press. p 135-155.

Son VD. 2003. Diet of Macaca fascicularis in a mangrove forest, Vietnam. Laboratory Primate Newsletter 42(4):1-5.

Spencer MA. 1999. Constraints on masticatory system evolution in anthropoid primates. Am J Phys Anthropol 108(4):483-506.

Stewart S, and German R. 1999. Sexual dimorphism and ontogenetic allometry of soft tissues in Rattus norvegicus. Journal of Morphology 242(1):57-66.

Taylor AB, Eng CM, Anapol FC, and Vinyard CJ. 2009. The functional correlates of jaw-muscle fiber architecture in tree-gouging and nongouging callitrichid monkeys. Am J Phys Anthropol 139(3):353-367.

Taylor AB, Terhune C.E., Hylander, W.L., Vinyard, C.J. 2014. In vitro sarcomere-length operating range of the masseter and temporalis muscles in Macaca fascicularis. Am J Phys Anthropol 153(S58):252.

Taylor AB, Terhune CE, Toler M, Holmes M, Ross CF, and Vinyard CJ. 2018. Jaw-Muscle Fiber Architecture and Leverage in the Hard-Object Feeding Sooty Mangabey are not Structured to Facilitate Relatively Large Bite Forces Compared to Other Papionins. Anat Rec 301(2):325-342.

Taylor AB, and Vinyard CJ. 2004. Comparative analysis of masseter fiber architecture in tree-gouging (Callithrix jacchus) and nongouging (Saguinus oedipus) callitrichids. J Morphol 261(3):276-285.

Taylor AB, and Vinyard CJ. 2009. Jaw-muscle fiber architecture in tufted capuchins favors generating relatively large muscle forces without compromising jaw gape. J Hum Evol 57(6):710-720.

Taylor AB, and Vinyard CJ. 2013. The relationships among jaw-muscle fiber architecture, jaw morphology, and feeding behavior in extant apes and modern humans. Am J Phys Anthropol 151(1):120-134.

Taylor AB, Yuan T, Ross CF, and Vinyard CJ. 2013. The scaling of jaw-muscle fiber architecture in anthropoid primates. Am J Phys Anthropol 150 Suppl 56: 269.

Taylor AB, Yuan T, Ross CF, and Vinyard CJ. 2015. Jaw-muscle force and excursion scale with negative allometry in platyrrhine primates. Am J Phys Anthropol 158(2):242-256.

Terhune CE, Hylander WL, Vinyard CJ, and Taylor AB. 2015. Jaw-muscle architecture and mandibular morphology influence relative maximum jaw gapes in the sexually dimorphic Macaca fascicularis. J Hum Evol 82:145-158.

Thierry, B. 2000. Covariation of conflict management patterns across macaque species. In: Aureli F, de Waal FBM (Eds.), Natural Conflict Resolution . Berkeley: University of California Press.

Thierry B. 2004. Social Epigenesis. In: Thierry B, Singh M, and Kaumanns W, editors. Macaque societies: a model for the study of social organization. Cambridge: Cambridge University Press. p 267-295.

Thierry B, Iwaniuk AN, and Pellis SM. 2000. The influence of phylogeny on the social behaviour of macaques (Primates: Cercopithecidae, genus Macaca). Ethology 106(8):713-728.

Troisi A, Aureli F, Schino G, Rinaldi F, and Angelis N. 1990. The influence of age, sex, and rank on yawning behavior in two species of macaques (Macaca fascicularis and M. fuscata). Ethology 86(4):303-310.

Turnbull WD. 1970. Mammalian masticatory apparatus. Fieldiana Geol 18:149-356.

van Eijden T, Korfage J, and Brugman P. 1997. Architecture of the human jaw-closing and jaw-opening muscles. Anat Rec 248(3):464-474.

van Minh N, Mouri T, Hamada Y. 2015. Aging-related changes in the skulls of Japanese macaques (Macaca fuscata). Anthropological Science 123(2): 107-119.

van Schaik CP, and van Noordwijk M, A. 1986. The hidden costs of sociality: intra-group variation in feeding strategies in Sumatran long-tailed macaques (Macaca fascicularis). Behaviour 99(3):296-314.

Vinyard CJ, Wall CE, Williams SH, and Hylander WL. 2003. Comparative functional analysis of skull morphology of tree-gouging primates. Am J Phys Anthropol 120(2):153-170.

Wainwright PC, Alfaro ME, Bolnick DI, and Hulsey CD. 2005. Many-to-one mapping of form to function: a general principle in organismal design? Integrative and Comparative Biology 45(2):256-262.

Wall CE, Briggs MM, Huq E, Hylander WL, and Schachat F. 2013. Regional variation in IIM myosin heavy chain expression in the temporalis muscle of female and male baboons (Papio anubis). Arch Oral Biol 58(4):435-443.

Ward SR, and Lieber RL. 2005. Density and hydration of fresh and fixed human skeletal muscle. J Biomech 38(11):2317-2320.

Weijs W, Brugman P, and Klok E. 1987. The growth of the skull and jaw muscles and its functional consequences in the New Zealand rabbit (Oryctolagus cuniculus). Journal of Morphology 194(2):143-161.

Wheatley B. 1980. Feeding and ranging of East Bornean Macaca fascicularis. In: Lindburg D, editor. The macaques: studies in ecology, behavior, and evolution. New York: Van Nostrand Reinhold. p 215-246.

Williams SH, Peiffer E, and Ford S. 2009. Gape and bite force in the rodents Onychomys leucogaster and Peromyscus maniculatus: does jaw-muscle anatomy predict performance? J Morphol 270(11):1338-1347.

Yeager CP. 1996. Feeding ecology of the long-tailed macaque (Macaca fascicularis) in Kalimantan Tengah, Indonesia. International Journal of Primatology 17(1):51-62.

Zielinski DE. 1965. A study of the normal anatomy of the masticatory apparatus of Macaca mulatta. Chicago: Loyola University Chicago (Masters Thesis).

Tables and Figures

Table 1. List of landmarks used in the determination of muscle lever-arm lengths, jaw length, condyle-molar length, basicranial length and TMJ height.

Landmark Name	Definition
Incisor	Centre of occlusal surface of the right mandibular first incisor
Molar	Centre of occlusal surface of the most posteriorly-positioned molar tooth within the dental row
Right condyle	Centre of superior (articulating) surface of the right mandibular condyle
Left condyle	Centre of superior (articulating) surface of the left mandibular condyle
Inion	Superior point of the external occipital protuberance
Basion	Midline point of the anterior margin of the foramen magnum
Temporalis origin	Superior margin of the temporalis muscle at the antero-posterior center of the muscle
Temporalis insertion	Anterior surface of the coronoid process at the lowest level of the mandibular notch
Superficial masseter origin	Anterior ⅔ point on the inferior surface of the zygomatic arch
Superficial masseter insertion	Centre of the masseteric scar denoting the muscle's insertion adjacent to the mandibular angle
Deep masseter origin	Posterior ¼ point on the inferior surface of the zygomatic arch
Deep masseter insertion	Lateral surface of the ascending ramus, at the inferior border of the related bony depression.

Table 2. Reduced major axis regression statistics for the variables of fiber length (FL), muscle mass, and PCSA within the jaw-adductor musculature against jaw length and condyle-molar length. Muscle mass and PCSA are adjusted to mass$^{1/3}$ and PCSA$^{1/2}$ respectively, such that a slope of 1.0 is equal to isometry.

Variable	Slope	Y-intercept	95% CI for slope	Standard Error	R^2	p
Versus jaw length						
Superficial masseter FL	1.597	-1.892	1.377-1.836	0.127	0.847	<0.01
Deep masseter FL	1.203	-1.333	0.932-1.480	0.152	0.616	<0.01
Temporalis FL	2.364	-3.210	1.953-2.823	0.202	0.825	<0.01
Superficial masseter mass	1.457	-2.602	1.186-1.695	0.122	0.831	<0.01
Deep masseter mass	1.407	-2.673	1.169-1.587	0.115	0.838	<0.01
Temporalis mass	1.674	-2.819	1.350-2.032	0.147	0.816	<0.01
Superficial masseter PCSA	1.503	-2.682	1.107-1.785	0.172	0.686	<0.01
Deep masseter PCSA	1.609	-3.038	1.225-1.855	0.151	0.789	<0.01
Temporalis PCSA	1.404	-2.277	1.062-1.738	0.157	0.701	<0.01
Versus condyle-molar length						
Superficial masseter FL	2.286	-2.373	1.680-2.784	0.356	0.419	<0.01
Deep masseter FL	1.722	-1.695	1.013-2.298	0.296	0.290	<0.01
Temporalis FL	3.385	-3.922	2.321-4.172	0.500	0.475	<0.01
Superficial masseter mass	2.086	-3.041	1.337-2.556	0.314	0.456	<0.01
Deep masseter mass	2.014	-3.096	1.251-2.436	0.312	0.422	<0.01
Temporalis mass	2.397	-3.323	1.588-2.996	0.363	0.448	<0.01
Superficial masseter PCSA	2.152	-3.134	1.286-2.719	0.341	0.399	<0.01
Deep masseter PCSA	2.303	-3.523	1.401-2.817	0.363	0.403	<0.01
Temporalis PCSA	2.100	-2.700	1.281-2.626	0.327	0.366	<0.01

Table 3. Reduced major axis regression statistics for biomechanical variables against jaw length, condyle-molar length, and basicranial length.

Variable	Slope	Y-intercept	95% CI for slope	Standard Error	R^2	p
Versus jaw length						
TMJ Height	2.058	-2.653	1.505-2.660	0.215	0.738	<0.01
Superficial Masseter Lever Arm	0.910	-0.364	0.780-1.084	0.074	0.842	<0.01
Deep Masseter Lever Arm	0.961	-0.660	0.809-1.108	0.083	0.823	<0.01
Temporalis Lever Arm	1.114	-0.809	0.974-1.271	0.066	0.915	<0.01
Versus condyle-molar length						
TMJ Height	2.947	-3.273	1.599-4.303	0.514	0.270	<0.01
Superficial Masseter Lever Arm	1.303	-0.638	0.834-1.710	0.206	0.400	<0.01
Deep Masseter Lever Arm	1.375	-0.949	0.982-1.706	0.231	0.320	<0.01
Temporalis Lever Arm	1.595	-1.145	1.141-1.928	0.251	0.403	<0.01
Versus Basicranial length						
Jaw length	1.259	-0.258	0.936-1.572	0.207	0.353	<0.01
Condyle-molar length	0.880	0.030	0.627-1.111	0.138	0.413	<0.01
Superficial Masseter Lever Arm	1.146	-0.599	0.863-1.489	0.173	0.455	<0.01
Deep Masseter Lever Arm	1.210	-0.908	0.873-1.526	0.197	0.363	<0.01
Temporalis Lever Arm	1.403	-1.097	0.956-1.775	0.237	0.317	<0.01

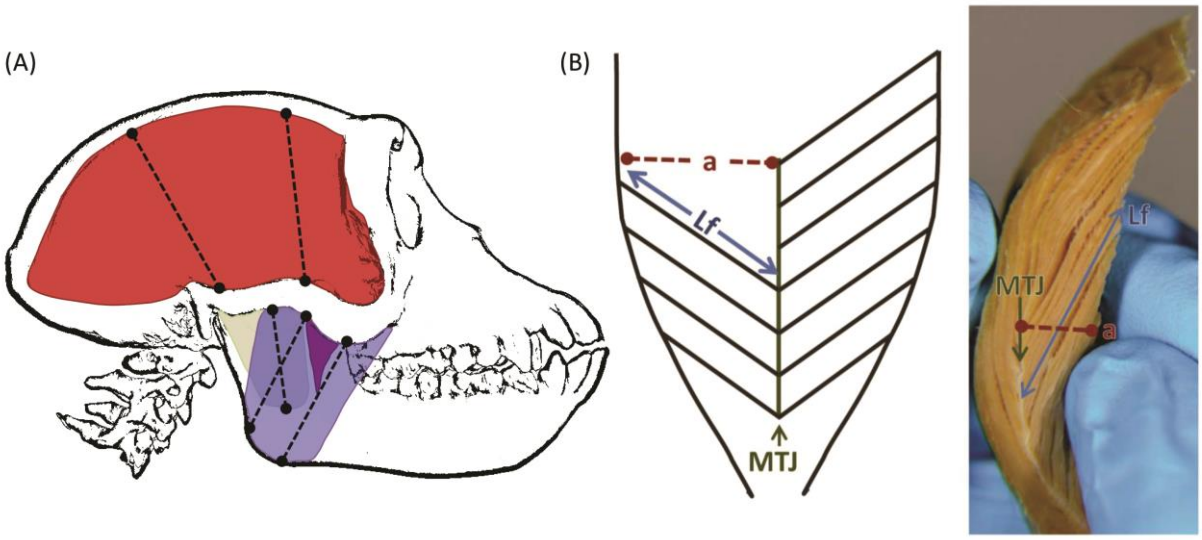

Figure 1. Technique used for determining architectural parameters. (A) Schematic illustration highlighting the configuration of the temporalis (red), superficial masseter (blue) and deep masseter (gray) within M. fascicularis. (B) Schematic and magnified cross-section through a muscle sample (temporalis) illustrating the internal configuration of fibers from which variables were collected. Lf= fiber length, MTJ= myotendinous junction, a= perpendicular distance from the myotendinous junction to the muscle's border.

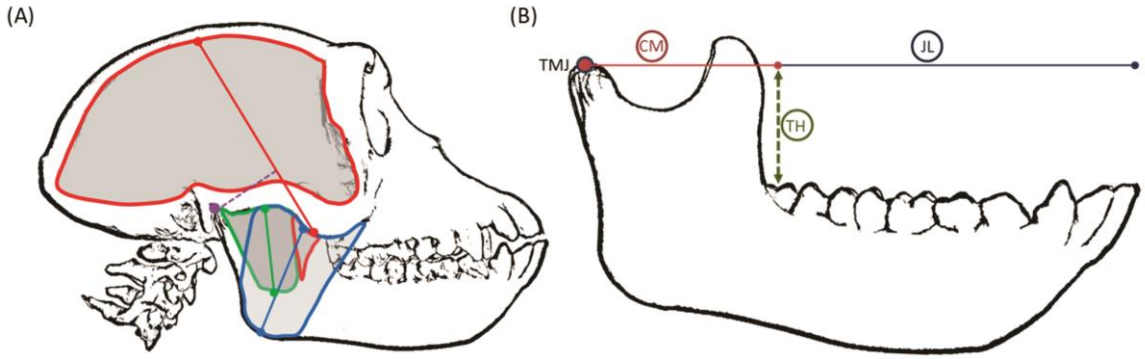

Figure 2. Schematic illustration of the measurements used to determine biomechanical variables. (A) Measurements used to determine lever arm lengths within the jaw adductor musculature. Each muscle's principal line of action (solid colored line) was denoted by a vector (temporalis in red, superficial masseter in blue, deep masseter in green). Lever arm lengths were calculated as the perpendicular distance (dashed line, example shown for the temporalis in purple) from each muscle-action vector to the temporomandibular joint. (B) easurements used to determine jaw length, condyle-molar length, and condyle height. Jaw length (JL) was measured as a horizontal vector from the center of the right mandibular condyle (TMJ) to a plane projected vertically (at a perpendicular angle to the occlusal plane) from the right I1 . Condyle-molar length (CM) was measured as a horizontal vector from the center of the right mandibular condyle to a plane projected vertically from the most posterior molar tooth within the dental row. TMJ Height (TH) represents the vertical distance from the center of the most posterior occluding molar tooth to the horizontal vector representing jaw length.

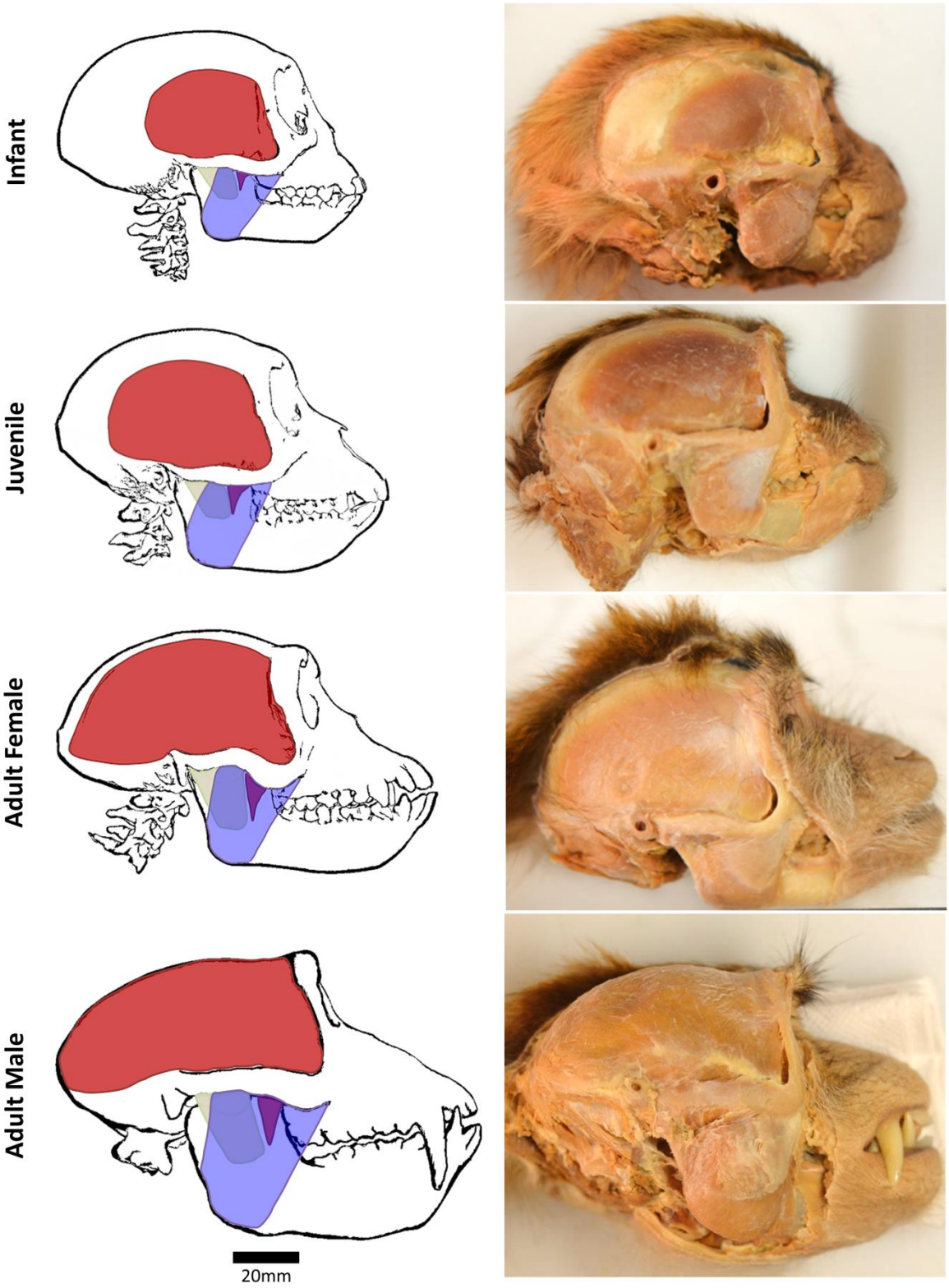

Figure 3. Schematic representation and photograph showing changes in muscle size and configuration between successive age and sex classifications. Temporalis is presented in red, superficial masseter in blue and deep masseter in gray. Scale bar represents 20mm.

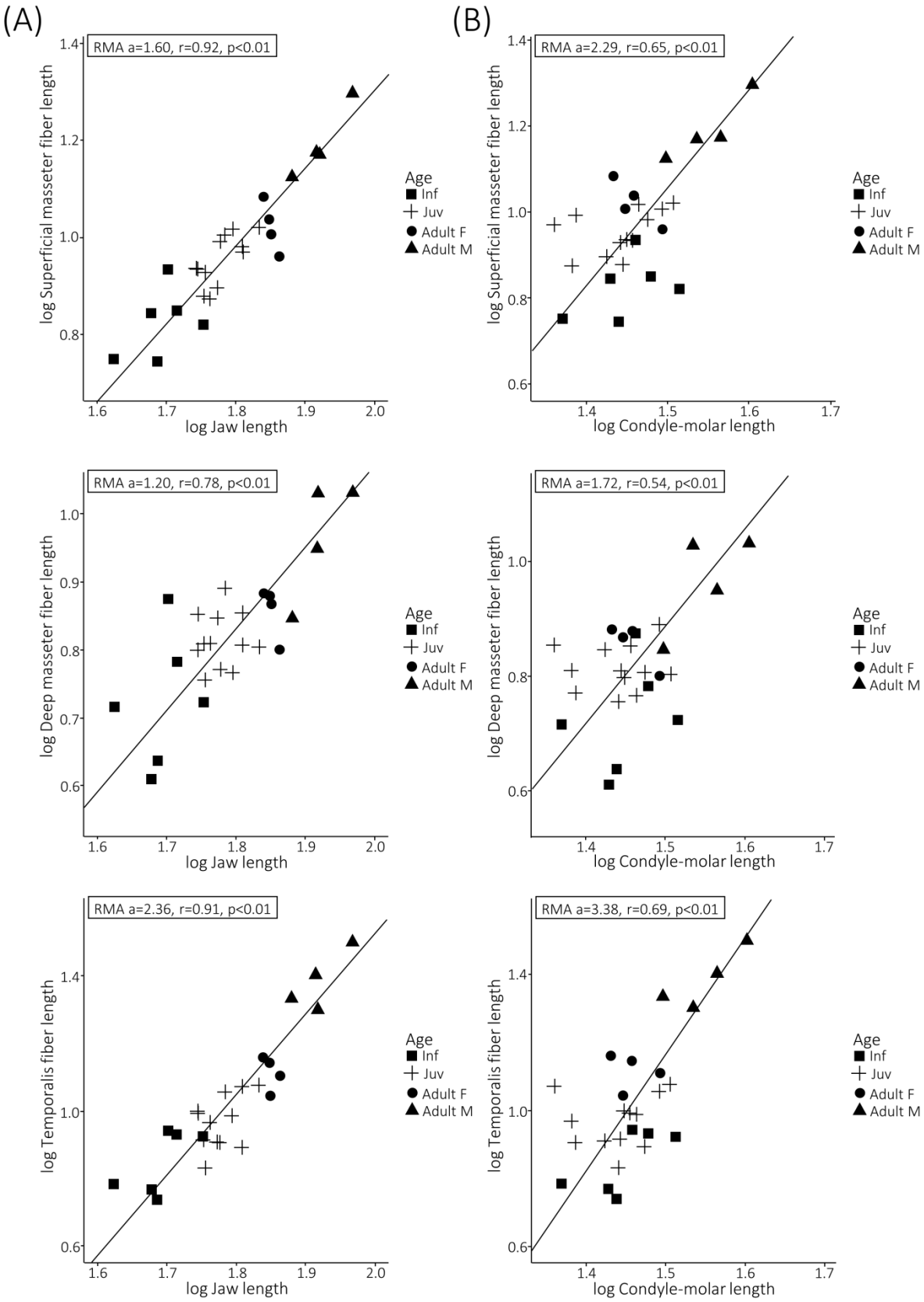

Figure 4. Bivariate plot of fiber lengths within the adductor musculature against (A) jaw length and (B) condyle-molar length. Both variables log-transformed.

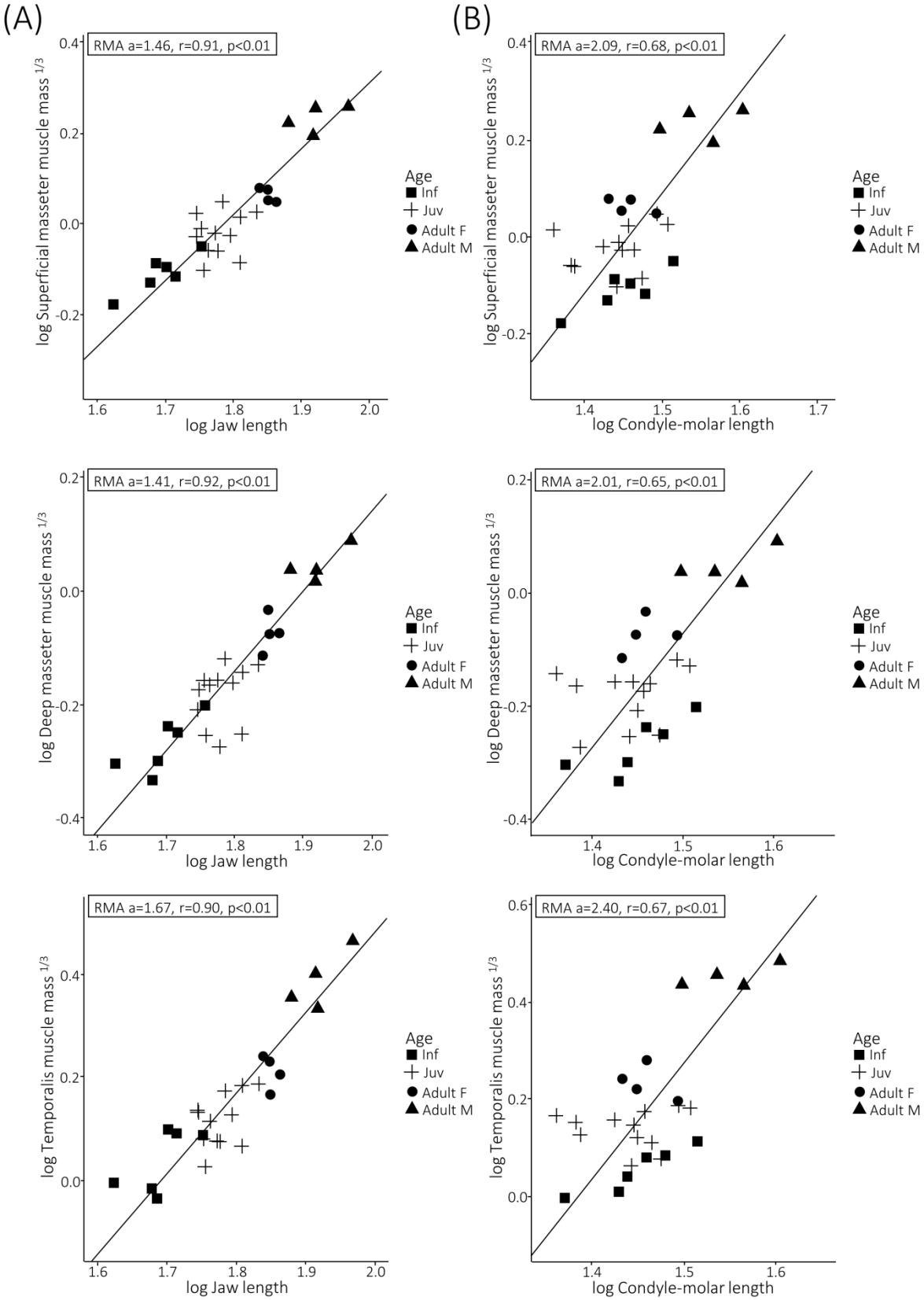

Figure 5. Bivariate plot of muscle mass within the adductor musculature against (A) jaw length and (B) condyle-molar length. Both variables log-transformed.

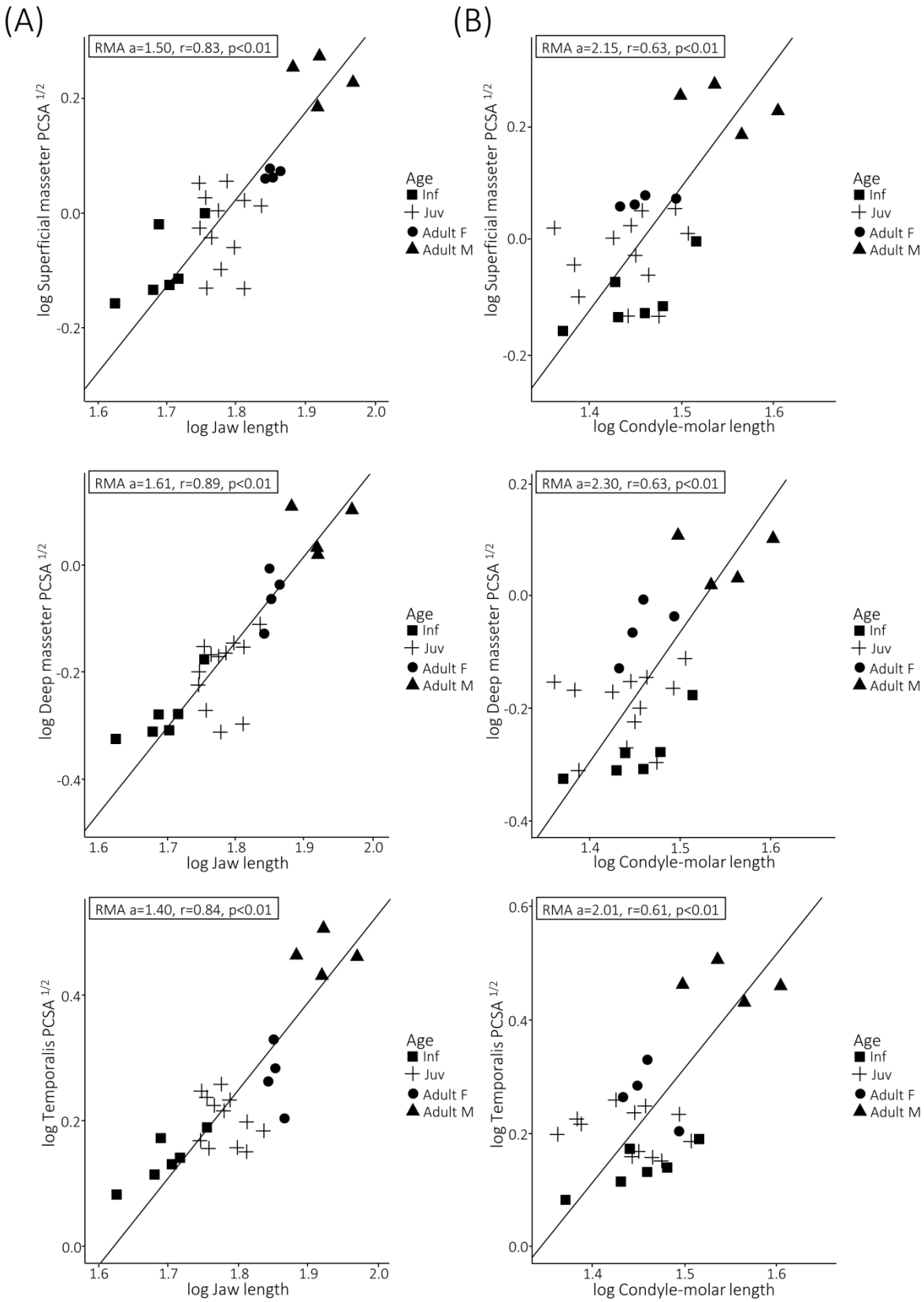

Figure 6. Bivariate plot of PCSA within the adductor musculature against (A) jaw length and (B) condyle-molar length. Both variables log-transformed.

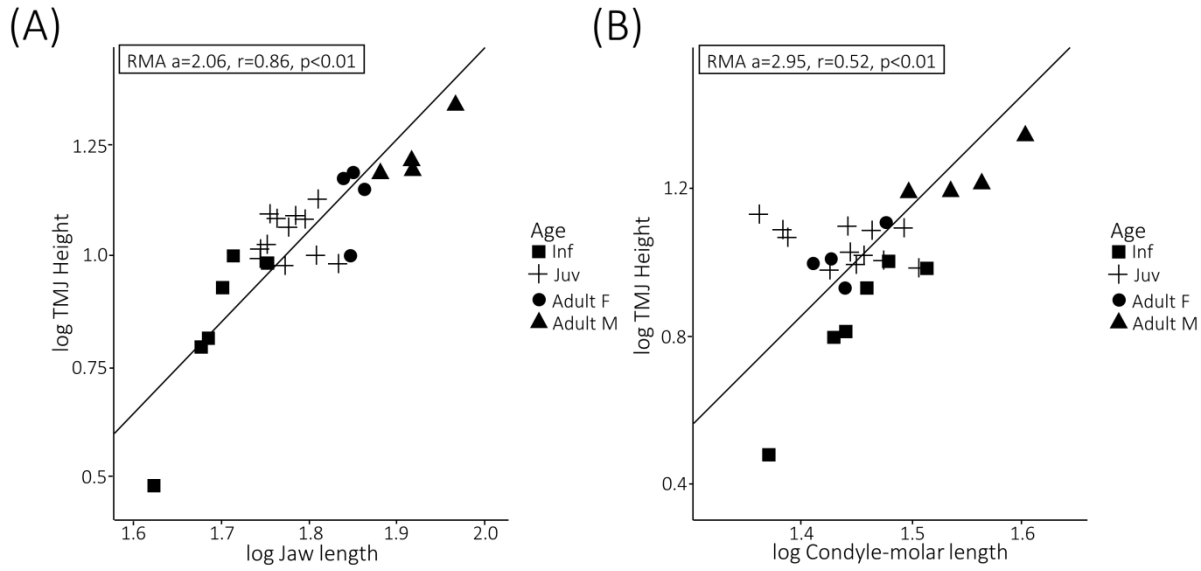

Figure 7. Bivariate plot of TMJ height against (A) jaw length and (B) condyle-molar length. Both variables log-transformed.

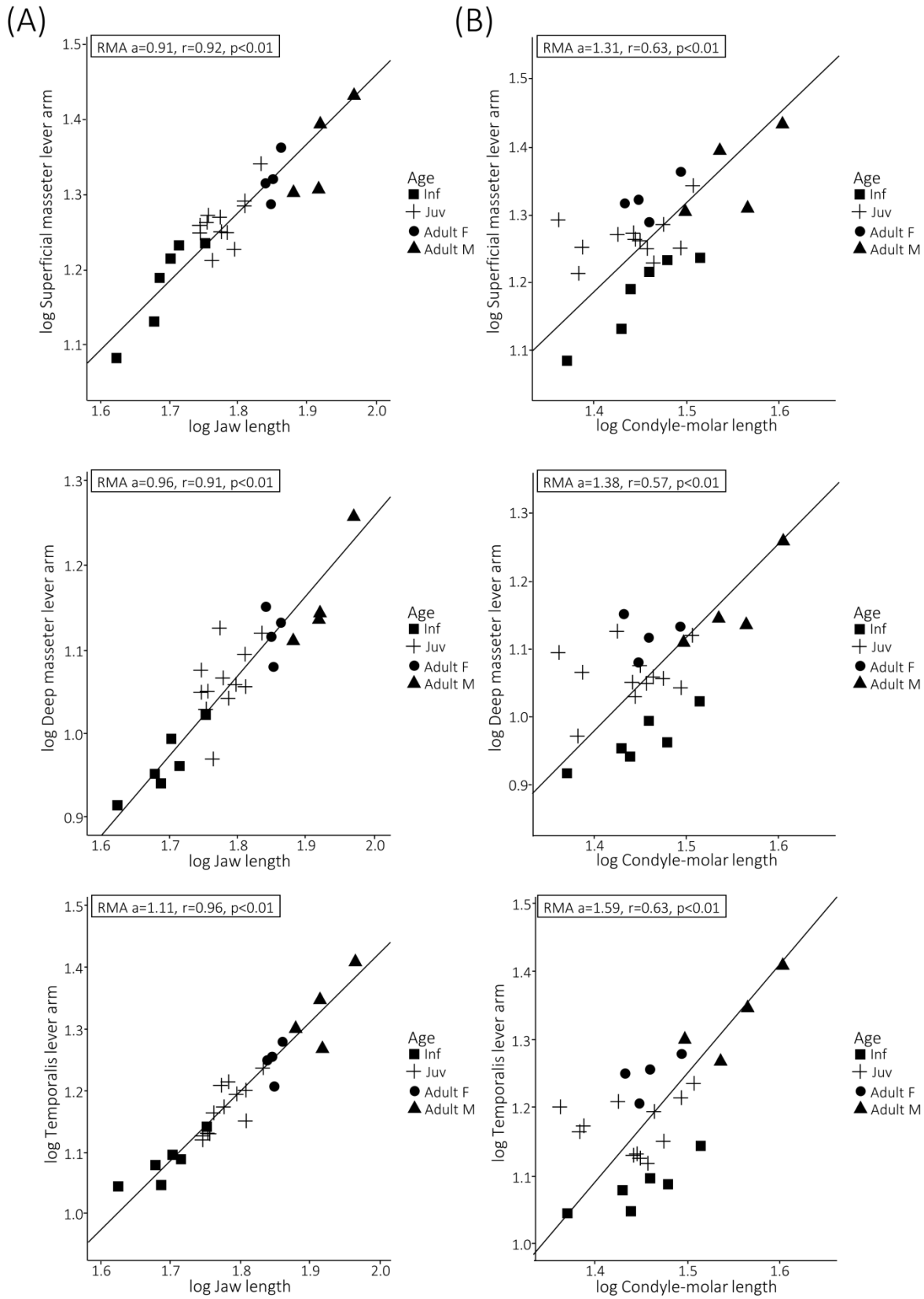

Figure 8. Bivariate plot of lever arm lengths for the adductor musculature against (A) jaw length and (B) condyle-molar length. Both variables log-transformed.

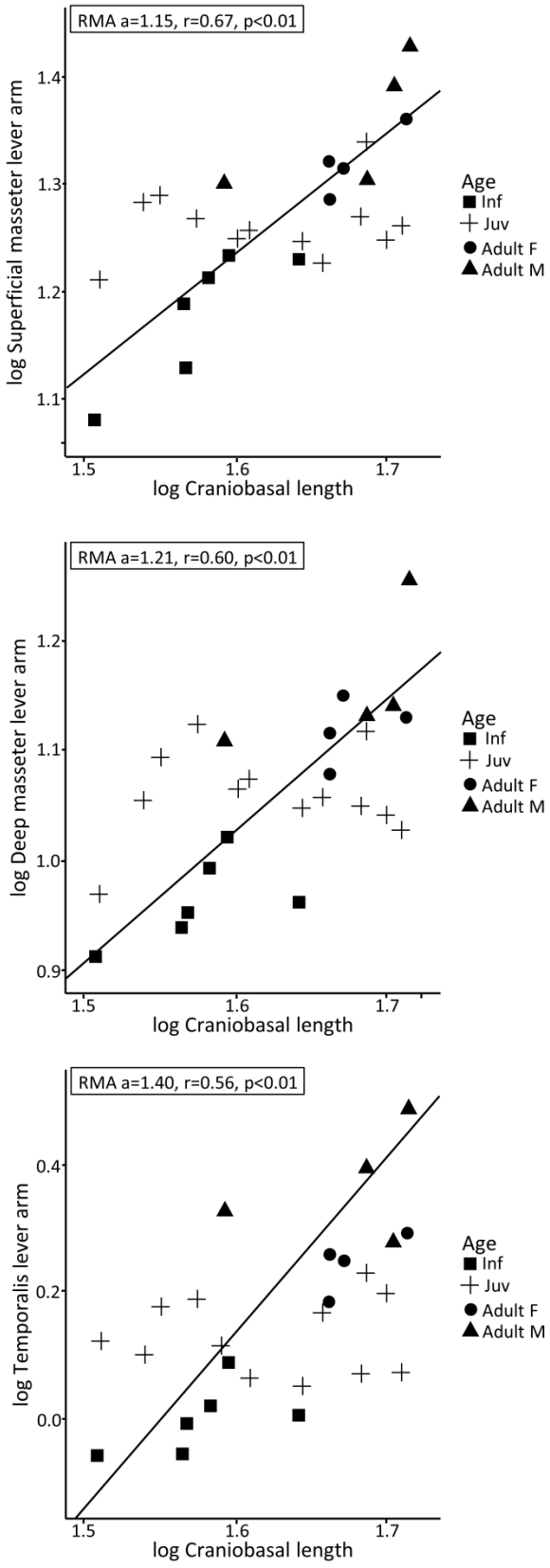

Figure 9. Bivariate plot of lever arm lengths for the adductor musculature against basicranial length.

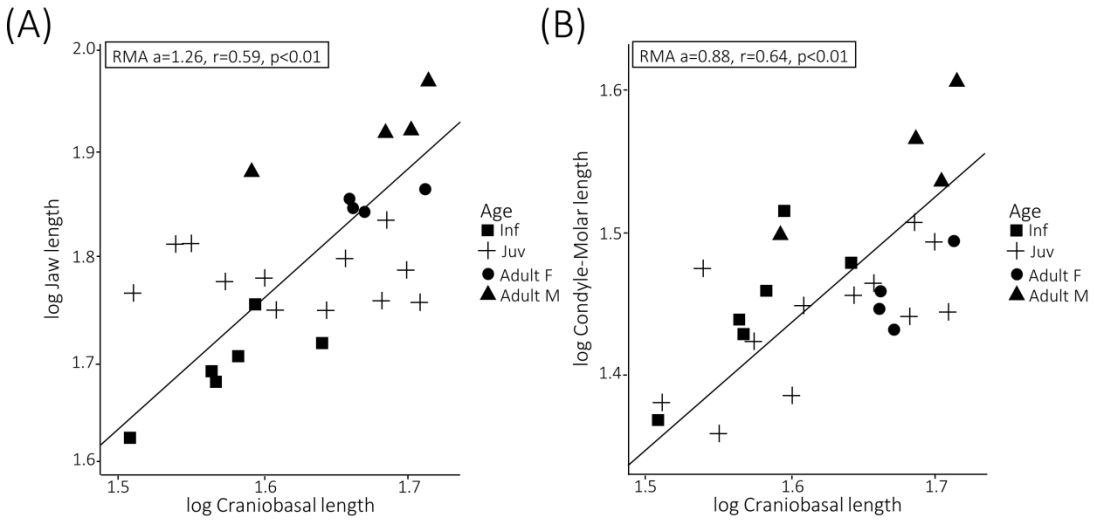

Figure 10. Bivariate plot of (A) jaw length and (B) condyle-molar length against basicranial length. Both variables log-transformed.

3. Non-destructive determination of muscle architectural variables through the use of DiceCT

Edwin Dickinson, Heiko Stark and Kornelius F. Kupczik

Published in *The Anatomical Record* 301: 363-377.

Abstract

The fascicular architecture of skeletal muscle dictates functional parameters such as force production and contractile velocity. Muscle microarchitecture is typically determined by means of manual dissection, a technique that is inherently destructive to specimens. Furthermore, fascicle lengths and pennation angles are commonly assessed at only a limited number of sampling sites per muscle. We present the results of a digital technique to non-destructively assess muscle architectural variables for three jaw-adductor muscles within a specimen of the cercopithecine primate *Macaca fascicularis* (crab-eating macaque). The specimen is first subjected to a contrast-enhanced staining protocol to increase the density of internal soft tissues. High-resolution mCT scans are then collected and segmented to isolate individual muscles. A textural orientation algorithm is then applied to each muscle volume to reconstruct constituent muscle fascicles in three dimensions. Using this technique, we report muscle volume, fascicle length, angle of pennation, and physiological cross-sectional area (PCSA) for each muscle. These data are compared to results collected using traditional dissection of the contralateral muscles.

Reconstructions of muscle volume and pennation angle closely correspond to the dissection results. The degree of similarity between measurements of fascicle length and PCSA varies between muscles, with temporalis demonstrating the greatest disparity between techniques; likely reflecting the complex geometry and fascicular arrangement of this muscle. The described technique samples a much larger number of fascicles than had previously been possible and non-destructively investigates the internal architecture of preserved specimens. We conclude that this approach demonstrates great potential for quantifying muscle internal architecture.

Non-Destructive Determination of Muscle Architectural Variables Through the Use of DiceCT

EDWIN DICKINSON,[1]* **HEIKO STARK**,[2] **AND KORNELIUS KUPCZIK**[1]
[1]Max Planck Weizmann Center for Integrative Archaeology and Anthropology, Max Planck Institute for Evolutionary Anthropology, Leipzig, Germany
[2]Institute of Systematic Zoology and Evolutionary Biology with Phyletic Museum, Friedrich-Schiller-University Jena, Jena, Germany

ABSTRACT

The fascicular architecture of skeletal muscle dictates functional parameters such as force production and contractile velocity. Muscle microarchitecture is typically determined by means of manual dissection, a technique that is inherently destructive to specimens. Furthermore, fascicle lengths and pennation angles are commonly assessed at only a limited number of sampling sites per muscle. We present the results of a digital technique to non-destructively assess muscle architectural variables for three jaw-adductor muscles within a specimen of the cercopithecine primate *Macaca fascicularis (crab-eating macaque)*. The specimen is first subjected to a contrast-enhanced staining protocol to increase the density of internal soft tissues. High-resolution μCT scans are then collected and segmented to isolate individual muscles. A textural orientation algorithm is then applied to each muscle volume to reconstruct constituent muscle fascicles in three dimensions. Using this technique, we report muscle volume, fascicle length, angle of pennation, and physiological cross-sectional area (PCSA) for each muscle. These data are compared to results collected using traditional dissection of the contralateral muscles. Reconstructions of muscle volume and pennation angle closely correspond to the dissection results. The degree of similarity between measurements of fascicle length and PCSA varies between muscles, with temporalis demonstrating the greatest disparity between techniques; likely reflecting the complex geometry and fascicular arrangement of this muscle. The described technique samples a much larger number of fascicles than had previously been possible and non-destructively investigates the internal architecture of preserved specimens. We conclude that this approach demonstrates great potential for quantifying muscle internal architecture. Anat Rec, 301:363–377, 2018. © 2018 Wiley Periodicals, Inc.

Key words: muscle fascicle architecture; PCSA; DiceCT; pennation angle; muscles of mastication

Over more than a century, there have been a plethora of studies investigating the structure of skeletal muscle and the functional correlates of fascicular arrangement (e.g., Weber, 1846; Morris, 1948; Gans & Bock, 1965; Gordon et al., 1966a, 1966b; Gans, 1982; Powell et al., 1984; Lieber & Friden, 2000; Lieber & Ward, 2011). Extensive research has also been made into quantifying inter- and intra- specific variation in muscle architectural

*Correspondence to: Edwin Dickinson, Max Planck Institute for Evolutionary Anthropology, Deutscher Platz 6, Leipzig 04103, Saxony, Germany., Telephone: +49 (0)341 3550 875. Fax: +49 (0)341 3550 119 Email: edwin_dickinson@eva.mpg.de

Received 23 June 2017; Accepted 18 September 2017.

DOI 10.1002/ar.23716
Published online in Wiley Online Library (wileyonlinelibrary.com).

properties within a wide variety of mammalian and non-mammalian taxa (e.g., Sacks & Roy, 1982; Roy et al., 1984a,b; Anapol & Jungers, 1986; Lieber & Blevins, 1989; Friederich & Brand, 1990; Lieber et al., 1992; Anapol & Barry, 1996; Murray et al., 2000; Kawakami et al., 2001; Payne et al., 2006; Oishi et al., 2008; Michilsens et al., 2009; Organ et al., 2009; Kikuchi, 2010; Hartstone-Rose et al., 2012; Furuuchi et al., 2013; Mathewson et al., 2014; Perry et al., 2014; Terhune et al., 2015; Ito & Endo, 2016; Ogihara et al., 2017). By quantifying and comparing muscle architecture, such studies have investigated the scaling relationship between muscle architecture and body mass (Antón, 1999, 2000; Anapol et al., 2008; Eng et al., 2008; Perry & Wall, 2008; Perry et al., 2011; Taylor & Vinyard, 2013; Taylor et al., 2015), as well as changes in muscle architecture over the course of ontogeny (Herring & Wineski, 1986; Weijs et al., 1987; Allen et al., 2010; Pfaller et al., 2011; Lamas et al., 2014). One common thread shared by these diverse studies, however, is that all have quantified these architectural characteristics by deploying a similar methodology: gross dissection.

Though capable of quantifying a number of architectural parameters, such a technique is inherently destructive to a specimen and therefore irreversible. Many dissection-based studies also rely upon sampling only a small number of fascicles (also known as muscle fiber bundles) within a given muscle, yet architectural profiles determined from only a small subset of fascicles may not represent the entire muscle as a whole.

Structure-Function Relationships within Muscle

Understanding muscle architecture is critical to interpretations of anatomical adaptations, as muscle architectural parameters directly relate to a muscle's functional capabilities. The two variables considered to be the most critical architectural determinants of function (see Lieber & Friden, 2000; Taylor et al., 2009) are the length of fascicles within a muscle, and the muscle's physiologic cross-sectional area (PCSA)—a multivariable product of muscle mass and density, fiber length, and fiber orientation. As muscle fibers consist of serially arranged sarcomeres, total fiber lengths are proportional to the muscle's contractile velocity (Bodine et al., 1982). Fiber length is also linked to muscle excursion, and therefore limits the range of postures at which forces can be produced (Bang et al., 2006; Gokhin et al., 2009). Meanwhile, PCSA is proportionally related to the maximal contractile force a muscle may generate (Powell et al., 1984). An increase in PCSA therefore signifies a higher intrinsic force-generating capability for a given muscle. For a given volume of muscle, an increase in fiber length will increase both contractile velocity and muscle stretch but subtract from PCSA and therefore potential force; while decreasing fiber length will limit the former factors but increase force-production capabilities (Lieber, 1986). The architectural structure of a specific muscle is therefore not only closely related to its functional role, but reflective of its place along a spectrum of optimization between these two dichotomized functional variables.

Digital Approaches to Modelling Muscle Architecture

In the past decade, new imaging modalities have been introduced as a means of quantifying muscle architectural structure. Diffusion tensor magnetic resonance imaging (DTI) has been successfully applied to visualize muscle volumes and approximate muscle fascicle orientations in the hindlimb musculature of humans, rabbits, rats, and mice (Damon et al., 2002; Heemskerk et al., 2005; Sinha et al., 2006; McMillan et al., 2011; Schenk et al., 2013). This method works by tracking the diffusion of water molecules through tissues and, in addition to its application to skeletal muscle, has also been used to visualize other structures in the heart (Reese et al., 1995), tongue (Napadow et al., 2001), and brain (Gössl et al., 2002; Klose et al., 2005). However, the clarity of contrast between tissues and overall resolution of imaged biological structures is relatively poor compared to other imaging modalities.

More recently still, a growing number of studies have deployed diffusible iodine-based contrast-enhanced computed tomography (diceCT) and associated contrast-enhanced staining protocols as a means of visualizing muscle portions *in situ* (e.g., Jeffery et al., 2011; Tsai & Holliday, 2011; Cox & Jeffery, 2011; Cox et al., 2012; Hautier et al., 2012; Holliday et al., 2013; Baverstock et al., 2013; Gignac & Kley, 2014; Cox & Faulkes, 2014; Gignac et al., 2016). Methodologically, contrast-enhanced μCT—which includes both iodine-based staining and the use of other staining agents, including phosphomolybdic acid, phosphotungstic acid, osmium tetroxide, and others (for reviews of the efficacy of different staining solutions, see Metscher, 2009; Pauwels et al., 2013; Descamps et al., 2014)—overcomes many of the problems associated with DTI, as it enables high-resolution data to be collected (through the use of μCT) with extremely good contrast between connective tissue and muscle. As such it is possible to easily visualize muscle portions through scan slices and, following segmentation, produce highly accurate 3D reconstructions of muscle volumes, documenting the spatial configuration of muscles alongside hard-tissue elements *in situ* (Gignac et al., 2016). A limitation of these existing studies, however, is that to date they have been unable to quantitatively assess the internal configuration of these muscles, and provide data upon fascicular arrangement (but see Kupczik et al., 2015).

Aims of the Present Study

This study reports on a quantitative method for determining muscle fascicle lengths and orientations *in situ* through the use of diceCT. This work builds on a previously published study by Kupczik et al., (2015), which introduced this methodology upon a single muscle from a domestic dog. However, elements of this approach (both in terms of the protocol for specimen preparation and staining, and the algorithmic reconstruction of muscle fascicles) have since been refined for comparative studies of primate muscle structure and the functional impact of variation therein. In the current study we present a digital reconstruction of three jaw-adductor muscles (temporalis, superficial masseter, deep masseter) from a specimen of the cercopithecine primate

Macaca fascicularis (crab-eating macaque). Muscle volume and the architectural variables of fascicle length, pennation angle, and PCSA are calculated for these muscles and compared to the results of dissection for the contralateral musculature of the same individual. We also assess the potential effect of model simplification parameters upon the digital reconstruction process by means of a sensitivity analysis. This digital technique of muscle reconstruction, which relies upon a pattern recognition algorithm to identify continuous structures within the muscle volume as individual fascicles, can produce both vector fields and streamline maps of fascicle distributions in three dimensions; as well as enabling us to produce quantitative summaries of fascicle properties such as length and orientation. The application of this method to diceCT datasets therefore allows us to garner additional data from these scans than had previously been possible, adding architectural information regarding the internal structure of the muscle to spatial and volumetric data on the size, orientation, and configuration of muscle portions.

MATERIALS & METHODS

Specimen Details

The head of one *M. fascicularis* specimen of approximate dimensions 80 × 50 × 40 mm (craniocaudal, mediolateral, dorsoventral) was selected for use in this study. The specimen was acquired *post-mortem* through Hull York Medical School, University of York, England, from a colony previously used in dental caries experiments (Smith & Beighton, 1986, 1987). Prior to our acquisition of the specimen, the sample had been fixed using a formaldehyde solution and stored in 70% ethanol, before being transferred into vacuum-sealed packages for long-term preservation. Due to the effects of volume loss associated with ethanol storage (Vickerton et al., 2013), absolute values for variables such as muscle mass and PCSA will be underestimated. The density of muscle tissue in calculations of PCSA has also been adjusted to reflect published values for formalin-fixed skeletal muscle tissue (Ward & Lieber, 2005). However, comparisons between contralateral muscles should not be affected, as any loss of volume is assumed to have affected both sides of the specimen in equal measure. The individual in question was immature, with full deciduous dentition present and the first permanent molar close to eruption. The jaw was closed with the upper and lower teeth in near centric occlusion.

Dissection of Muscles

In order to provide a comparative dataset for our results, we first dissected the three primary jaw-adductor muscles (temporalis, superficial masseter, and deep masseter) on the right side of the specimen. To begin, the skin and any overlying facial musculature were removed to expose the muscles of interest. These muscles were then collected from the specimen by blunt dissection. Following removal, all muscles were blotted dry, trimmed of any excess connective tissues, and weighted to the nearest 0.0001 g using a Kern analytical balance (Kern & Sohn, Balingen, Germany). Fascicle lengths and orientations were measured immediately post-weighing, following the protocol outlined by Taylor et al. (2009). Muscles were sectioned along their lengths following the orientation of visible surface fascicles, and divided into anterior, middle (where applicable) and posterior portions. Ten fascicles were measured from temporalis (five anterior and five posterior) and superficial masseter (five anterior and five posterior) at evenly spaced intervals. Five fascicles were measured from deep masseter (all from the middle portion). Fascicle length was measured as the linear distance between each fascicle's proximal and distal points of termination. Though the fascicles selected to be measured were approximately linear, it is possible that this methodology may underestimate fascicle length. As it was not possible to incorporate sarcomere length correction into this study, raw measured fascicle lengths are used both here and in the subsequent calculation of physiologic cross-sectional area. Though the comparison between methods is not affected, it should be noted that our reported data for fascicle lengths and PCSA may not reflect muscle fascicles measured at their optimal lengths (Anapol & Barry, 1996; Felder et al., 2005; Winters et al., 2011). The perpendicular distance between the distal junction of the fascicle and the muscle's central tendon was also measured to calculate the angle of pennation for each fascicle. Both measurements were taken under a magnifying lens, using digital callipers accurate to the nearest 0.01 mm.

Staining of the Specimen

The corresponding muscles on the left side of the specimen were left intact. The skin had been simultaneously removed from both sides of the specimen during the dissection process; however, ongoing work on other specimens has demonstrated that the removal of the overlying skin is not necessary for high-quality staining of the underlying masticatory musculature. After dissection was complete, the specimen was immersed within a prewash solution of 20% w/v sucrose dissolved in distilled water to minimise any risk of volume loss during the staining procedure (Morhardt & Witmer, 2016). Full dissolution of the sucrose was ensured prior to immersion of the specimen. The specimen remained immersed in this solution for approximately 48 hours at room temperature. The specimen was then immersed in a 5 L volume of low concentration (1.25%) Lugol's Iodine (I_2KI), and placed upon a laboratory rocker to circulate the solution around the specimen. A low concentration was selected to ensure that no overstaining of the superficial layers of musculature would occur prior to the full staining of the deepest portions (Gignac et al., 2016), and to further minimise the risk of changes in muscle volume (Vickerton et al., 2013).

After six weeks, a test scan was made using a custom-made diondo d3 μCT system housed at the Department of Human Evolution, Max Planck Institute for Evolutionary Anthropology, Leipzig. This test scan revealed that though the superficial portions were stained to a satisfactory level, the deepest elements of the sample had not yet been fully permeated by the staining solution. The specimen was therefore returned to a freshly prepared Lugol's solution and immersed for a further four weeks. A complete scan was then performed on the same μCT system at 150 kV and 150 mA with a 0.5 mm brass filter. The resulting dataset was reconstructed in 16 bit, resulting in

isometric voxel sizes (0.027 × 0.027 × 0.027 mm). The use of such high resolution ensured that muscle fascicles could be clearly distinguished within our dataset, as the cross-sectional area of muscle fascicles within juvenile macaques are reported as between 0.44 mm and 2.09 mm in the masseter, and 1.51–2.23 mm in temporalis (Maxwell et al., 1979). Prior to both scans, the specimen was transferred from I_2KI solution into a matching volume of distilled water for 48 hr in order to circumvent overstaining of any superficial elements. The staining protocol used here is based upon recommendations outlined in Gignac et al. (2016) and comments provided by Orsbon (2016, personal communication).

Image Processing and Fascicle Recognition

The final image stack was manually segmented in Avizo 8.0 (FEI, Thermo Fisher Scientific) to separate the individual muscle portions (Fig. 1). Three-dimensional (3D) volumes representing each muscle were generated in order to quantify the overall volume of each muscle (Fig. 2). Using a published value of 1.055 g/cm^3 to represent the density of formaldehyde-fixed mammalian muscle tissue (Ward & Lieber, 2005), these volumes were converted into estimations of muscle mass to facilitate comparisons to our dissection data. New image stacks were then created for each muscle object, containing only the muscle in question. These image stacks were independently imported into the freely available custom software imagexd (http://starkrats.de). A textural orientation algorithm was applied to each dataset to recognise continuous structures within each muscle object. It was expected that lower variation in grey values would be found along a continuing fascicle than between adjacent fascicles/other biological tissues. Therefore, the fascicle recognition algorithm analyzed the standard deviation (SD) of grey values in voxels surrounding a central reference voxel, and followed the path defined by the lowest SD. The resultant texture map defining structures of high grey value homogeneity was used to project a vector field of muscle fascicles within each muscle object. The vector field was then used to compute 3D streamlines representing individual fascicle distributions, using randomly distributed seedpoints throughout the muscle volume. Consequently, it is possible for multiple seed points to be generated at different stages across a single continuing fascicle. Full details regarding the operational steps and underlying algorithms of this streamline mapping procedure may be found in Kupczik et al. (2015).

During the process of streamline generation, a preliminary analysis was first conducted to assess the sensitivity of our output to simplification parameters within the fascicle reconstruction process. Our streamlines (representing muscle fascicles) were generated at a specified number of randomly distributed seedpoints throughout the muscle volume. By increasing or decreasing the number of potential seedpoints, the resultant fascicle field may itself change. To ascertain the effects of model simplification upon the final fascicular reconstructions, multiple streamline datasets were generated for a single muscle volume (superficial masseter) using an increasingly high number (500, 1,000, 2,500, 5,000, and 10,000) of potential seed points.

Following the streamline generation procedure, the created streamlines were then uploaded into the software package Trackvis (Wang & Weeden, Martinos Center for Biomedical Imaging, Massachusetts General Hospital) for visualization and quantification. This software measured the length of streamlines based on the voxel sizes of the original μCT dataset, and has been used extensively in the past to track fibrous structures in the brain (e.g., Kaplan et al., 2010, Baur et al., 2013). In order to assess the raw capabilities of the fascicle recognition process, no manual post-processing of the final streamline array was instituted. The same streamline dataset was also uploaded into the freely available custom software package cloud2 (http://starkrats.de). This software was used to compute the angle of pennation for fascicles within each muscle. To begin, the muscle volume was reoriented in such a way as to align the central myotendinous junction to a single axis (Y) within our global coordinate system. The myotendinous junction could be visually identified as a narrow area within the 3D streamline field (approximately mid-way between the muscle's medial and lateral borders) through which few fascicles passed. The orthogonal Z-axis passed through the muscle in an antero-posterior direction. A 3D grid was then projected through the muscle using evenly-distributed nodes. The angles of all fascicles within each grid portion was measured relative to the plane denoting the myotendinous junction and averaged, resulting in a summary of fascicle orientations at locations throughout the muscle (Fig. 3): providing measurements of average angles of pennation at several locations spanning between the anterior and posterior borders of the muscle.

The results of these three variables (muscle volume/mass, fascicle length, and pennation angle) are ultimately combined to calculate the PCSA of each muscle. This variable is calculated independently for the data derived from dissection and from digital reconstruction. Using data derived during dissection, PCSA (cm^2) was calculated using the formula:

$$\frac{\{muscle\ mass\ (g)\times cos\,\theta\}}{\{fiber\ length\ (cm)\times 1.055\ (g/cm^3)\}}$$

in which θ represents the angle of pennation and 1.055 represents the density of formaldehyde-fixed mammalian muscle tissue (Ward & Lieber, 2005). As our specimens were also stored in ethanol prior to dissection and staining, it is likely that this estimate may slightly overestimate true muscle density within our specimen.

The PCSA (cm^2) of our digital reconstruction is calculated using the muscle's 3D volume in place of mass, using the formula:

$$\frac{\{muscle\ volume\ (cm^3)\times\cos\theta\}}{\{fiber\ length\,(cm)\}}$$

RESULTS

Sensitivity Analysis

We generated five versions of a single muscle volume (superficial masseter), using an increasing number of potential seed points: 500, 1,000, 2,500, 5,000, and

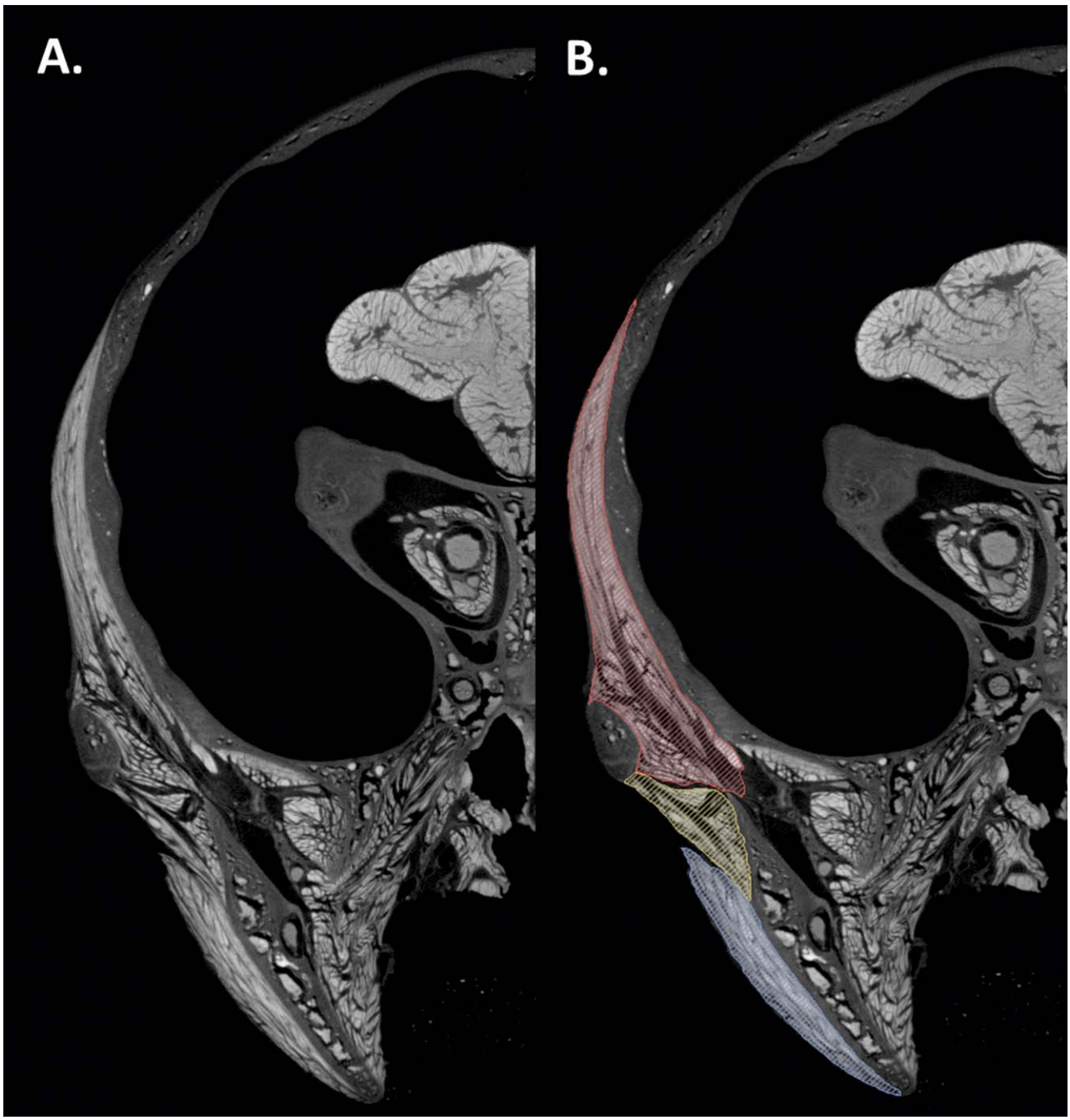

Fig. 1. Coronal contrast-enhanced microCT slice through the cranial region of Macaca fascicularis. Key jaw-adductor muscles are highlighted in **B**: temporalis in red, superficial masseter in blue, and deep masseter in yellow.

10,000. Increasing the number of seedpoints increased the number of generated fascicles. Mean fascicle length also decreased with an increasing number of seedpoints (Fig. 4), as smaller streamlines could be captured and included within the final streamline field. Models using low numbers of seedpoints failed to produce sufficient streamlines as to accurately describe the fascicular arrangement of the muscle. Meanwhile, analysis of the distribution of fascicle lengths within each iteration of the model demonstrated that the use of 10,000 seedpoints resulted in a high number of extremely short (<1 mm) streamlines. Therefore, 5,000 seedpoints was considered an appropriate value for use within this study. Analyses of the deep masseter and temporalis using 5,000 seedpoints and two bracketing models (2,500 and 10,000 seedpoints) confirmed the use of 5,000 seedpoints to additionally be most suitable for these muscles.

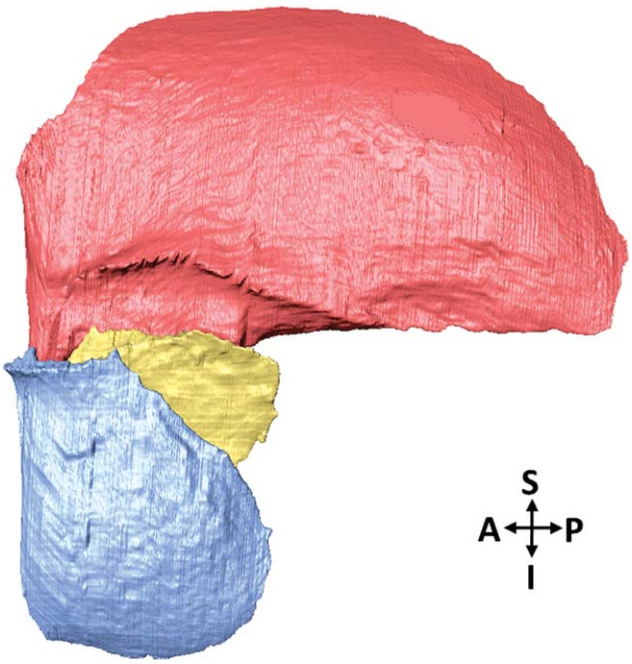

Fig. 2. Three-dimensional volume reconstructions of key jaw-adductor muscles within Macaca fascicularis, shown in lateral view. Colors as defined in Figure 1.

Digital Reconstruction of Muscle Mass

Estimations of muscle mass from 3D diceCT reconstructions of muscle volume closely match the measurements derived from manual dissection of the contralateral muscle (Table 1). This correspondence is greatest for the two components of masseter; for which the computed and measured mass values differ by only 0.02 g and 0.01 g for superficial masseter and deep masseter, respectively. The estimation for temporalis corresponds less well, overestimating muscle mass by 0.16 g.

Digital Reconstruction of Fascicle Lengths

Streamlines representing muscle fascicles were generated for all three muscle volumes (Fig. 5), using 5,000 seedpoints in each case. The number of digitally reconstructed fascicles within each muscle totaled 467 for deep masseter, 526 for superficial masseter, and 603 for temporalis.

Estimations of fascicle length using digitally constructed streamlines most closely match the range of dissected muscle fascicles within the deep masseter (Table 2). The mean reconstructed fascicle length fell towards the lower range of dissected muscle fascicles within the contralateral muscle. However, the streamlines generated for the superficial masseter and (particularly) the temporalis appear to correspond less well; producing longer fascicles than those discovered during dissection of the contralateral muscle. The mean reconstructed fascicle length for superficial masseter falls slightly above the upper range of fascicles measured within the corresponding muscle during dissection; in the case of temporalis, this discrepancy is greater still.

Unnatural fascicle trajectories were also noted within temporalis, most notably in the posterior portion of this muscle. Dissection of the contralateral muscle indicated a number of posteriorly-positioned fascicles possessing horizontal orientations that ran near-orthogonal to the muscle's axis of force generation. However, such fascicles were not recognized by our fascicle tracking algorithm.

Digital Reconstruction of Pennation Angle

Angles of pennation were calculated for muscle fascicles in both superficial masseter and temporalis (during dissection of the contralateral muscles, muscle fascicles within deep masseter were found to follow a predominantly parallel-fibered arrangement with no distinct myotendinous junction present, and thus no pennation angle was measured for this muscle). These results are presented in Table 3.

Reconstructions of pennation angle from the diceCT dataset closely correspond to those measured during manual dissection of the contralateral muscles. Within superficial masseter, the mean reconstructed pennation angle is within 1 degree of the average angle measured during dissection. Our reconstruction for temporalis corresponds similarly well (26.51 degrees vs. 25.29 degrees; Table 3). However, the upper and lower boundaries of the total range of angles are greater within our digital reconstructions for both muscles: 16.3–26.0 degrees compared to 15.3–20.5 degrees in superficial masseter, and 14.3–43.0 degrees compared to 22.1–28.6 degrees in temporalis.

Physiologic Cross-Sectional Area

These data were used to calculate PCSA for each of our three muscles (Table 4). Reconstructed PCSA for deep masseter matched the results derived from dissection. Digital reconstructions of PCSA for superficial masseter and temporalis correspond less well: with estimates that are 25% and 32% smaller than the calculations derived from dissection of the contralateral muscles, respectively. These differences reflect the increased muscle fascicle lengths recorded within the digital reconstruction of these muscles.

DISCUSSION

Muscle Mass

Reconstructions of muscle mass using volumetric diceCT data closely approximated the measured weights of the contralateral muscles acquired during dissection. Of the three analyzed muscles, our volumetric reconstruction of the temporalis corresponded least closely to the results of dissection. We suggest one reason for this to be that the digital reconstruction of this muscle enabled the entirety of this muscle around its insertions (particularly in the case of medial attachment sites upon the mandible) to be quantified as a part of the muscle volume. During dissection, meanwhile, it is often challenging to remove intact the entirety of the muscle around such obscured sites of insertion. In the case of all muscles, it is necessary to be aware that small differences may reflect changes in overall muscle volume between dissection and digital reconstruction, as a product of the staining process. High concentrations of iodine

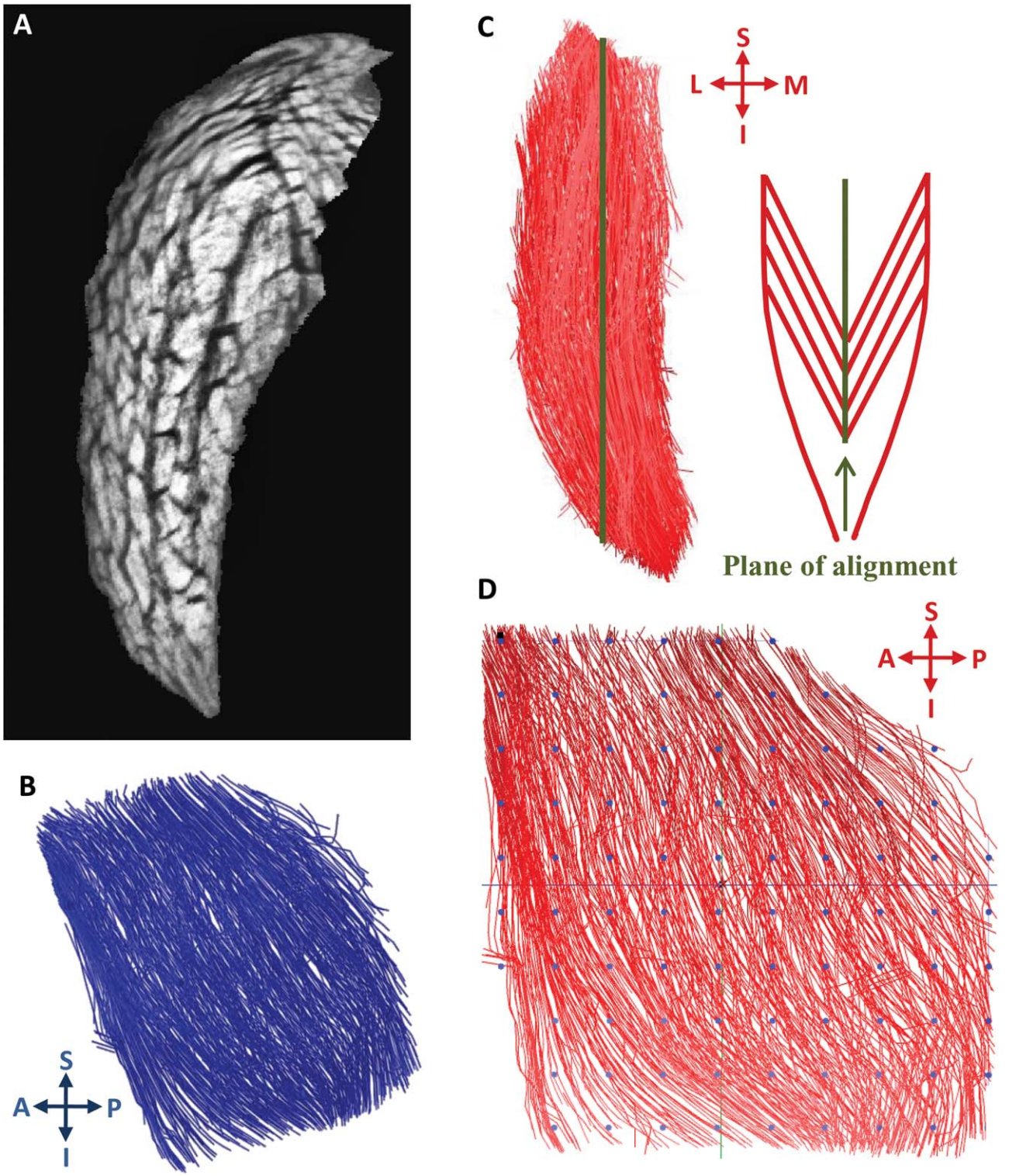

Fig. 3. Illustration of the workflow used to calculate architectural parameters: individual muscles are manually segmented from a high-resolution iodine-enhanced μCT stack and isolated (**A**). A textural orientation algorithm extracts continuous features from this volume, representing muscle fascicles (**B**). The resultant streamline dataset is then aligned to best fit the muscle's internal myotendinous junction (highlighted in Fig. 5) onto a central plane, against which angles of pennation are measured (**C**). A three-dimensional grid is then projected through the muscle using evenly-distributed nodes; each column is used to divide the muscle into portions which are used to calculate regional changes in pennation angle, as illustrated in Figure 5 (**D**).

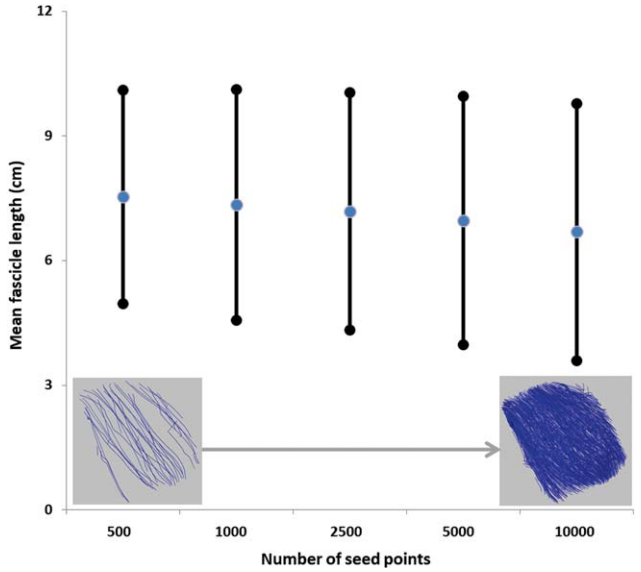

Fig. 4. Analysis of the effects of model resolution (defined as the number of potential seed points used for fascicle reconstruction) upon measures of fascicle length within a single muscle (superficial masseter). Mean fascicle lengths shown in blue; standard deviation shown in black. Below, images are included of the output data for our least complex (500 seed point) and most complex (10,000 seed point) models.

TABLE 1. Reconstructed volumes and weights of superficial masseter, deep masseter, and temporalis (derived from segmentation of the diceCT image stack) compared to measured weights collected during dissection of the contralateral muscles

Muscle	Digital volume (cm^3)	Reconstructed weight[a] (g)	Measured weight (g) (opposite side)
Superficial masseter	0.257	0.272	0.293
Deep masseter	0.108	0.114	0.123
Temporalis	1.083	1.142	0.982

[a]In order to transform our volumetric data into an estimate of muscle mass, muscle volumes were converted into estimations of muscle weight using previously published data (Ward & Lieber, 2005) on the density of formaldehyde-fixed mammalian muscle tissue to be approximately 1.055 g/cm^3. As our specimens were also stored in ethanol prior to dissection and staining, it is possible that this estimate may slightly overestimate true muscle density within our specimen.

can result in the shrinkage of tissues (Vickerton et al., 2013). To combat this potential effect, we used a low concentration iodine stain (1.25%), and additionally applied a sucrose prewash to the specimen to minimize the risk of volume less (Morhardt & Witmer, 2016).

Finally, one additional complication when analyzing all variables reported here is the matter of bilateral asymmetry between the dissected muscles and those used as part of the diceCT procedure. As muscles from the right-hand side of the individual were dissected and those of the left-hand side used for our diceCT analyses, any discrepancies in size or architectural configuration between these pairs of muscles would naturally lead to variation between these two sets of results. Data on muscle asymmetry within the postcranium is reported for *Pan troglodytes* (Carlson, 2006), and demonstrates that bilateral differences in muscle mass average 7% across the forelimb and hindlimb, with a maximum difference of 17% in the plantar flexors. Bilateral differences within our jaw-adductor sample displayed a similar range (8% in superficial masseter, 8% in deep masseter, 14% in temporalis). Though behavioural asymmetry between left- and right-hand side may be more exaggerated in the muscles of the postcranium, it should be noted that bilateral asymmetry may account for some degree of variation between all muscle data reported here.

Muscle Fascicle Lengths

Estimations of fascicle lengths most closely resembled the results of our dissection data for the deep masseter. Fascicle lengths within superficial masseter were slightly overestimated by the digital reconstruction, while fascicle length estimations for temporalis greatly exceeded the measured range observed during dissection. The greater disparity observed within temporalis may reflect the increased complexity of the fascicular trajectory in the temporalis muscle, which involves the muscle wrapping around the curvature of the cranium and passing beneath structures such as the zygomatic arch (by comparison, the trajectories of fascicles in superficial and deep masseter are more simple, running from the medial and inferior surface of the zygomatic arch to the lateral surfaces of the ascending ramus and gonial angle of the mandible). This may render these fascicles more difficult to accurately identify using the fascicle tracking algorithm. It is further possible that the complex curvature of muscles—in particular that of temporalis—resulted in an underestimation of fascicle length measurements during dissection. Muscles were sectioned along their lines of action, and fascicle lengths measured from the resultant cross-sectional faces. However, these measurements would not fully reflect the 3D length of curved muscle fascicles along their full trajectory.

Methodological differences between the data collected during dissection and the results of our digital reconstruction might also explain disparities between our two sets of results. It is expected that the method of digital reconstruction will inherently produce longer measures of fascicle length that those found during our dissection. This is due to the fact that our digital approach quantified the length of fascicles in three dimensions; by comparison, measurements gathered during dissection were derived from a two-dimensional cross-sectional plane through the muscle. Consequently, the increased fascicle lengths reported using this digital approach may be more reflective of the full lengths of the internal fascicles themselves. However, an earlier study analysing the canine masseter (Kupczik et al., 2015) also recognized a number of muscle fascicles as being non-physiological in length (defined there as exceeding the longest fascicles recorded during dissection). The potential for the results of our reconstruction to overestimate the length of individual fascicles (by failing to accurately

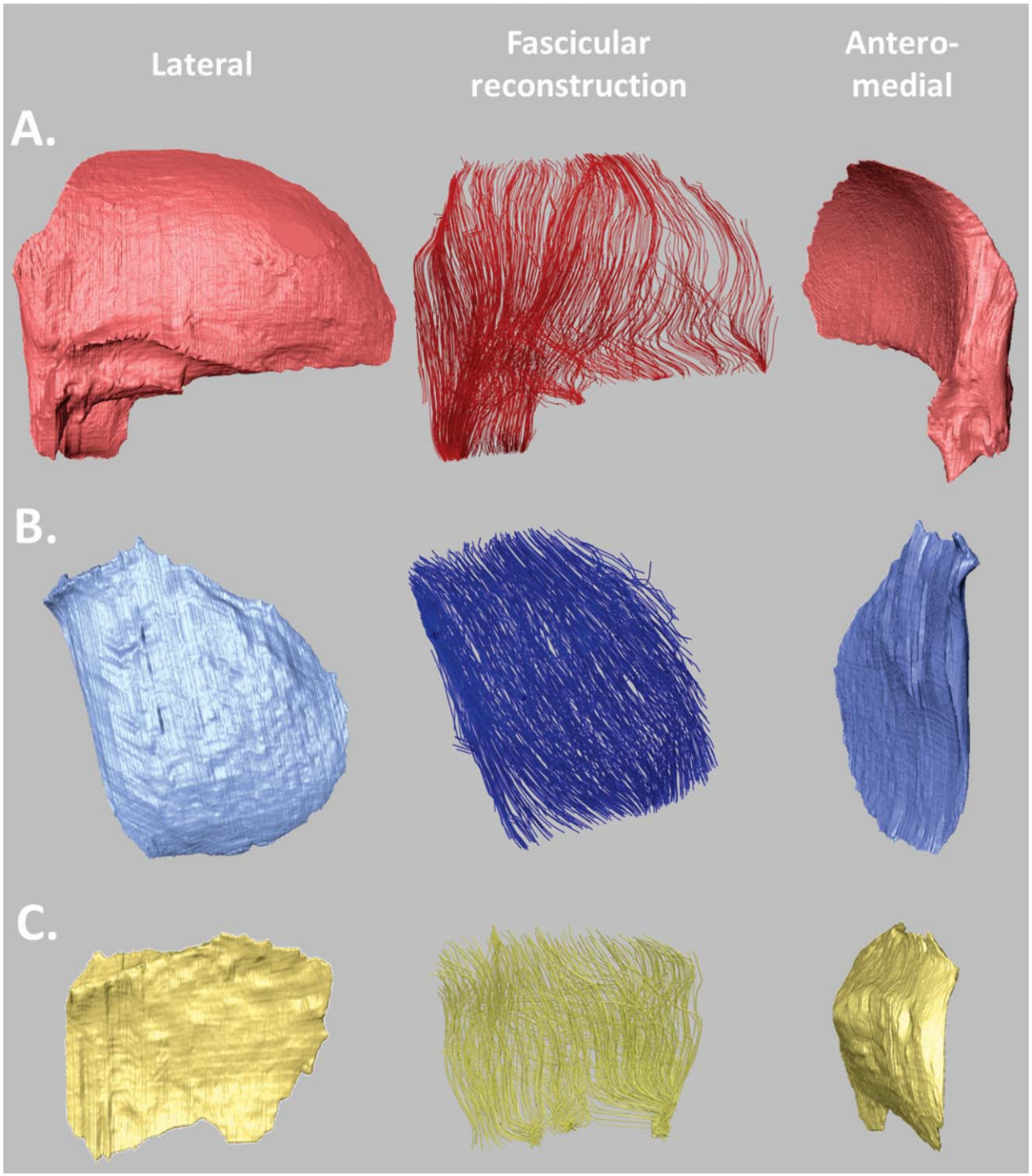

Fig. 5. Three-dimensional volumes and fascicular reconstructions of temporalis (**A**), superficial masseter (**B**), and deep masseter (**C**).

determine the points of termination for a given fascicle) should therefore be noted.

Comparative datasets on immature individuals of *Macaca fascicularis* are scarce. Muscle architectural data for adult females is reported by Antón (1999) for the superficial masseter, and data on adults of both sexes are reported by Terhune et al. (2015) for superficial masseter and temporalis. Antón (1999) reports average fascicle lengths of 6.9–12.2 mm for superficial masseter; these are comparable to the data for adult

TABLE 2. Fascicle lengths (mean, standard deviation, number of fascicles) derived from digitally reconstructed muscle fascicles compared to muscle dissection

Muscle	Reconstructed fascicle length (mm)	Dissected fascicle length (mm)
Superficial masseter	6.96 ± 2.99 (N = 526)	5.64 ± 0.38 (N = 10)
Deep masseter	4.78 ± 1.91 (N = 467)	5.20 ± 0.48 (N = 5)
Temporalis	10.51 ± 5.54 (N = 603)	6.12 ± 0.71 (N = 10)

TABLE 3. Pennation angles (mean, *SD*) derived from digitally reconstructed muscle fascicles compared to muscle dissection

Muscle	Reconstructed pennation angle (degrees)	Dissection pennation angle (degrees)
Superficial masseter	19.40 ± 3.19	18.53 ± 1.74
Temporalis	26.51 ± 9.59	25.29 ± 3.86

TABLE 4. PCSA derived from digitally reconstructed muscle fascicles compared to results gathered from dissection of the contralateral muscles

Muscle	Reconstructed PCSA (cm^2)	Dissection PCSA (cm^2)
Superficial masseter	0.36	0.48
Deep masseter	0.23	0.23
Temporalis	0.99	1.46

females (10.81–12.53 mm) found by Terhune et al. (2015). Adult males present significantly longer muscle fascicles, averaging 12.8–21.1 mm. Terhune et al. also report that fascicle lengths are considerably greater within temporalis than superficial masseter in both adult females (14.2–17.7 mm) and males (24.4–29.7 mm). Our own data suggest that the relative lengths of fascicles within superficial masseter and temporalis are much more similar within juvenile individuals than in the adult specimens analyzed in previous studies. As would be expected, adult individuals possess absolutely longer fascicles than those found within our own immature specimen within all muscles.

Terhune et al. (2015) further report that anterior fibers in temporalis were shorter than posterior fibers, in both males and females. However, the opposite was true within superficial masseter, where anterior fibers were longer than posterior fibers. Data collected during the dissection of our juvenile specimen support the pattern observed by Terhune et al. within the temporalis, with posterior fascicles (averaging 6.48 mm) longer than their anterior counterparts (5.75 mm); however, no meaningful differences were observed in fascicle lengths between anterior and posterior portions of superficial masseter (5.59 vs. 5.68 mm).

When comparing the two methods presented here, it is important to consider that only a small subset of the total number of muscle fascicles were measured during our dissection (N = 10 for superficial masseter and temporalis; N = 5 for deep masseter). This sampling method may have failed to capture the longest fascicles present within the muscle, resulting in an incomplete range of fascicle lengths and a lower average fascicle length than if every fascicle had been quantified. However, this method was selected to resemble a number of comparable muscle architectural studies which rely upon selecting sampling sites at different sections through the muscle and measuring a subset of the exposed fascicles (e.g., Anapol & Barry, 1996; Taylor et al., 2009; Lamas et al., 2014; Terhune et al., 2015). The application of an alternative method, such as chemical digestion (as in Perry & Wall, 2008; Organ et al., 2009; Hartstone-Rose et al., 2012; Perry et al., 2014) may have produced different results. Furthermore, as with muscle mass, some differences between left- and right- sided muscle fascicle lengths may be attributable to natural asymmetry: mean bilateral differences in fascicle length of 9.3% are reported within the chimpanzee postcranium (Carlson, 2006).

Pennation Angles

The reconstructed angles of pennation for both muscles closely matched the results gathered during dissection, to within approximately 1 degree. However, the sampling method used within our digital reconstruction also allowed us to analyse the distribution of fascicle orientations throughout the muscle volume. During dissection, fascicle lengths and orientations were measured at two locations within each muscle: the interface between anterior and middle portions (one-third of the way through the muscle) and the interface between middle and posterior portions (two-thirds of the way through the muscle). By comparison, angles of pennation were digitally reconstructed for fascicles throughout each muscle. As these angles appear to change dependent upon the location of fascicles within the muscle (Fig. 5), we would expect our digital approach to capture a greater range of variation in fascicle orientation. In the case of superficial masseter, the average angle of pennation is lowest toward the centre of the muscle and increases towards the anterior and posterior borders (Fig. 6).

Digital reconstruction of a full muscle fascicle field therefore enables us to map changes in architectural variables between different portions of single muscles. Such observations into regional differences in architectural properties may prove to be useful in addressing questions raised in recent studies (e.g., Wall et al., 2008; Vinyard et al., 2008) into regionalised specialisation within single muscles of mastication.

By comparison to data reported by Terhune et al. (2015) on angles of pennation within adult *M. fascicularis*, the constitutent fascicles reported for our immature specimen are considerably more pinnate in both superficial masseter and temporalis. An increase in pennation angle would theoretically improve the ability to generate high masticatory forces, by increasing the total number of fascicles that may be accommodated within a given muscle or muscle portion. The higher degree of

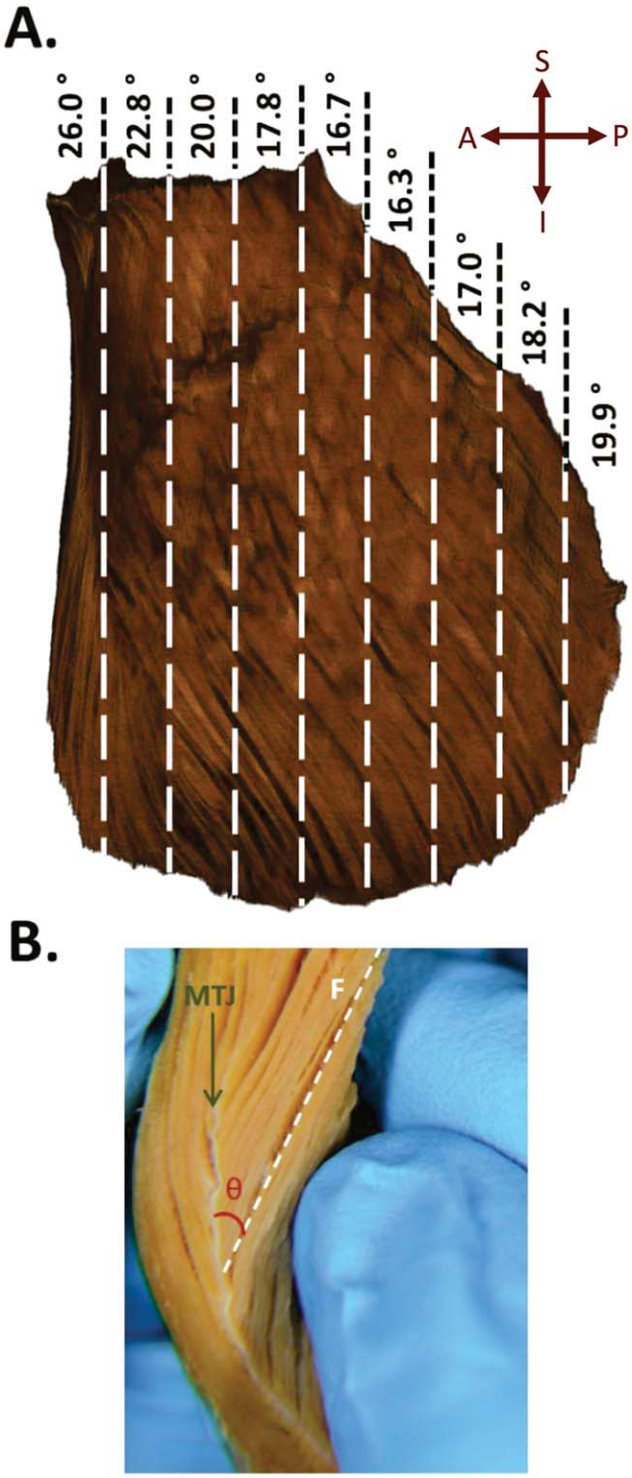

Fig. 6. Changes in pennation angle within superficial masseter: (**A**) mean angle of pennation for fascicles within each portion of superficial masseter, calculated through digital fascicular reconstruction; (**B**) illustration of the myotendinous junction (MTJ) and muscle fascicles (F) between which pennation angle (θ) is measured.

pinnation observed within our juvenile specimen preliminarily suggests that these individuals may be more optimized toward force production than their more mature counterparts. Further data is necessary, however, to determine the extent to which pennation angle can be seen to follow any form of consistent trend during development within this species.

In terms of regional differentiation in pennation angle, meanwhile, we find slight differences between anterior and posterior portions of muscles. Within our reconstruction of superficial masseter, fascicles were more pinnate within the anterior portion of our juvenile specimen than the posterior (Fig. 5); these findings also matched the results of our dissection of this individual (in which anterior fibers had an average pennation angle of 19.5 degrees, and posterior fascicles an angle of 17.6 degrees). The opposite trend is reported within adult specimens, though the differences are again slight (10.5 vs. 15.6 degrees in females; 12.8 vs. 18.5 degrees in males) (Terhune et al., 2015).

Physiologic Cross-Sectional Area

The calculation of PCSA for deep masseter produced equivalent results for both the gross dissection and digital reconstruction. However, our digital reconstruction of superficial masseter and temporalis resulted in lower PCSA values than those derived from dissection of the contralateral muscles. This disparity appears largely driven by differences in mean fascicle lengths between the two datasets. As mentioned above, such disparities may reflect the differences between the two-dimensional lengths measured during dissection and the 3D trajectories of the fascicles, an overestimation of individual muscle fascicle lengths within our digital reconstructions, or some degree of bilateral asymmetry between the muscles of the left- and right- hand sides.

As raw measured fascicle lengths (without sarcomere length correction) were used during the calculation of PCSA, our values may not reflect muscle fascicles at their optimal length. Whilst the comparison between methods is not affected, this should be accounted for when comparing the architectural variables reported here to other datasets.

Evaluation of Technique

Digital fascicle reconstruction offers a number of potential advantages over traditional gross dissection techniques. The first of these relates to the number of fascicles that are analyzed within a muscle, or muscle portion. Dissection-based studies typically rely upon sampling a subset of fascicles (either directly from cross-sections of muscle portions, or following chemical digestion of the connective tissues) to represent the muscle's architectural profile (e.g., Anapol & Barry, 1996, Taylor et al., 2009, Hartstone-Rose et al., 2012, Perry et al., 2014)). Our digital reconstruction approach allows us to analyse the fascicular distribution of an entire muscle or muscle portion simultaneously—providing a much greater depth of data from which to determine the muscle's structure. By analyzing large numbers of fascicles across multiple regions of a muscle, we may begin to observe regions of functional specialization and relate differences in architectural properties to other functional determinants of muscle function, such as biomechanical efficiency. As mechanical advantage will vary throughout a single muscle, regional differences in architectural

parameters such as fascicle length or pennation angle may be related to differences in moment arm length between anteriorly- and posteriorly-positioned fascicles within this muscle. Integrating data on muscle fascicle length and orientation into digital mediums of biomechanical modeling such as multibody dynamics (Curtis et al., 2008; Shi et al., 2012; Fitton et al., 2012; Gröning et al., 2013; Watson et al., 2014) or finite element analysis (Kupczik et al., 2007, 2009; Chalk et al., 2011; Wang et al., 2010; Dumont et al., 2011; Ross et al., 2011; Tseng et al., 2011; Cox et al., 2011; Fitton et al., 2012; Smith et al., 2015) may allow us to directly address the relationship between muscle architectural variables and other functional determinants of muscle performance.

Furthermore, as opposed to gross dissection (which results in the loss of tissue and thus is inherently irreversible), the use of diceCT and digital fascicle reconstruction enables muscle architectural properties to be derived without the need to remove the muscles from the specimen. Specimens may even be destained through the use of a sodium thiosulphate ($Na_2S_2O_3$) postwash (Gignac et al., 2016); such that the specimen may be later used for other research purposes. Consequently, this method is considered to represent a reversible and non-destructive 3D imaging tool (Morhardt & Witmer, 2016; Gignac et al., 2016).

Though this technique therefore offers great potential, it is necessary to be aware of possible inaccuracies in the mapping process. By allowing the path of fascicles to be identified using fully-automated processes, it is possible for false signals to be incorporated into the results. Within our own models, we may have identified regions (such as the posterior portion of temporalis) wherein fascicles follow seemingly unnatural trajectories. Dissection of this muscle indicated a number of posteriorly-positioned fascicles with a horizontal orientation, running orthogonally to the muscle's axis of force generation. However, such fascicles were not recognized by our fascicle tracking algorithm. In addition to the failure to recognize certain fascicles, small artifacts relating either to the staining or scanning procedures may cause fascicle lengths to be under- or over-measured. As muscle form and architecture become more complex and heterogenous (as in the case of temporalis), registration issues appear more frequent and differences between the results of dissection and digital reconstruction appear more pronounced. An understanding of the underlying anatomy is therefore crucial to being able to interpret the resultant fascicle maps, and identify portions in which mapping errors may be present. Finally, as shown by the results of our sensitivity analysis, simplifications in the modeling process (such as a reduction in the number of potential seed points analyzed when constructing a fascicle field) may have some small effect upon the final results.

The extended period of time necessary to enact the workflow should also be noted. To begin, staining of the specimen can itself be time-consuming. For a juvenile individual of *Macaca fascicularis*, our staining process took ten weeks to be completed. Other diceCT studies report shorter periods of staining time, at higher concentrations: 3 weeks for the head of an adult *Ornithorhynchus anatinus* in 7.5% I2KI (Gignac et al., 2016); 4 weeks for the head of a subadult *Alligator mississippiensis* in 11.25% I2KI (Gignac & Kley, 2014); and 7 weeks for the head of an adult *Sciurus carolinensis* in 25% I2KI (Jeffery et al., 2011). Higher concentration solutions of staining agent may have expedited the staining process for our specimen, but this can result in the shrinkage of tissues (Vickerton *et al*. 2013) and poses a risk of overstaining superficial tissues, thus compromising the quality of final data (Gignac et al., 2016). In addition to our use of a low-concentration iodine stain, we additionally applied a sucrose prewash to the specimen in order to minimize the risk of volume loss through specimen shrinkage during the staining process (Morhardt & Witmer, 2016). Following staining and scanning, manual segmentation of each muscle was then necessary, to create the requisite image stacks upon which to perform the fascicular reconstruction. Both of these steps are themselves demanding in terms of time and computational power.

Overall, this technique provides a novel and potentially powerful tool for analyzing the internal structure of skeletal muscle in high resolution, and without destruction of the specimen. We demonstrate that key architectural parameters such as fascicle lengths and pennation angles can be calculated from iodine-stained μCT datasets. Within muscles which present more simple and consistent fascicular orientations (such as the components of masseter), the results of our digital reconstruction were largely similar to those data collected during dissection of the contralateral muscles. However, data for the temporalis were less well-matched, perhaps as a result of the muscle's more complex shape and curved fascicular trajectories. Unnatural fascicle orientations within the posterior portion of temporalis demonstrate that heterogeneity in fascicle orientation throughout the muscle volume can lead to misidentification artifacts. Future work will continue to refine and improve the algorithm's ability to identify internal structures within muscle, and develop the tools used to quantify and analyze these architectural variables. Additional analyses will expand this methodology to analyze further muscle groups, including postcranial elements. Future work will also be focused upon integrating the output of these analyses into new methods for quantifying musculoskeletal performance, such as multibody dynamics analysis. We propose that this technique presents a highly useful supplement to the existing toolkit used in the quantification of muscle microarchitecture: to be used alongside gross dissection in order to visualize fascicular arrangement in three-dimensions, or to be applied in situations where muscle architectural parameters are required but non-destructive methodologies are preferred.

ACKNOWLEDGEMENTS

We thank Adam Hartstone-Rose for inviting us to contribute to this special issue. We are grateful to the following individuals for their help during the course of this study: Laura Fitton and Paul O'Higgins (Centre for Anatomical and Human Sciences, Hull York Medical School) for providing the specimen for use; Callum Ross and Courtney Osborn (Ross lab, University of Chicago) for advice regarding the staining protocol; David Plotzki for CT scanning assistance; and Silke Brauer and Tina Kottek for their help with storage of the specimen. We would also like to thank two anonymous reviewers for

their comments to improve this manuscript. Financial support was provided by the Max Planck Society.

LITERATURE CITED

Allen V, Elsey RM, Jones N, Wright J, Hutchinson JR. 2010. Functional specialization and ontogenetic scaling of limb anatomy in Alligator mississippiensis. J. Anat 216:423–445.

Anapol F, Barry K. 1996. Fiber architecture of the extensors of the hindlimb in semiterrestrial and arboreal guenons. Am J Phys Anthropol 99:429–447.

AnapolF, Shahnoor N, Ross CF. 2008. Scaling of reduced physiologic cross-sectional area in primate muscles of mastication. In: Primate craniofacial function and biology. Berlin: Springer. p. 201–216.

Anapol FC, Jungers WL. 1986. Architectural and histochemical diversity within the quadriceps femoris of the brown lemur (Lemur fulvus). Am J Phys Anthropol 69:355–375.

Antón SC. 1999. Macaque masseter muscle: Internal architecture, fiber length and cross-sectional area. Int J Primatol 20:441–462.

Antón SC. 2000. Macaque pterygoid muscles: internal architecture, fiber length, and cross-sectional area. Int J Primatol 21:131–156.

Bang M-L, Li X, Littlefield R, Bremner S, Thor A, Knowlton KU, Lieber RL, Chen J. 2006. Nebulin-deficient mice exhibit shorter thin filament lengths and reduced contractile function in skeletal muscle. J Cell Biol 173:905–916.

Baverstock H, Jeffery NS, Cobb SN. 2013. The morphology of the mouse masticatory musculature. J Anat 223:46–60.

Baur V, Hänggi J, Langer N, Jäncke L. 2013. Resting-state functional and structural connectivity within an insula—amygdala route specifically index state and trait anxiety. Biological Psychiatry 73:85–92.

Bodine SC, Roy RR, Meadows DA, Zernicke RF, Sacks RD, Fournier M, Edgerton VR. 1982. Architectural, histochemical, and contractile characteristics of a unique biarticular muscle: The cat semitendinosus. J Neurophysiol 48:192–201.

Carlson KJ. 2006. Muscle architecture of the common chimpanzee (Pan troglodytes): Perspectives for investigating chimpanzee behavior. Primates 47:218–229.

Chalk J, Richmond BG, Ross CF, Strait DS, Wright BW, Spencer MA, Wang Q, Dechow PC. 2011. A finite element analysis of masticatory stress hypotheses. Am J Phys Anthropol 145:1–10.

Cox PG, Fagan MJ, Rayfield EJ, Jeffery N. 2011. Finite element modelling of squirrel, guinea pig and rat skulls: Using geometric morphometrics to assess sensitivity. J Anat 219:696–709.

Cox PG, Faulkes CG. 2014. Digital dissection of the masticatory muscles of the naked mole-rat, Heterocephalus glaber (Mammalia, Rodentia). Peer J 2:e448.

Cox PG, Jeffery N. 2011. Reviewing the morphology of the jaw-closing musculature in squirrels, rats, and guinea pigs with contrast-enhanced microCT. Anat Rec 294:915–928.

Cox PG, Rayfield EJ, Fagan MJ, Herrel A, Pataky TC, Jeffery N. 2012. Functional evolution of the feeding system in rodents. PLoS One 7:e36299.

Curtis N, Kupczik K, O'higgins P, Moazen M, Fagan M. 2008. Predicting skull loading: Applying multibody dynamics analysis to a macaque skull. Anat Rec 291:491–501.

Damon BM, Ding Z, Anderson AW, Freyer AS, Gore JC. 2002. Validation of diffusion tensor MRI-based muscle fiber tracking. Magn Reson Med 48:97–104.

Descamps E, Sochacka A, D, Kegel B, Van Loo D, Van Hoorebeke L, Adriaens D. 2014. Soft tissue discrimination with contrast agents using micro-CT scanning. Belg J Zool 144:20–40.

Dumont ER, Davis JL, Grosse IR, Burrows AM. 2011. Finite element analysis of performance in the skulls of marmosets and tamarins. J Anat 218:151–162.

Eng CM, Smallwood LH, Rainiero MP, Lahey M, Ward SR, Lieber RL. 2008. Scaling of muscle architecture and fiber types in the rat hindlimb. J Exp Biol 211:2336–2345.

Felder A, Ward SR, Lieber RL. 2005. Sarcomere length measurement permits high resolution normalization of muscle fiber length in architectural studies. J Exp Biol 208:3275–3279.

Fitton LC, Shi JF, Fagan MJ, O'Higgins P. 2012. Masticatory loadings and cranial deformation in Macaca fascicularis: A finite element analysis sensitivity study. J Anat 221:55–68.

Friederich JA, Brand RA. 1990. Muscle fiber architecture in the human lower limb. J Biomech 23:91–95.

Furuuchi K, Koyabu D, Mori K, Endo H. 2013. Physiological cross-sectional area of the masticatory muscles in the giraffe (Giraffa camelopardalis). Mammal Study 38:67–71.

Gans C. 1982. Fiber architecture and muscle function. Exerc Sport Sci Rev 10:160–207.

Gans C, Bock WJ. 1965. The functional significance of muscle architecture – A theoretical analysis. Ergeb Anat Entwicklungsgesch 38:115.

Gignac PM, Kley NJ. 2014. Iodine-enhanced micro-CT imaging: Methodological refinements for the study of the soft-tissue anatomy of post-embryonic vertebrates. J Exp Zool Part B Mol Dev Evol 322:166–176.

Gignac PM, Kley NJ, Clarke JA, Colbert MW, Morhardt AC, Cerio D, Cost IN, Cox PG, Daza JD, Early CM, etal. 2016. Diffusible iodine-based contrast-enhanced computed tomography (diceCT): An emerging tool for rapid, high-resolution, 3-D imaging of metazoan soft tissues. J Anat 228:889–909.

Gokhin DS, Bang M-L, Zhang J, Chen J, Lieber RL. 2009. Reduced thin filament length in nebulin-knockout skeletal muscle alters isometric contractile properties. Am J Physiol Physiol 296:C1123–C1132.

Gordon AM, Huxley AF, Julian FJ. 1966a. Tension development in highly stretched vertebrate muscle fibres. J Physiol 184:143.

Gordon AM, Huxley AF, Julian FJ. 1966b. The variation in isometric tension with sarcomere length in vertebrate muscle fibres. J Physiol 184:170.

Gössl C, Fahrmeir L, Pütz B, Auer LM, Auer DP. 2002. Fiber tracking from DTI using linear state space models: Detectability of the pyramidal tract. Neuroimage 16:378–388.

Gröning F, Jones MEH, Curtis N, Herrel A, O'Higgins P, Evans SE, Fagan MJ. 2013. The importance of accurate muscle modelling for biomechanical analyses: A case study with a lizard skull. J R Soc Interface 10:20130216.

Hartstone-Rose A, Perry JMG, Morrow CJ. 2012. Bite force estimation and the fiber architecture of felid masticatory muscles. Anat Rec 295:1336–1351.

Hautier L, Lebrun R, Cox PG. 2012. Patterns of covariation in the masticatory apparatus of hystricognathous rodents: Implications for evolution and diversification. J Morphol 273:1319–1337.

Heemskerk AM, Strijkers GJ, Vilanova A, Drost MR, Nicolay K. 2005. Determination of mouse skeletal muscle architecture using three-dimensional diffusion tensor imaging. Magn Reson Med 53: 1333–1340.

Herring SW, Wineski LE. 1986. Development of the masseter muscle and oral behavior in the pig. J Exp Zool Part A Ecol Genet Physiol 237:191–207.

Holliday CM, Tsai HP, Skiljan RJ, George ID, Pathan S. 2013. A 3D interactive model and atlas of the jaw musculature of Alligator mississippiensis. PLoS One 8:e62806.

Ito K, Endo H. 2016. Compartive study of physiological cross-sectional area of masticatory muscles among species of Carnivora. Mammal Study 41:181–190.

Jeffery NS, Stephenson RS, Gallagher JA, Jarvis JC, Cox PG. 2011. Micro-computed tomography with iodine staining resolves the arrangement of muscle fibres. J Biomech 44:189–192.

Kaplan E, Naeser MA, Martin PI, Ho M, Wang Y, Baker E, Pascual-Leone A. 2010. Horizontal portion of arcuate fasciculus fibers track to pars opercularis, not pars triangularis, in right and left hemispheres: a DTI study. Neuroimage 52:436–444.

Kawakami Y, Akima H, Kubo K, Muraoka Y, Hasegawa H, Kouzaki M, Imai M, Suzuki Y, Gunji A, Kanehisa H, etal. 2001. Changes in muscle size, architecture, and neural activation after 20 days of bed rest with and without resistance exercise. Eur J Appl Physiol 84:7–12.

Kikuchi Y. 2010. Comparative analysis of muscle architecture in primate arm and forearm. Anat Histol Embryol 39:93–106.

Klose U, Erb M, Saur R, Seeger U, Grodd W. 2005. Segmentierung der weißen Hirnsubstanz auf der Grundlage von MR-DTI-Vorzugsrichtungen. Z Med Phys 15:247–255.

Kupczik K, Dobson CA, Fagan MJ, Crompton RH, Oxnard CE, O'Higgins P. 2007. Assessing mechanical function of the zygomatic region in macaques: Validation and sensitivity testing of finite element models. J Anat 210:41–53.

Kupczik K, Dobson CA, Crompton RH, Phillips R, Oxnard CE, Fagan MJ, O'Higgins P. 2009. Masticatory loading and bone adaptation in the supraorbital torus of developing macaques. Am J Phys Anthropol 139:193–203.

Kupczik K, Stark H, Mundry R, Neininger FT, Heidlauf T, Röhrle O. 2015. Reconstruction of muscle fascicle architecture from iodine-enhanced microCT images: A combined texture mapping and streamline approach. J Theor Biol 382:34–43.

Lamas LP, Main RP, Hutchinson JR. 2014. Ontogenetic scaling patterns and functional anatomy of the pelvic limb musculature in emus (Dromaius novaehollandiae). Peer J 2:e716.

Lieber RL. 1986. Skeletal muscle adaptability. I: Review of basic properties. Dev Med Child Neurol 28:390–397.

Lieber RL, Blevins FT. 1989. Skeletal muscle architecture of the rabbit hindlimb: Functional implications of muscle design. J Morphol 199:93–101.

Lieber RL, Friden J. 2000. Functional and clinical significance of skeletal muscle architecture. Muscle Nerve 23:1647–1666.

Lieber RL, Jacobson MD, Fazeli BM, Abrams RA, Botte MJ. 1992. Architecture of selected muscles of the arm and forearm: Anatomy and implications for tendon transfer. J Hand Surg Am 17:787–798.

Lieber RL, Ward SR. 2011. Skeletal muscle design to meet functional demands. Philos Trans R Soc B Biol Sci 366:1466–1476.

Mathewson MA, Kwan A, Eng CM, Lieber RL, Ward SR. 2014. Comparison of rotator cuff muscle architecture between humans and other selected vertebrate species. J Exp Biol 217:261–273.

Maxwell LC, Carlson DS, McNamara JA, Faulkner JA. 1979. Histochemical characteristics of the masseter and temporalis muscles of the rhesus monkey (Macaca mulatta). Anat Rec 193:389–401.

McMillan AB, Shi D, Pratt SJP, Lovering RM. 2011. Diffusion tensor MRI to assess damage in healthy and dystrophic skeletal muscle after lengthening contractions. Biomed Res Int 2011:1.

Metscher BD. 2009. MicroCT for comparative morphology: Simple staining methods allow high-contrast 3D imaging of diverse non-mineralized animal tissues. BMC Physiol 9:11.

Michilsens F, Vereecke EE, D'Août K, Aerts P. 2009. Functional anatomy of the gibbon forelimb: Adaptations to a brachiating lifestyle. J Anat 215:335–354.

Morhardt RC; Witmer, LM AR. 2016. ABSTRACT: Diffusible iodine-based contrast enhancement of large, post-embryonic, intact vertebrates for CT scanning: Staining, destaining, and long-term storage. Presented at International Congress of Vertebrate Morphology 2016, Washington, D.C.

Morris CB. 1948. The measurement of the strength of muscle relative to the cross section. Res Quarterly Am Assoc Heal Phys Educ Recreat 19:295–303.

Murray WM, Buchanan TS, Delp SL. 2000. The isometric functional capacity of muscles that cross the elbow. J Biomech 33:943–952.

Napadow VJ, Chen Q, Mai V, So PTC, Gilbert RJ. 2001. Quantitative analysis of three-dimensional-resolved fiber architecture in heterogeneous skeletal muscle tissue using NMR and optical imaging methods. Biophys J 80:2968–2975.

Ogihara N, Oishi M, Kanai R, Shimada H, Kondo T, Yoshino-Saito K, Ushiba J, Okano H. 2017. Muscle architectural properties in the common marmoset (Callithrix jacchus). Primates 1–12.

Oishi M, Ogihara N, Endo H, Asari M. 2008. Muscle architecture of the upper limb in the orangutan. Primates 49:204–209.

Organ JM, Teaford MF, Taylor AB. 2009. Functional correlates of fiber architecture of the lateral caudal musculature in prehensile and nonprehensile tails of the Platyrrhini (Primates) and Procyonidae (Carnivora). Anat Rec 292:827–841.

Pauwels E, Van Loo D, Cornillie P, Brabant L, Van Hoorebeke L. 2013. An exploratory study of contrast agents for soft tissue visualization by means of high resolution X-ray computed tomography imaging. J Microsc 250:21–31.

Payne RC, Crompton RH, Isler K, Savage R, Vereecke EE, Gunther MM, Thorpe SKS, D'Aout K. 2006. Morphological analysis of the hindlimb in apes and humans. I. Muscle architecture. J Anat 208: 709–724.

Perry JMG, Hartstone-Rose A, Wall CE. 2011. The jaw adductors of strepsirrhines in relation to body size, diet, and ingested food size. Anat Rec 294:712–728.

Perry JMG, Macneill KE, Heckler AL, Rakotoarisoa G, Hartstone-Rose A. 2014. Anatomy and adaptations of the chewing muscles in Daubentonia (Lemuriformes). Anat Rec 297:308–316.

Perry JMG, Wall CE. 2008. Scaling of the chewing muscles in prosimians. In: Primate craniofacial function and biology. Berlin: Springer. p. 217–240.

Pfaller JB, Gignac PM, Erickson GM. 2011. Ontogenetic changes in jaw-muscle architecture facilitate durophagy in the turtle Sternotherus minor. J Exp Biol 214:1655–1667.

Powell PL, Roy RR, Kanim P, Bello MA, Edgerton VR. 1984. Predictability of skeletal muscle tension from architectural determinations in guinea pig hindlimbs. J Appl Physiol 57:1715–1721.

Reese TG, Weisskoff RM, Smith RN, Rosen BR, Dinsmore RE, Wedeen VJ. 1995. Imaging myocardial fiber architecture in vivo with magnetic resonance. Magn Reson Med 34:786–791.

Ross CF, Berthaume MA, Dechow PC, Iriarte-Diaz J, Porro LB, Richmond BG, Spencer M, Strait D. 2011. In vivo bone strain and finite-element modeling of the craniofacial haft in catarrhine primates. J Anat 218:112–141.

Roy RR, Bello MA, Powell PL, Simpson DR. 1984. Architectural design and fiber-type distribution of the major elbow flexors and extensors of the monkey (cynomolgus). Am J Anat 171:285–293.

Roy RR, Powell PL, Kanim P, Simpson DR. 1984. Architectural and histochemical analysis of the semitendinousus muscle in mice, rats, guinea pigs, and rabbits. J Morphol 181:155–160.

Sacks RD, Roy RR. 1982. Architecture of the hind limb muscles of cats: Functional significance. J Morphol 173:185–195.

Schenk P, Siebert T, Hiepe P, Güllmar D, Reichenbach JR, Wick C, Blickhan R, Böl M. 2013. Determination of three-dimensional muscle architectures: Validation of the DTI-based fiber tractography method by manual digitization. J Anat 223:61–68.

Shi J, Curtis N, Fitton LC, O'Higgins P, Fagan MJ. 2012. Developing a musculoskeletal model of the primate skull: Predicting muscle activations, bite force, and joint reaction forces using multibody dynamics analysis and advanced optimisation methods. J Theor Biol 310:21–30.

Sinha S, Sinha U, Edgerton VR. 2006. In vivo diffusion tensor imaging of the human calf muscle. J Magn Reson Imaging 24: 182–190.

Smith AL, Benazzi S, Ledogar JA, Tamvada K, Smith LCP, Weber GW, Spencer MA, Dechow PC, Grosse IR, Ross CF. 2015. Biomechanical implications of intraspecific shape variation in chimpanzee crania: Moving towards an integration of geometric morphometrics and finite element analysis. Anat Rec (Hoboken, NJ 2007) 298:122.

Smith K, Beighton D. 1986. The effects of the availability of diet on the levels of exoglycosidases in the supragingival plaque of macaque monkeys. J Dent Res 65:1349–1352.

Smith K, Beighton D. 1987. Proteolytic activities in the supragingival plaque of monkeys (Macaca fascicularis). Arch Oral Biol 32: 473–476.

Taylor AB, Eng CM, Anapol FC, Vinyard CJ. 2009. The functional correlates of jaw-muscle fiber architecture in tree-gouging and nongouging callitrichid monkeys. Am J Phys Anthropol 139:353–367.

Taylor AB, Vinyard CJ. 2013. The relationships among jaw-muscle fiber architecture, jaw morphology, and feeding behavior in extant apes and modern humans. Am J Phys Anthropol 151:120–134.

Taylor AB, Yuan T, Ross CF, Vinyard CJ. 2015. Jaw-muscle force and excursion scale with negative allometry in platyrrhine primates. Am J Phys Anthropol 158:242–256.

Terhune CE, Hylander WL, Vinyard CJ, Taylor AB. 2015. Jaw-muscle architecture and mandibular morphology influence relative maximum jaw gapes in the sexually dimorphic Macaca fascicularis. J Hum Evol 82:145–158.

Tsai HP, Holliday CM. 2011. Ontogeny of the Alligator cartilago transiliens and its significance for sauropsid jaw muscle evolution. PLoS One 6:e24935.

Tseng ZJ, Mcnitt-Gray JL, Flashner H, Wang X, Enciso R. 2011. Model sensitivity and use of the comparative finite element method in mammalian jaw mechanics: Mandible performance in the gray wolf. PLoS One 6:e19171.

Vickerton P, Jarvis J, Jeffery N. 2013. Concentration-dependent specimen shrinkage in iodine-enhanced microCT. J Anat 223:185–193.

Vinyard CJ, Wall CE, Williams SH, Hylander WL. 2008. Patterns of variation across primates in jaw-muscle electromyography during mastication. Integr Comp Biol 48:294–311.

Wall CE, Vinyard CJ, Williams SH, Johnson KR, Hylander WL. 2008. Specialization of the superficial anterior temporalis in baboons for mastication of hard foods. In: Primate craniofacial function and biology. Berlin: Springer. p. 113–124.

Wang Q, Smith AL, Strait DS, Wright BW, Richmond BG, Grosse IR, Byron CD, Zapata U. 2010. The global impact of sutures assessed in a finite element model of a macaque cranium. Anat Rec 293:1477–1491.

Ward SR, Lieber RL. 2005. Density and hydration of fresh and fixed human skeletal muscle. J Biomech 38:2317–2320.

Watson PJ, Gröning F, Curtis N, Fitton LC, Herrel A, McCormack SW, Fagan MJ. 2014. Masticatory biomechanics in the rabbit: A multi-body dynamics analysis. J R Soc Interface 11:20140564.

Weber E. 1846. Wagner's Handworterbuche der Physiologie. Braunschweig: Vieweg.

Weijs WA, Brugman P, Klok EM. 1987. The growth of the skull and jaw muscles and its functional consequences in the New Zealand rabbit (Oryctolagus cuniculus). J Morphol 194:143–161.

Winters TM, Takahashi M, Lieber RL, Ward SR. 2011. Whole muscle length-tension relationships are accurately modeled as scaled sarcomeres in rabbit hindlimb muscles. J Biomech 44:109–115.

4. Modelling developmental changes in masticatory function within *Macaca fascicularis*.

Edwin Dickinson, Kornelius F. Kupczik and Laura C. Fitton

In preparation for publication.

Abstract

Both soft- and hard-tissue components of the masticatory apparatus undergo significant anatomical changes during development. However, the combined effect of these changes upon the functional capacity of the masticatory system at various stages of development is not known. Here, we present a series of three-dimensional biomechanical models representing the masticatory apparatus of *M. fascicularis* at four stages of development (infant, juvenile, adult female, and adult male). We measure gape potential and maximum bite force in each model at four bitepoints along the dental row. We also evaluate biting performance at a series of predetermined gapes to simulate feeding performance on items of a controlled size. Spheres of an increasingly large diameter (0 cm – 5 cm) were placed at an incisor (I1) and premolar (P4) bitepoint, and biting performance was measured within each model. Finally, we present a hypothetical model in which a juvenile is iteratively warped towards an adult morphology. By accounting for changes in bite force and gape potential during each stage, we assess the impact of individual components of the masticatory system upon overall masticatory performance.

Maximum bite force and gape potential were both observed to increase consistently during development. Changes in muscle size contributed most significantly to increases in bite force potential, while craniofacial form imparted a more significant effect upon gape potential than muscle architectural changes. As a result, adults displayed an improved ability to consume larger and more mechanically challenging food items. This trend mirrors observed dietary shifts within this species towards the increased consumption of larger and more mechanically resistant foods with increasing age. These findings demonstrate the close relationship between masticatory form and dietary consistency during ontogeny, in which functional constraints imposed by the masticatory anatomy of younger individuals may impact upon dietary selection, precluding them from the exploitation of larger or more mechanically challenging food items which are consumed more frequently by adult conspecifics.

Introduction

The primate masticatory apparatus performs a diverse array of critical roles, which combine food acquisition and processing techniques with several non-masticatory functions such as social display behaviours (Hiiemae, 1984; Conroy, 1990; Fleagle, 1998). The functional capabilities of the masticatory system, particularly maximum bite force and gape, are therefore likely to represent key determinants of an individual's dietary and social ecology (Troisi *et al.,* 1990; Plavcan and van Schaik 1992; Taylor and Vinyard, 2009; Taylor *et al.*, 2018). Maximum bite force along the dental row may constrain the dietary repertoire by limiting the range of foodstuffs which can be exploited (Turnbull 1970); consequently, individuals that process more mechanically resistant food items often display adaptations towards generating high masticatory forces, such as increasing the mass and cross sectional area of the adductor musculature (Taylor and Vinyard, 2009; Santana *et al.,* 2010), and altering the lever-arm mechanics of the jaw so as to improve the mechanical advantage of the masticatory musculature (Singleton, 2005; Koyabu and Endo, 2010; Santana *et al.,* 2012; Dumont *et al.,* 2014). Adaptations within the facial skeleton towards resisting the associated increase in masticatory stresses have also been recorded (Anapol and Lee, 1994; Wright 2005; Daegling *et al., 2*011).

Maximum gape similarly impacts dietary selection by imposing limits on dental clearance, dictating the maximum size of food items that can be orally ingested (Perry and Hartstone-Rose 2010; Hartstone-Rose *et al.*, 2012). Maximizing clearance at the canine is also important in relation to an individual's social ecology, both in terms of enhancing the efficacy of canine-baring social display behaviours (Altmann 1967; Troisi *et al.,* 1990; Plavcan and van Schaik 1992; Plavcan, 2001) and ensuring sufficient canine gape as to enable the use of the canine as a weapon during direct agonistic conflicts (Plavcan and van Schaik, 1997; Soltis, 2004; Thierry, 2004). Indeed, a strong association has been demonstrated between maximum gape potential and canine height across catarrhine primates (Plavcan et al 1995; Hylander and Vinyard 2006, Hylander 2009; Hylander 2013). Adult male individuals of strongly competitive taxa display a marked increase in canine height, alongside adaptations towards enhancing maximum gape such as an elongation of the jaw and increases in the lengths of muscle fibers (Terhune *et al.,* 2015; Taylor *et al.,* 2018). As the success of both direct and indirect inter-male conflicts can have a direct effect upon the social status and , ultimately, reproductive success of an individual, adaptations towards maximizing gape have been hypothesized to experience strong positive selection within adult male catarrhines (Herring and Herring, 1974; Smith, 1984; Hylander, 2013; Terhune *et al., 2*015; Taylor et al., 2018).

Anatomical correlates of masticatory function

As noted above, adaptations towards enhancing bite force and gape potential may be observed in both soft- and hard-tissue components of the craniofacial complex. As the cross-sectional area of the adductor musculature is proportionally related to the maximal contractile force that these muscles may generate (Powell, 1984), increasing muscle volume enhances force generation potential (Gans and Bock, 1965; Gans, 1982; Lieber 1986). The length of constituent muscle fibers also affects contractile properties. As muscle fiber lengths are proportionally related to a muscle's contractile velocity and maximal excursion potential (Bodine *et al.,* 1982; Bang *et al., 2*006; Gokhin *et al., 2*009), longer muscle fibers facilitate an increase in maximum gape by extending the range of postures at which forces can be produced (Herring et al., 1979; Taylor and Vinyard 2004, 2009; Williams et al., 2009). For a given muscle volume, however, longer muscle fibers reduces force generation potential by reducing total fiber count and thus maximal force potential. As a result, a functional trade-off

exists within the architecture of skeletal muscle, in which a muscle cannot be wholly optimized for both maximizing force and gape (Gans and Bock, 1965; Gans, 1982; Lieber, 2002).

The spatial configuration of the adductor musculature relative to the jaw also impacts functional performance. This configuration can be divided into two distinct components: the relationship between each muscle of mastication and the TMJ (referred to as the lever arm, or 'in-lever' of the system), and that between the TMJ and the terminal bitepoint (the load arm, or 'out-lever') (Greaves 1978; Spencer 1999). For a given muscle, an increase in relative lever arm length – achieved either by reconfiguring the muscle's position relative to the temporomandibular joint, or by decreasing load arm length by moving the bitepoint closer to the TMJ – improves mechanical advantage (and thus the efficiency of force transfer to the bitepoint in question). By contrast, increasing relative load arm length enables the generation of wider gapes, by extending the distance between the dentition and the TMJ to create a wider arc of rotation around the joint center during jaw opening (Smith 1984; Williams *et al.,* 2009; Hylander, 2013). Meanwhile, reducing lever-arm lengths will decrease muscle stretch per degree of jaw rotation, similarly enabling a greater maximum attainable gape (Herring and Herring, 1974; Dechow and Carlson, 1990; Terhune *et al.,* 2015; Taylor *et al.,* 2018).

Developmental changes to the primate masticatory apparatus are likely to alter these relationships, and in so doing may impact upon overall functional performance. Throughout ontogeny, the primate face undergoes many changes in form, which include the elongation of the rostrum (Corner and Richtsmeier 1991; Richtsmeier *et al.,* 1993; O'Higgins and Jones 1998), lateral extension of the zygomatic arches (Cochard 1985), and an increase in both the length and breadth of the mandible associated with the eruption of the permanent dentition and the extension of the postcanine tooth row (Taylor 2002). Such changes affect biomechanical relationships within the masticatory apparatus (Singleton, 2015) and may impact upon overall masticatory performance during ontogeny. For example, an increase in jaw length enables wider absolute gapes at the anterior dentition per degree of jaw rotation, but decreases the mechanical advantage of these dental elements by placing them further from the temporomandibular joints (Radinsky, 1981; Dechow and Carlson, 1990; Spencer, 1999).

The muscles of mastication also undergo intrinsic structural changes during development, though detailed data on the nature and magnitude of such changes are largely unreported within primate taxa. During ontogeny, adductor muscle mass and cross-sectional area are both reported to increase (Cachel, 1984; Dickinson *et al.,* 2018; see also Herring and Wineski, 1986, Weijs *et al. ,* 1987 for non-primate taxa), resulting in an increase in contractile force potential. However, fiber lengths are also reported to increase substantively during development (Weijs *et al.,* 1987; Dickinson *et al.,* 2018), which may reduce force generation potential but increase maximum gape.

Understanding the interaction between these developmental changes is critical to interpreting the ontogeny of the primate face from a functional perspective. Quantifying the cumulative impact of ontogeny upon bite force and gape potential within a primate species also enables us to contextualize observed differences in dietary and social within primates during development, and to explore the extent to which these ecological differences reflect constraints imposed by the anatomy of the masticatory system at various stages of development.

Overview of the study

In a previous study, developmental changes to muscle architectural properties within an ontogenetic sequence of *Macaca fascicularis* were reported (Dickinson et al., 2018). Muscle mass, fiber lengths, and physiologic cross-sectional were all reported to increase during development, scaling with positive allometry relative to two biomechanical proxies (jaw length and condyle-molar length). These data suggest that both gape and bite force potential may increase within this species during development due to soft-tissue changes. However, the length of the jaw was also observed to scale with positive allometry (relative to basicranial length) during development, potentially reducing the mechanical advantage of the jaw adductors. Similarly, the height of the temporomandibular joint (TMJ) above the occlusal plane scaled with positive allometry relative to all size proxies, increasing muscle stretch per degree of jaw rotation (Dickinson *et al.,* 2018). The resultant effect of both soft- and hard-tissue changes upon the functional capacity of the masticatory system, and the magnitude of any changes in bite force and gape potential during ontogeny, therefore remains unknown. Similarly, the question of which anatomical components – muscle size, architectural properties, and craniofacial form – play the largest role in dictating developmental changes in functional performance is also yet to be addressed.

Here, we present a series of three-dimensional biomechanical models representing the masticatory apparatus of *M. fascicularis* at differing stages of development. Four models are presented, representing an infant, juvenile, adult female and adult male specimen, respectively. Through simple simulations of masticatory actions using multibody dynamics analysis (MDA), these models enable us to quantify the impact of developmental changes to the masticatory complex upon functional parameters of performance such as gape and bite force.

Multibody dynamic modelling techniques have been previously employed to investigate masticatory performance within several taxa (e.g. Langenbach *et al., 2*002; Sellers and Crompton 2004; Koolstra and van Eijden, 2005; Curtis *et al., 2*010; Bates and Falkingham, 2012; Gröning *et al., 2*013; Watson *et al., 2*014), including an adult male *M. fascicularis* (Curtis *et al., 2*008; Fitton *et al.,* 2012; Shi *et al.,* 2012). This technique enables the calculation of key parameters such as maximal gape potential and maximum bite force at various bitepoints along the dental row (Curtis *et al., 2*011). Moreover, it is possible to compare feeding performance between models for a range of food item sizes; while hypothetical models with modified parameters can also be constructed to explore form-function relationships within the masticatory system. Such analyses allow us to directly quantify how developmental changes to the masticatory complex impact upon functional parameters of performance across a series of scenarios.

Analysing ontogenetic changes in masticatory performance within *M. fascicularis* is of particular interest to studies of form-function relationships within the jaw, due to developmental shifts in both dietary and social ecology within this species during life. Observational data on feeding behaviours in wild Sumatran populations of *M. fascicularis* report that food item size increases during development (van Schaik and Noordwijk, 1986). The highest percentage of items consumed by infants were classified as small (<10mm diameter) foodstuffs, whilst juveniles fed most frequently on medium-sized foods (10-20mm). Meanwhile, adults most frequently fed on large (>20mm) food items (van Schaik and Noordwijk, 1986). Moreover, adults are further reported to consume a greater frequency of mechanically challenging food items than juvenile or infant conspecifics; just 21% of the food items ingested by infant individuals over the study period were classified as mechanically challenging,

compared to 47% for juveniles and 59% for adults (van Schaik and Noordwijk, 1986). These data suggest that changes to the masticatory complex during ontogeny may be critical in enabling older individuals to exploit larger and more mechanically-resistant foods which younger group members may be incapable of ingesting.

In addition to differences in dietary ecology between age groups, the role of the masticatory apparatus in social behaviours also differs between individuals of different ages and, within adults, between sexes. Wide-gape yawning displays, which are frequently employed as a means of dominance assertion between agonistic competitors (Altmann, 1967; Troisi et al., 1990; Thierry, 2000, 2004; Soltis, 2004), undergo an almost fourfold increase in frequency between sub-adulthood and adulthood in both males and females (Deputte, 1994). Within each age group, males demonstrated these postures more frequently than equivalently-aged females; though adult female yawning frequency was still greater than that of juvenile males (Deputte, 1994). The increased importance (as a means of establishing hierarchical status) and prevalence of such display behaviours within adult individuals, particularly adult males, has therefore been suggested to result in specific adaptations towards maximizing gape within these groups (Terhune *et al.,* 2015; Taylor *et al.,* 2018).

The developmental series of models presented here therefore allow us to explore the relationship between dietary/social ecology and masticatory anatomy, and to determine the extent to which differences or similarities in dietary ecologies between juvenile and adults represent constraints imposed by the anatomy of the masticatory system upon food selection.

Aims and Predictions

This study aims to quantify ontogenetic changes in masticatory performance within *M. fascicularis*, and evaluate the potential effect of such changes upon the dietary and social ecology of this species. We explore the hypothesis that functional differences in both force generation and gape generation potential between infant, juvenile and adult *M. fascicularis* contribute to niche separation in dietary ecology between these age groups by imposing constraints upon the dietary repertoire of younger individuals. We also aim to explore developmental and dimorphic differences in maximum gape potential, which may reflect the increased social pressures upon adult individuals (particularly adult males) towards an aggressive and highly competitive social environment in which wide-gape jaw postures are frequently used to assert social status. Finally, we aim to investigate how changes to individual anatomical elements during development– muscle size, architectural configuration, and craniofacial form – affect overall measures of masticatory performance.

Prediction 1. Gape generation

Due to the increasing prevalence and importance of wide-gape canine-baring display postures within adult *M. fascicularis*, we predict that maximum gape capacity will increase during development, with adults demonstrating an increase in gape potential relative to juveniles and infants. As a functional link between the increased canine size observed within adult male *M. fascicularis* and maximum gape has been previously demonstrated (Hylander, 2013), we also predict that our adult male model will demonstrate an increase in gape potential relative to our adult female model.

Prediction 2. Bite force generation

Assuming an approximately similar occlusal morphology, the ability to generate absolutely higher bite forces along the dental row enables the exploitation of more mechanically resistant food items.

As the proportion of mechanically challenging foodstuffs within the *M. fascicularis* diet increases during development (from 21% in infants to 47% in juveniles and 59% in adults), we predict that bite force will follow the same trend: with infants and juveniles demonstrating reduced bite force relative to adults at all bite points along the dental row at all degrees of gape. Maximizing bite force potential is also critical during inter-male conflicts, in which the canines are used as weapons during agonistic encounters with rivals. We therefore predict that our adult male model will demonstrate an increase in bite force potential relative to our adult female model.

Prediction 3. Maximum food item size vs. bite force capacity

As reported by van Schaik and Noordwijk (1986), younger individuals demonstrate a steep decline in the consumption of large (>20mm) foods relative to adults of either sex. This may reflect an inability among infant and juvenile individuals to generate appropriately high masticatory forces at gapes above this threshold, thus restricting their dietary repertoire. We therefore predict that juveniles and (particularly) infants will struggle to generate appropriate masticatory forces at gapes beyond this threshold, and demonstrate a smaller maximum food item size than adult individuals.

Prediction 4. Form-function relationships within the primate jaw

Within hypotheses 1-3, adults are predicted to produce larger gapes and higher magnitudes of bite force than juvenile conspecifics. Using a series of hypothetical models, it is possible to analyse which aspects of morphology contribute to these hypothesized differences, and the extent to which changes to individual components of the masticatory system impact upon functional performance. We predict that developmental increases in muscle mass will enhance bite force potential within *M. fascicularis* during development. Meanwhile, ontogenetic changes to muscle architectural properties and craniofacial form will serve to improve maximum gape potential. Though adaptations associated with an increased gape – including elongation of muscle fibers, and an extension of load-arm lengths within the masticatory apparatus – also reduce bite force potential, we predict that the magnitude of muscle growth is such that bite force will remain significantly higher within an adult morphology.

Materials and Methods

Specimen preparation

Four cranial specimens of *Macaca fascicularis* were selected for analysis from a collection housed at Hull York Medical School, York, United Kingdom. Each specimen had been previously dissected as part of a broader ontogenetic study, and architectural data for the temporalis, superficial masseter and deep masseter reported (Dickinson *et al.,* 2018). Specimens were selected to represent unique stages of development on the basis of mandibular dental eruption patterns. The youngest specimen (infant model) was in possession of only deciduous dental elements; the intermediate specimen (juvenile model) possessed permanent M_1 dentition in occlusion; and our two adult specimens (one male, one female) each demonstrated full permanent dentition. No specimens presented any recognisable soft or hard tissue deformities or pathologies.

Prior to dissection, CT scans were collected for each cranium. Three specimens were scanned using an X-Tek HMX160 µCT system ((XTek Systems Ltd, Tring, UK) housed at the University of Hull, UK and reconstructed in 8-bit using isometric voxel sizes of approximately 0.1 x 0.1 x 0.1 mm. The final specimen (adult male model) was scanned on a Medical CT system housed at York Medical Imaging Centre at a lower resolution (0.5 x 0.5 x 0.5 mm) due to constraints of specimen size.

The muscles of mastication were physically dissected from one half of the cranium, following the protocol outlined in Dickinson *et al.* (2018). In brief, the skin and any overlying facial musculature were first removed to expose the muscles of interest. These muscles were excised from their skeletal attachments using blunt dissection, blotted dry and trimmed of any excess connective tissues, and weighted to the nearest 0.0001 g using a Kern analytical balance (Kern & Sohn, Balingen, Germany). Muscles were then sectioned, following the orientation of visible surface fascicles, into anterior and posterior portions (the larger muscles of temporalis and superficial masseter were sectioned into three portions representing anterior, middle, and posterior portions respectively). Fibers were then measured from the exposed cross-sections at evenly-spaced intervals. Fiber lengths were measured as the distance between each fiber's proximal and distal points of termination, while the perpendicular distance between the distal junction of each fiber and the muscle's central tendon was also measured to calculate the angle of pennation. In addition to the temporalis, superficial masseter, and deep masseter analysed in the previous study, the medial pterygoid was also analysed here to ensure full representation of the adductor musculature within our model.

Following dissection, each specimen was immersed within a prewash solution of 20% w/v sucrose dissolved in distilled water for 48 to 72 hours, to minimise the risk of volume loss as a result of the subsequent staining procedure (Morhardt *et al., 2*016). The crania were then each immersed in separate 5L volumes of low concentration (1.25%) Lugol's Iodine (I2KI). A low concentration was selected to mitigate the risk of overstaining superficial layers of the adductor musculature and to further minimize the risk of change in muscle volume (Vickerton *et al., 2*013; Gignac *et al., 2*016). Throughout the staining process, specimens were placed upon a laboratory rocker to circulate the solution around each specimen. Total staining time ranged from 10 weeks (infant model) to 20 weeks (adult male model), after which all four specimens were subjected to a second µCT scan at a higher resolution (0.03 x 0.03 x 0.03 mm) using a custom-made diondo d3 mCT system housed at the Department of Human Evolution, Max Planck Institute for Evolutionary Anthropology, Leipzig.

Model construction

Resultant image stacks from both the initial and post-staining µCT scans were manually segmented in Avizo 8.0 (FEI, Thermo Fisher Scientific) to separate the cranium, mandible, temporalis, superficial masseter, deep masseter, and medial pterygoid. Bony elements were segmented from the first series of scans, while soft-tissue components were segmented from our stained µCT datasets. Three-dimensional (3D) volumes representing each object were then generated, and the two datasets merged together using manual landmark registration.

To reduce model processing times, each 3D volume was simplified down to approximately 250,000 surface elements (cranium) or 100,000 surface elements (other objects) (Figure 1). Landmark configurations were then placed upon each specimen, representing origination and insertion points for each muscle portion, using the three-dimensional muscle volumes as a guide. Division of each muscle into portions followed the protocol used for sectioning the tissue during dissection. This resulted in three portions (anterior, middle, and posterior) for the two larger adductors (temporalis and superficial masseter) and two portions – anterior and posterior – for the two smaller adductors (deep masseter and medial pterygoid).

Each model was imported into Maya 2016 (Autodesk Inc.) and rotated to a predefined coordinate system in order to align all models comparably. The aligned models were then scaled and converted into the appropriate file format (.asc) using a custom Matlab script (Vivian Allen, pers. comm.). The

resultant files were then uploaded into the software package SIMM (Software for Interactive Musculoskeletal Modeling) version 6.1, a musculoskeletal modelling toolkit that facilitates the construction and analysis of 3D biomechanical models (Delp and Loan, 1995).

Within SIMM, wrapping objects were applied to the model where direct connections between origination and insertion points would result in penetration of the muscle through bony elements, in order to replicate the biological curvature of each muscle strand (Figure 2). Each muscle strand was then assigned unique contractile properties representing the average fiber profiles of the corresponding muscle section. Fiber lengths were averaged across each muscle portion, while optimal fiber length (OFL) was estimated at 115% of this average length. To produce region-specific estimates of muscle force, physiologic cross-sectional area (PCSA) was calculated for each muscle portion and converted into force using a universal muscle strength estimate of 30 N/cm^2 (Richmond et al., 2005). As the musculature had undergone volumetric reduction due to formaldehyde fixation prior to our acquisition of the sample, it was necessary to adjust our measures of muscle mass prior to calculating PCSA. To account for this shrinkage, we conducted a comparison of four adult female specimens and four adult male specimens from our sample against a series of ten adult *M. fascicularis* specimens dissected by Terhune et al. (2015), of which five were female and five male. We observed a consistent reduction in volume across all muscles, with muscle volumes ranging from 38.0-46.4% of the baseline values reported by Terhune et al. (2015). As the degree of reduction was consistent within all muscles and across both sexes, we applied a universal correction factor of 2.4x to all muscle volumes to account for this effect. Finally, the tendon slack length (TSL) – which contributes to the elastic properties of the muscle – was estimated for each muscle strand using the numerical method (Manal and Buchanan, 2004), using published range of motion data for adult male and adult female *M. fascicularis* of 75° and 55° degrees respectively (Hylander, 2013). Range of motion data was subsequently estimated at 45° and 35° for the juvenile and infant models, respectively. The mean calculated tendon slack length was applied to each muscle strand, with the exception of strands for the temporalis muscle within the adult male model. A slightly larger TSL ($\bar{x}$ + 1 S.D.) was used for these strands to represent the larger tendon found within this muscle in adult males.

Force data was generated within each muscle strand using a standardized Hill-type model, with muscle strands considered active when between 50% and 160% of resting length (Figure 3). To minimize potential errors in the projection of passive forces towards extreme musculotendon lengths, only active muscle forces were considered within our analyses.

Data analysis in SIMM and quantification of performance

Both bony elements within each model (cranium and mandible) were modelled in SIMM as rigid bodies. The model was constrained to prohibit motion within the cranium, and to create a simple hinge at the temporomandibular joints around which the mandible experienced rotation. While these parameters represent a simplification of the biological condition, in which jaw abduction and adduction also involves anteroposterior translation of the mandibular condyle within the glenoid fossa, kinematic data was not available for individuals across the developmental spectrum. Further, by controlling each model to the same simple motion, we may directly compare the impact of differences in craniofacial morphology and muscle architectural properties upon masticatory performance between models. However, it should be understood that the kinematics of our simulated bites will differ slightly from those experienced by *M. fascicularis in vivo.*

Two performance variables (bite force and gape) were measured during our simulations. Potential bite force was measured at four bitepoints along the dental row: incisor (I1), canine (C), premolar (P4) and the most posterior tooth within the postcanine row (which ranged from dP4 to M3 within our specimens). As the deciduous fourth premolar (dP4) also served as the most posterior tooth within the infant postcanine dental row, the P4 bitepoint also serves as the most posterior bitepoint within this model. Maximum gape was measured at the most anteriorly-positioned tooth (I1). Each model underwent incremental jaw abduction from a neutral pose (with the jaw in occlusion), with the above variables recalculated at every 0.5° interval of rotation. This provided a measure of bite force potential across the full gape spectrum, as well as indicating the gape at which each model's maximum bite force could be produced and the magnitude of this peak in bite force potential. Once the total adductive force capability of the model dropped below 5N, the model was considered to have reached its maximal functional gape, and the jaw movement was returned towards its neutral pose.

In addition to testing the absolute limits of performance within each model, we also evaluated biting performance at a series of predetermined gapes to simulate feeding performance on items of a controlled size. Bite force was measured at an incisor (I1) and premolar (P4) bitepoint at 1cm, 2cm, 3cm, 4cm and 5cm gapes to assess both anterior and postcanine feeding performance on items of an increasing diameter. Such analyses enable us to investigate whether differences in masticatory performance during development may contribute to niche separation between the dietary repertoires of infant, juvenile and adult *M. fascicularis*.

In order to address the fourth hypothesis, we finally explore the role of individual components of the masticatory system through the use of an iteratively warped hypothetical model. Bite force and gape potential at a P4 bitepoint were measured in a series of models in which soft- and hard-tissue parameters were sequentially altered. To first establish the effect of muscle mass alone upon bite force and gape potential, we applied the muscle mass parameters of an adult model to an otherwise unaltered juvenile model. Secondly, we reconfigured the architectural parameters of this model to also match the adult configuration; creating a hybrid model in which fully adult musculature were combined with a juvenile craniofacial skeleton. Finally, we measure the impact of craniofacial form upon masticatory performance by comparing the results of this model to our original adult male model, which possessed identical muscular parameters but a distinct craniofacial configuration.

Results

Gape generation

Maximum gape increased consistently during development, and was greater within adult males than females, in line with Prediction 1. This increase was observed in both the degree of rotation possible at the temporomandibular joint, and the absolute gape generated at the anterior dentition as a result of this jaw movement (Table 1). The degree of rotation possible at the jaw joint increased from 28.5° in our infant model to 37° in the juvenile model, 51.5° in the adult female, and 65.5° in the adult male model. In terms of absolute gape, these translated to gape capacities of 20.4mm within the infant model, 36.7mm in the juvenile, 60.4 mm for the adult female and 88.0mm in the adult male model (Table 1).

Bite force generation

Maximum bite force at each bitepoint across the gape spectrum is presented in Figure 4. Bite force potential increased during development across all four bitepoints and was increased in adult males relative to females, supporting Prediction 2 (Table 2). Meanwhile, bite force was universally higher at more posteriorly-positioned teeth, due to their relatively shorter load arm lengths (Table 2).

Bite force potential was also evaluated at a series of predetermined gapes to simulate feeding performance on items of a controlled size. At each specified gape (1cm, 2cm, 3cm, 4cm and 5cm), the adult male model possessed the greatest bite force at both an anterior and postcanine bitepoint, followed by the adult female, the juvenile, and finally the infant model (Figure 5).

Not all models were capable of generating the full series of gapes. At the first incisor (I1), infants failed to generate bite forces above a 2cm gape, while juveniles could not generate gapes above a 3cm threshold. At the premolar bitepoint, meanwhile, infants could not generate bite forces with a 2cm clearance at the P4 while juveniles could not generate forces at a 3cm P4 gape. Our prediction that infants and juveniles would demonstrate a poor ability to feed on items above a 2cm diameter (Prediction 3) was therefore supported.

By contrast, both adult models attained a 5cm gape at the first incisor. However, adult males continued to generate relatively high bite forces at a 5cm gape, while females could produce only a small fraction of their maximum bite force as a 5cm incisor gape approached their maximal functional limit. Further, adult females could not reach a 5cm gape at the P4. Our adult male model could successfully accommodate a 5 cm at this bitepoint; however, only a small amount of potential bite force (20N) could be generated at this gape (Figure 5).

Hypothetical model and form-function hypothesis testing

The addition of an adult muscle mass to our initial juvenile model resulted in a significant increase in bite force potential (Figure 6A), in line with Prediction 4. Additionally adding adult architectural properties to the model resulted in a decrease in bite force potential, due to the longer muscle fibers found within the adult condition. Bite force was significantly higher in magnitude within this model, however, than in our original juvenile model. Finally, the effect of an adult craniofacial configuration was a further reduction in maximum bite force potential, demonstrating the improved mechanical efficiency of the juvenile facial skeleton in terms of force transfer from the adductor musculature to a P4 bitepoint (Figure 6C).

In terms of gape potential, meanwhile, allocating adult muscle mass increases gape potential by universally increasing bite force potential, thus translating the threshold below which adductive force becomes negligible to a later point within the gape cycle (Figure 6B, 6C). Allocating adult architectural properties further increases maximal gape capacity, in line with Prediction 4, as the longer fibers found within the jaw adductors of adult males result in an increased excursion potential. Finally, the effect of an adult craniofacial configuration is an additional increase in potential gape, further supporting Prediction 4 and demonstrating that the craniofacial configuration observed within adult males is significantly better at producing wide gapes than the juvenile facial skeleton (albeit at a slight cost to the efficiency of force transmission) (Figure 6B, 6C).

Discussion

Validation of the model

To assess the biological validity of this model, both bite force and gape data were compared to previously published findings on the functional capabilities of the masticatory apparatus within *Macaca*. Our bite force estimations were compared to *in vivo* bite force data collected through electric stimulation of the adductor musculature within anaesthetized specimens of the sister taxon *Macaca mulatta* (Dechow and Carlson, 1990). Within this study, maximum occlusal forces were measured with a bite force transducer positioned at an incisor, premolar, and molar bitepoint for juvenile, adult female, and adult male individuals across a 132 specimen sample. The results of our simulation accord well with these published findings. Peak occlusal forces at the incisors averaged 70.3N in juveniles, 133.1N in adult females, and 151.1N in adult males; our *in silico* estimates of maximal incisor bite forces within *M. fascicularis* measured 51.6N in juveniles, 98.3N in adult females, and 184.7N in adult males. At a molar bitepoint, meanwhile, Dechow and Carlson (1990) report peak occlusal forces of 139.8N in juveniles, 286.2N in adult females, and 369.3N in adult males, which closely correspond to our bite force estimates of 120N (juvenile), 237.4N (adult female) and 436.1N (adult male) within *M. fascicularis*. While some discrepancies between these results are expected (both due to minor anatomical differences between the sister taxa, and the differing methodologies employed), the strong congruence between these data suggest validity of this biomechanical model.

Our estimates of maximal potential gape were compared to data reported by Hylander *et al.* (2013) in which maximal jaw rotation was measured in a series of anaesthetized adult *M. fascicularis*, comprising both male and female specimens. A maximal rotation of 55° was reported for adult females, and 74° for adult males. These data correspond well to our predictions of maximum gape generated within our adult female and male models, which report maximal jaw rotations of 51.5° and 65.5°, respectively. This agreement further supports our interpretation of biological validity within our model.

The ontogeny of gape within *M. fascicularis*

Our data demonstrate that maximum gape increases significantly during development, both in terms of the degree of jaw rotation permitted at the temporomandibular joint and in the absolute inter-tooth distances generated during maximal jaw abduction. To facilitate this increase in gape potential, several anatomical adaptations towards maximizing gape are observed within older individuals, most prominently adult males. Changes in craniofacial form during ontogeny serve to increase maximum gape by elongating the jaw, which improves gape (Fig. 3B, 3C), even at the cost of mechanical advantage (3A). Similarly, elongation of fiber lengths between juveniles and adults help to maximize gape potential by increasing muscle excursion potential (Fig. 3B, 3C). As a result, both the degree of jaw rotation (65.5°) and absolute gape potential (88.0 mm) within our adult male model far exceed the capabilities of our juvenile (37°; 36.7 mm) and adult female (51.5°; 60.4mm) models (Table 1).

Differences in social ecology might contribute to these observed developmental changes in maximum gape. Adult males have been theorized to experience particularly strong pressures towards maximizing the efficacy of canine-baring display behaviours (Plavcan and van Schaik, 1997; Hylander, 2013; Terhune *et al.,* 2015; Taylor *et al.,* 2018) and employ such behaviours more frequently than either juveniles or adult females (Deputte, 1994). An increase in gape potential

within males is also required to ensure requisite canine clearance for the enlarged dental elements found within these individuals (Plavcan, van Schaik and Kappeler, 1995; Hylander and Vinyard, 2006; Hylander, 2009; Hylander, 2013).

As well as maximizing the efficacy of social display behaviours, increases in gape potential during development also impart advantages to older individuals in terms of dietary ecology. Enhancing gape potential broadens the dietary niche by allowing adults to ingest larger food items; indeed, as illustrated in figure 5, ontogenetic changes to masticatory form impart significant effects upon the maximum size of foodstuffs which may be consumed. At a P_4 bitepoint, juveniles can generate only 23N of bite force on a 2cm diameter food item, while a 3cm diameter object could not be accommodated between these teeth. By contrast, adult females can accommodate objects up to 4cm (though bite force potential approaches negligible margins at this gape), while adult males can produce meaningful bite forces at a 4cm gape and can even accommodate 5cm food items between the premolars (Figure 5). A similar trend is also demonstrated for the incisors (Figure 5), though all individuals show increases in gape potential (and reductions in bite force potential) at this more anteriorly-positioned bitepoint due to the wider absolute gapes generated at the incisor during jaw rotation, and the decreased mechanical advantage of the adductor musculature at this bitepoint.

Importantly, these findings mirror reported trends in feeding behaviours within wild *M. fascicularis*. Observational data demonstrate that infants and juveniles ingest lower proportions of large (>20mm) food items compared to adults, while infants also exploit fewer medium-sized (10-20 mm diameter) relative to juveniles (van Schaik and Noordwijk, 1986). As these food items approach the functional limits of maximum ingestive food item size predicted within infants and juveniles by our biomechanical models, it seems likely that differences in dietary consistency during development may reflect functional constraints imposed by the masticatory anatomy of younger individuals upon dietary selection, precluding them from the exploitation of larger food items which are consumed more frequently by adult conspecifics.

The ability of larger-bodied, older individuals to exploit a wider diversity of food items may reflect a form of niche diversification; by broadening their subsistence pool, older individuals may more easily fulfil the elevated caloric demands enforced by their increased body sizes (within *Papio anubis*, which shows a similar level of dimorphism to *M. fascicularis*, resting metabolic rate (RMR) is almost twice as high in adult males (798 kcal/day) than adult females (434 kcal/day), while the caloric demands of immature individuals are hypothesized to be lesser still (Leonard and Robertson, 1992)). This may be of particular importance during periods of resource scarcity (initiated either by the seasonal absence of preferred foods, or environmental factors which limit resource abundance) in which the ability to fulfil daily caloric needs becomes more difficult, particularly for larger individuals.

The ontogeny of bite force within *M. fascicularis*

Our findings demonstrate that maximum potential bite force increases during development, and is greater within adult males than females, across a range of bitepoints (Table 2). The universal increase in bite force potential during development appears to reflect increases in overall muscle size between age groups. Though infants and juveniles present both shorter muscle fibers and a more mechanically advantageous craniofacial form (Figure 6B, 6C), the overall increase in muscle size (summed adductor muscle mass is 229% greater in juveniles compared to infants, 294% greater in adult females compared to juveniles, and 323% greater in adult males compared to adult females) and resultant PCSA drives significant increases in bite force potential between each model. The

magnitude of this effect is illustrated in Figure 6A, in which the addition of adult muscle mass to our juvenile model results in a ~900% increase in bite force potential.

From a functional perspective, the limitations placed on force production by the smaller muscles found in juveniles and (particularly) infants may provide an anatomical explanation for observed dietary differences across the developmental trajectory of *M. fascicularis*. Feeding observational data from van Schaik and Noordwijk (1986) report that only 21% of the food items ingested by infant individuals were considered mechanically challenging, compared to 47% for juveniles and 59% for adults. As previously discussed, the ability of larger-bodied, older individuals to exploit a wider diversity of food items may represent; an important form of niche diversification; while the additional muscle mass observed within adults – particularly adult males – may also serve a secondary role in minimizing the accumulation of muscle fatigue within the masticatory apparatus during extended feeding bouts necessitated by their increased caloric demands.

An increase in bite force potential during development might also impart benefits beyond the sphere of dietary ecology. Though adult male and female *M. fascicularis* exploit a similar proportion of mechanically resistant foods (van Schaik and Noordwijk, 1986), males possess muscles three times as large, and can produce anterior bite forces of twice the magnitude attainable by females (Table 2; Figure 4). Such defined dimorphism in bite force potential might indicate the importance of maximizing bite force for adult males within a social context, in which the jaw is used as a weapon during agonistic conflicts. Both direct and indirect aggressive conflicts between male *M. fascicularis* are common (Altmann, 1967; Thierry, 2004; Soltis, 2004), while other features of the masticatory apparatus – such as the increased size of the canine dentition in adult males – have similarly been suggested as an adaptation towards their highly competitive social ecology (Plavcan, van Schaik and Kappeler, 1995; Plavcan and van Schaik, 1997; Hylander, 2013). Maximizing anterior bite force within adult males might therefore represent part of a broad suite of anatomical adaptations within *Macaca* towards a social environment in which agonistic conflicts represent a key determinant of an individual's hierarchical status and, ultimately, reproductive potential.

Form-function relationships within the primate masticatory system

Analysis of our hypothetical model demonstrates that both soft- and hard-tissue changes during ontogeny affect masticatory function within *M. fascicularis*. Muscle architectural properties, driven by an increase in fiber lengths across the adductor complex, display adaptations towards maximizing gape by increasing excursion potential during ontogeny. Simultaneously, elongation of the jaw and changes to the lever-arm mechanics of the masticatory musculature enhance gape potential from a biomechanical perspective. In terms of magnitude, these craniofacial changes were observed to result in a more significant increase in gape potential than changes to muscle architectural properties (Figure 6B, 6C).

While enhancing gape, however, both architectural and biomechanical changes impart a negative impact upon bite force potential (Figure 6A). Longer muscle fibers reduce the PCSA, and therefore intrinsic force potential, of a muscle; meanwhile, a longer mandible reduces the mechanical advantage of the jaw adductors by increasing the load-arm lengths of the masticatory musculature at bitepoints along the dental row. However, a developmental decline in overall bite force bite potential is circumvented by simultaneous increases in muscle mass throughout the adductor complex. Moreover, the magnitude of this increase is sufficient that, despite a decline in mechanical efficiency, bite force potential is significantly enhanced during development.

This relationship demonstrates that while a functional trade-off between bite force and gape exists within individual components of the masticatory system, developmental changes across this system as a whole can function to circumvent this dichotomy. Functional integration between soft- and hard-tissue components of the masticatory apparatus during development allow *M. fascicularis* to overcome these individual trade-offs, enabling both bite force and gape to increase during ontogeny. As previously discussed, this may be critical in enabling older individuals to occupy their unique dietary and social niche, in which a diverse array of pressures may exhibit positive selection for enhancing both bite force and gape potential. This relationship reflects the highly integrated nature of the primate masticatory apparatus (Vinyard *et al.,* 2003; Ross *et al., 2*012), in which numerous components contribute to single masticatory functions. As a result, many possible adaptations may incur similar functional effects, and changes to specific components may be counterbalanced by adaptations within other portions of this system to produce an optimal morphology that supports the specific dietary (or social) niche of a species (Wainwright *et al.,* 2005).

Modelling masticatory function

Our findings demonstrate clear functional differences in both bite force and gape potential within *M. fascicularis* during development, with younger individuals demonstrating reduced bite force potential and a smaller maximum gape (measured in terms of both jaw rotation potential and absolute gape distances). These differences in masticatory performance are hypothesized to contribute towards differences in dietary consistency observed during development within this species, in which functional constraints imposed by the masticatory anatomy of infants and juveniles preclude these individuals from exploiting the full range of foods available to adult conspecifics, such that younger individuals consume relatively fewer large and mechanically challenging food items relative to adult individuals (as reported by van Schaik and Noordwijk, 1986).

It should be noted, however, that not all primates display similar patterns of dietary variation during development. Within *Cercocebus atys*, a durophagous specialist within the cercopithecoid clade, four of the five foods most frequently consumed by adults (the nut *Sacoglottis gabonensis,* the seeds of *Anthonata fragrans*, the fruits *Dialium aubrevillei*, and assorted fungi) were also among the five most-consumed foods by juveniles (McGraw *et al.,* 2011). Of these food items, adults consumed significantly more *D. aubrevillei* and fungi, while nonadults ate significantly more *S. gabonensis* and *A. fragrans*. As the nuts *S. gabonensis* rank among the most mechanically challenging foods consumed by this taxon (with a Young's modulus in excess of 200 MPa, and toughness values of 2,000-7,000 Jm^{-2}) as well as being relatively large (averaging 32 mm along their major axis and 24 mm along their minor axis; Daegling *et al., 2*011), juvenile *C. atys* demonstrate a dietary ecology which imposes similar or greater demands upon the masticatory apparatus than that of adult conspecifics (McGraw *et al.,* 2011). Further research exploring ontogenetic patterns of masticatory performance within this taxon, or indeed within other species which demonstrate similar consistency in dietary ecology during development, would therefore prove highly interesting. Differences in fiber length and PCSA have previously been shown to exist between adult male and female *C. atys* (Taylor *et al.,* 2018), and quantifying similar variables throughout ontogeny would provide a valuable insight into the impact of dietary ecology upon the scaling of bite force potential during development.

Similarly, while the series of models presented here incorporate data on muscle size, configuration, architecture and craniofacial form to quantify masticatory performance, a number of factors not analysed here also contribute towards feeding performance. Most notably, changes in dental

morphology during development may alter the mechanics of food breakdown between juvenile and adult individuals. The postcanine dentition within juveniles represents reduced degrees of dental wear compared to the corresponding occlusal morphologies of found within adults (*e.g.* Dennis *et al.,* 2004; Cuozzo *et al.,* 2014). The increased sharpness of newly-erupted dental cusps in younger individuals may enable food items to be processed with reduced masticatory forces, allowing juveniles to overcome their relative disadvantage in masticatory force production relative to adult conspecifics (Popowics and Fortelius, 1997; Evans and Sanson, 1998; Logan and Sanson, 2002; Lucas, 2004).

Beyond the sphere of dietary ecology, it is equally important to consider the effects of a species' social environment and ecology upon anatomical features of the masticatory apparatus. A number of recent studies (Plavcan *et al.,* 1995; Plavcan and van Schaik, 1997; Hylander, 2013; Terhune *et al., 2*015; Taylor *et al.,* 2018) have emphasized the importance of social display as a factor driving masticatory form within primates, particularly within adult males. Indeed, Taylor *et al.* (2018) demonstrate that, even within strongly durophagous primate taxa, adaptations towards maximizing gape supersede those towards the enhancement of bite force potential. As a result, they argue that the strongest selective pressures experienced by the masticatory apparatus within papionins may be towards maximizing the efficacy of gape display behaviours, even at the cost of mechanical advantage and bite force (Taylor *et al.,* 2018). The findings of our study, which demonstrate that adult males do indeed display significant advantages in terms of gape potential relative to females (Table 1) and that both soft- and hard-tissue features contribute towards gape enhancement during development (Figure 6B, 6C) provide support for these hypotheses. These findings mirror results by Terhune *et al.* (2015) on differences in masticatory form between adult male and female *M. fascicularis*, which similarly report a number of adaptations within the male masticatory system towards gape maximization (Terhune *et al.,* 2015).

While clarity on dimorphic differences in the primate masticatory apparatus has emerged within recent years, our results also show that adult females display adaptations towards gape enhancement relative to juveniles. Adult females also participate in social display behaviours as a means of establishing social rank, albeit less frequently than their male counterparts (Troisi *et al.,* 1990; Deputte, 1994; Thierry, 2004; Soltis, 2004). Future studies should therefore endeavour to further explore the social roles of the masticatory apparatus within both juvenile and adult individuals across a broad range of primate taxa. Such data, in addition to anatomical observations on the developing masticatory apparatus within other primate species, will be crucial to our understanding of how social behaviours can be seen to relate to anatomical features of the jaw, and the extent to which ontogenetic and dimorphic differences in masticatory form reflect the social ecology of a species.

Conclusions

Our findings show that both gape and bite force potential (at all bitepoints along the dental row) increase within *M. fascicularis* during development, and are enhanced within adult males relative to females. As a result, adults showed the greatest potential for feeding on larger and more mechanically resistant food items, followed by juveniles, with infants reporting the lowest ability to feed on such foods. These findings support observations of niche separation within the dietary ecology of *M. fascicularis*, in which adults are reported to exploit a higher proportion of large and mechanically challenging foods than juvenile or infant conspecifics. Such data demonstrate the close relationship between masticatory form and dietary consistency during ontogeny, in which functional

constraints imposed by the masticatory anatomy of younger individuals may impact upon dietary selection, precluding them from the exploitation of larger or more mechanically challenging food items which are consumed more frequently by adult conspecifics.

While masticatory anatomy therefore corresponds to developmental shifts in dietary ecology, ontogenetic and dimorphic differences in masticatory form also appear to reflect the social environment of a species. Indeed, though adult male and female *M. fascicularis* exploit a similar diet, males demonstrate both an increase in bite force potential and a significantly wider maximum gape, which may reflect unique social pressures towards direct and indirect inter-male conflicts. These data fall in line with an increasing volume of recent literature emphasizing the importance of maximizing gape for social display behaviors within adult male papionins (*e.g.* Terhune *et al*., 2015; Taylor *et al.,* 2018), which suggest that social pressures towards enhancing gape for canine-baring displays may be critical in driving differences in craniofacial anatomy between male and female individuals. It is therefore important to consider components of the masticatory system not just in light of dietary ecology and feeding performance, but to account for the diverse roles performed by the masticatory system within primates and to consider how this broad array of competing pressures may interact in an evolutionary context to produce the diversity in craniofacial form observed across extant primate taxa.

Literature Cited

Altmann S. 1967. The structure of primate social communication. In: Altmann S, editor. Social communication among primates. Chicago: University of Chicago Press. p 3325-3362.

Anapol F, and Lee S. 1994. Morphological adaptation to diet in platyrrhine primates. American Journal of Physical Anthropology 94(2):239-261.

Bang M-L, Li X, Littlefield R, Bremner S, Thor A, Knowlton KU, Lieber RL, and Chen J. 2006. Nebulin-deficient mice exhibit shorter thin filament lengths and reduced contractile function in skeletal muscle. The Journal of cell biology 173(6):905-916.

Bates KT, and Falkingham PL. 2012. Estimating maximum bite performance in Tyrannosaurus rex using multi-body dynamics. Biology Letters:rsbl20120056.

Bodine SC, Roy R, Meadows D, Zernicke R, Sacks R, Fournier M, and Edgerton V. 1982. Architectural, histochemical, and contractile characteristics of a unique biarticular muscle: the cat semitendinosus. Journal of Neurophysiology 48(1):192-201.

Cachel S. 1984. Growth and allometry in primate masticatory muscles. Arch Oral Biol 29(4):287-293.

Cochard LR. 1985. Ontogenetic allometry of the skull and dentition of the rhesus monkey (Macaca mulatta). In: Jungers WL, editor. Size and scaling in primate biology. New York: Plenum Press. p 231-255.

Conroy GC. 1990. Primate Evolution. New York: Norton.

Corner BD, and Richtsmeier JT. 1991. Morphometric analysis of craniofacial growth in Cebus apella. American Journal of Physical Anthropology 84(3):323-342.

Cuozzo FP, Head BR, Sauther ML, Ungar PS, and O'Mara MT. 2014. Sources of tooth wear variation early in life among known-aged wild ring-tailed lemurs (Lemur catta) at the Bezà Mahafaly Special Reserve, Madagascar. American journal of primatology 76(11):1037-1048.

Curtis N. 2011. Craniofacial biomechanics: an overview of recent multibody modelling studies. Journal of anatomy 218(1):16-25.

Curtis N, Jones ME, Evans SE, Shi J, O'Higgins P, and Fagan MJ. 2010. Predicting muscle activation patterns from motion and anatomy: modelling the skull of Sphenodon (Diapsida: Rhynchocephalia). Journal of the Royal Society Interface 7(42):153-160.

Curtis N, Kupczik K, O'higgins P, Moazen M, and Fagan M. 2008. Predicting skull loading: applying multibody dynamics analysis to a macaque skull. The Anatomical Record 291(5):491-501.

Daegling DJ, McGraw WS, Ungar PS, Pampush JD, Vick AE, and Bitty EA. 2011. Hard-object feeding in sooty mangabeys (Cercocebus atys) and interpretation of early hominin feeding ecology. PLoS One 6(8):e23095.

Dechow PC, and Carlson DS. 1990. Occlusal force and craniofacial biomechanics during growth in rhesus monkeys. American Journal of Physical Anthropology 83(2):219-237.

Delp SL, and Loan JP. 1995. A graphics-based software system to develop and analyze models of musculoskeletal structures. Computers in biology and medicine 25(1):21-34.

Dennis JC, Ungar PS, Teaford MF, and Glander KE. 2004. Dental topography and molar wear in Alouatta palliata from Costa Rica. American Journal of Physical Anthropology 125(2):152-161.

Deputte BL. 1994. Ethological study of yawning in primates. I. Quantitative analysis and study of causation in two species of Old World monkeys (Cercocebus albigena and Macaca fascicularis). Ethology 98(3-4):221-245.

Dickinson E, Stark H, and Kupczik K. 2018. Non-Destructive Determination of Muscle Architectural Variables Through the Use of DiceCT. The Anatomical Record 301(2):363-377.

Dumont ER, Samadevam K, Grosse I, Warsi OM, Baird B, and Davalos LM. 2014. Selection for mechanical advantage underlies multiple cranial optima in new world leaf-nosed bats. Evolution 68(5):1436-1449.

Evans A, and Sanson G. 1998. The effect of tooth shape on the breakdown of insects. Journal of Zoology 246(4):391-400.

Fitton LC, Shi J, Fagan M, and O'Higgins P. 2012. Masticatory loadings and cranial deformation in Macaca fascicularis: a finite element analysis sensitivity study. Journal of Anatomy 221(1):55-68.

Fleagle JG. 1998. Primate adaptation and Evolution, 2nd Ed. New York: Academic Press.

Gans C. 1982. Fiber architecture and muscle function. Exercise and sport sciences reviews 10(1):160-207.

Gans C, and Bock WJ. 1965. The functional significance of muscle architecture--a theoretical analysis. Ergebnisse der Anatomie und Entwicklungsgeschichte 38:115.

Gignac PM, Kley NJ, Clarke JA, Colbert MW, Morhardt AC, Cerio D, Cost IN, Cox PG, Daza JD, and Early CM. 2016. Diffusible iodine-based contrast-enhanced computed tomography (diceCT): an emerging tool for rapid, high-resolution, 3-D imaging of metazoan soft tissues. Journal of anatomy 228(6):889-909.

Gokhin DS, Bang ML, Zhang J, Chen J, and Lieber RL. 2009. Reduced thin filament length in nebulin-knockout skeletal muscle alters isometric contractile properties. Am J Physiol Cell Physiol 296(5):C1123-1132.

Greaves WS. 1978. The jaw lever system in ungulates: a new model. Journal of Zoology 184(2):271-285.

Gröning F, Jones ME, Curtis N, Herrel A, O'Higgins P, Evans SE, and Fagan MJ. 2013. The importance of accurate muscle modelling for biomechanical analyses: a case study with a lizard skull. Journal of The Royal Society Interface 10(84):20130216.

Hartstone-Rose A, Perry JM, and Morrow CJ. 2012. Bite force estimation and the fiber architecture of felid masticatory muscles. The Anatomical Record 295(8):1336-1351.

Herring SW, Grimm AF, and Grimm BR. 1979. Functional heterogeneity in a multipinnate muscle. Developmental Dynamics 154(4):563-575.

Herring SW, and Herring SE. 1974. The superficial masseter and gape in mammals. The American Naturalist 108(962):561-576.

Herring SW, and Wineski LE. 1986. Development of the masseter muscle and oral behavior in the pig. Journal of Experimental Zoology Part A: Ecological Genetics and Physiology 237(2):191-207.

Hiiemae K. 1984. Functional aspects of primate jaw morphology. Food acquisition and processing in primates: Springer. p 257-281.

Hylander WL. 2009. The functional significance of canine height reduction in early hominins. Am J Phys Anthropol Suppl 48:154.

Hylander WL. 2013. Functional links between canine height and jaw gape in catarrhines with special reference to early hominins. Am J Phys Anthropol 150(2):247-259.

Hylander WL, and Vinyard CJ. 2006. The evolutionary significance of canine reduction in hominins: functional links between jaw mechanics and canine size. Am J Phys Anthropol Suppl 42:107.

Koolstra J, and Van Eijden T. 2005. Combined finite-element and rigid-body analysis of human jaw joint dynamics. Journal of biomechanics 38(12):2431-2439.

Koyabu DB, and Endo H. 2010. Craniodental mechanics and diet in Asian colobines: morphological evidence of mature seed predation and sclerocarpy. Am J Phys Anthropol 142(1): 137-48.

Langenbach G, Zhang F, Herring S, and Hannam A. 2002. Modelling the masticatory biomechanics of a pig. Journal of Anatomy 201(5):383-393.

Leonard WR, and Robertson ML. 1992. Nutritional Requirements and Human Evolution: A Bioenergetics Model. American Journal of Human Biology 4:179-195.

Lieber RL. 1986. Skeletal muscle adaptability. I: Review of basic properties. Developmental Medicine & Child Neurology 28(3):390-397.

Lieber RL. 2002. Skeletal muscle structure, function, and plasticity: Lippincott Williams & Wilkins.

Lucas PW. 2004. Dental functional morphology: how teeth work: Cambridge University Press.

Manal K, and Buchanan TS. 2004. Subject-specific estimates of tendon slack length: a numerical method. Journal of Applied Biomechanics 20(2):195-203.

McGraw WS, Vick AE, and Daegling DJ. 2011. Sex and age differences in the diet and ingestive behaviors of sooty mangabeys (Cercocebus atys) in the Tai Forest, Ivory Coast. Am J Phys Anthropol 144(1):140-153.

Morhardt AR, RC; Witmer, LM. 2016. ABSTRACT: Diffusible iodine-based contrast enhancement of large, post-embryonic, intact vertebrates for CT scanning: staining, destaining, and long-term storage. International Congress of Vertebrate Morphology. Washington, D.C.

O'Higgins P, and Jones N. 1998. Facial growth in Cercocebus torquatus: an application of three-dimensional geometric morphometric techniques to the study of morphological variation. Journal of Anatomy 193(2):251-272.

Perry JM, and Hartstone-Rose A. 2010. Maximum ingested food size in captive strepsirrhine primates: scaling and the effects of diet. American Journal of Physical Anthropology 142(4):625-635.

Plavcan JM. 2001. Sexual dimorphism in primate evolution. American Journal of Physical Anthropology 116(S33):25-53.

Plavcan JM, and van Schaik CP. 1992. Intrasexual competition and canine dimorphism in anthropoid primates. American Journal of Physical Anthropology 87(4):461-477.

Plavcan JM, and van Schaik CP. 1997 Interpreting hominid behavior on the basis of sexual dimorphism. J Hum Evol 32:345–374.

Plavcan JM, van Schaik CP, Kappeler PM. 1995. Competition, coalitions and canine size in primates. J Hum Evol 28:245–276.

Popowics TE, and Fortelius M. 1997. On the cutting edge: tooth blade sharpness in herbivorous and faunivorous mammals. Annales Zoologici Fennici: JSTOR. p 73-88.

Powell PL, Roy RR, Kanim P, Bello MA, and Edgerton VR. 1984. Predictability of skeletal muscle tension from architectural determinations in guinea pig hindlimbs. Journal of Applied Physiology 57(6):1715-1721.

Radinsky LB. 1981. Evolution of skull shape in carnivores I: Representative modern carnivores. Biol J Linn Soc 15:369–388.

Richmond BG, Wright BW, Grosse I, Dechow PC, Ross CF, Spencer MA, and Strait DS. 2005. Finite element analysis in functional morphology. The Anatomical Record 283(2):259-274.

Richtsmeier JT, Cheverud J, Danahey S, Corner B, and Lele S. 1993. Sexual dimorphism of ontogeny in the crab-eating macaque (Macaca fascicularis). Journal of Human Evolution 25(1):1-30.

Ross CF, Iriarte-Diaz J, and Nunn CL. 2012. Innovative approaches to the relationship between diet and mandibular morphology in primates. International Journal of Primatology 33(3):632-660.

Santana SE, Dumont ER, and Davis JL. 2010. Mechanics of bite force production and its relationship to diet in bats. Functional Ecology 24(4):776-784.

Santana SE, Grosse IR, and Dumont ER. 2012. Dietary hardness, loading behavior, and the evolution of skull form in bats. Evolution 66(8):2587-2598.

Sellers WI, and Crompton RH. 2004. Using sensitivity analysis to validate the predictions of a biomechanical model of bite forces. Annals of Anatomy-Anatomischer Anzeiger 186(1):89-95.

Shi J, Curtis N, Fitton LC, O'Higgins P, and Fagan MJ. 2012. Developing a musculoskeletal model of the primate skull: predicting muscle activations, bite force, and joint reaction forces using multibody dynamics analysis and advanced optimisation methods. Journal of theoretical biology 310:21-30.

Singleton M. 2005. Functional shape variation in the cercopithecine masticatory complex. In: Slice DE, editor. Modern Morphometrics in Physical Anthropology. New York: Plenum Press. p 319-348.

Singleton M. 2015. Functional geometric morphometric analysis of masticatory system ontogeny in papionin primates. Anat Rec (Hoboken) 298(1):48-63.

Smith R. 1984. Comparative functional morphology of maximum mandibular opening (gape) in primates. In: Chivers DJ WB, Bilsborough A., editor. Food acquisition and processing in primates. New York: Plenum Press. p 231-255.

Soltis J. 2004. Mating Systems. In: Thierry B, Singh M, and Kaumanns W, editors. Macaque societies: a model for the study of social organization. Cambridge: Cambridge University Press. p 135-155.

Spencer MA. 1999. Constraints on masticatory system evolution in anthropoid primates. American Journal of Physical Anthropology 108(4):483-506.

Taylor AB. 2002. Masticatory form and function in the African apes. American Journal of Physical Anthropology 117(2):133-156.

Taylor AB, Terhune CE, Toler M, Holmes M, Ross CF, and Vinyard CJ. 2018. Jaw-Muscle Fiber Architecture and Leverage in the Hard-Object Feeding Sooty Mangabey are not Structured to Facilitate Relatively Large Bite Forces Compared to Other Papionins. The Anatomical Record 301(2):325-342.

Taylor AB, and Vinyard CJ. 2004. Comparative analysis of masseter fiber architecture in tree-gouging (Callithrix jacchus) and nongouging (Saguinus oedipus) callitrichids. Journal of Morphology 261(3):276-285.

Taylor AB, and Vinyard CJ. 2009. Jaw-muscle fiber architecture in tufted capuchins favors generating relatively large muscle forces without compromising jaw gape. J Hum Evol 57(6):710-720.

Terhune CE, Hylander WL, Vinyard CJ, and Taylor AB. 2015. Jaw-muscle architecture and mandibular morphology influence relative maximum jaw gapes in the sexually dimorphic Macaca fascicularis. J Hum Evol 82:145-158.

Thierry B. 2004. Social Epigenesis. In: Thierry B, Singh M, and Kaumanns W, editors. Macaque societies: a model for the study of social organization. Cambridge: Cambridge University Press. p 267-295.

Thierry B, Iwaniuk AN, and Pellis SM. 2000. The influence of phylogeny on the social behaviour of macaques (Primates: Cercopithecidae, genus Macaca). Ethology 106(8):713-728.

Troisi A, Aureli F, Schino G, Rinaldi F, and Angelis N. 1990. The influence of age, sex, and rank on yawning behavior in two species of macaques (Macaca fascicularis and M. fuscata). Ethology 86(4):303-310.

Turnbull WD. 1970. Mammalian masticatory apparatus. Fieldiana Geol 18:149-356.

van Schaik CP, and van Noordwijk M, A. 1986. The hidden costs of sociality: intra-group variation in feeding strategies in Sumatran long-tailed macaques (Macaca fascicularis). Behaviour 99(3):296-314.

Vickerton P, Jarvis J, and Jeffery N. 2013. Concentration-dependent specimen shrinkage in iodine-enhanced microCT. Journal of anatomy 223(2):185-193.

Vinyard CJ, Wall CE, Williams SH, and Hylander WL. 2003. Comparative functional analysis of skull morphology of tree-gouging primates. Am J Phys Anthropol 120(2):153-170.

Wainwright PC, Alfaro ME, Bolnick DI, and Hulsey CD. 2005. Many-to-one mapping of form to function: a general principle in organismal design? Integrative and comparative biology 45(2):256-262.

Watson PJ, Gröning F, Curtis N, Fitton LC, Herrel A, McCormack SW, and Fagan MJ. 2014. Masticatory biomechanics in the rabbit: a multi-body dynamics analysis. Journal of The Royal Society Interface 11(99):20140564.

Weijs W, Brugman P, and Klok E. 1987. The growth of the skull and jaw muscles and its functional consequences in the New Zealand rabbit (Oryctolagus cuniculus). Journal of Morphology 194(2):143-161.

Williams SH, Peiffer E, and Ford S. 2009. Gape and bite force in the rodents Onychomys leucogaster and Peromyscus maniculatus: Does jaw-muscle anatomy predict performance? Journal of Morphology 270(11):1338-1347.

Wright BW. 2005. Craniodental biomechanics and dietary toughness in the genus Cebus. Journal of Human Evolution 48(5):473-492.

Tables and Figures

Table 1. Maximum gape potential within *M. fascicularis* at each stage of development.

Model	Maximum functional jaw rotation	Maximum gape potential
Infant	28.5°	20.4mm
Juvenile	37°	36.7mm
Adult Female	51.5°	60.4mm
Adult Male	65.5°	88.0mm

Table 2. Maximum bite force potential within *M. fascicularis* at each stage of development, measured at various bitepoints along the dental row.

Model	I1 bitepoint	C bitepoint	P4 bitepoint	Posterior bitepoint
Infant	31.5N	38N	56.8N	56.8N
Juvenile	51.6N	60.8N	80.9N	120N
Adult Female	98.3N	117.3N	145.2N	237.4N
Adult Male	184.7N	220N	280.5N	436.1N

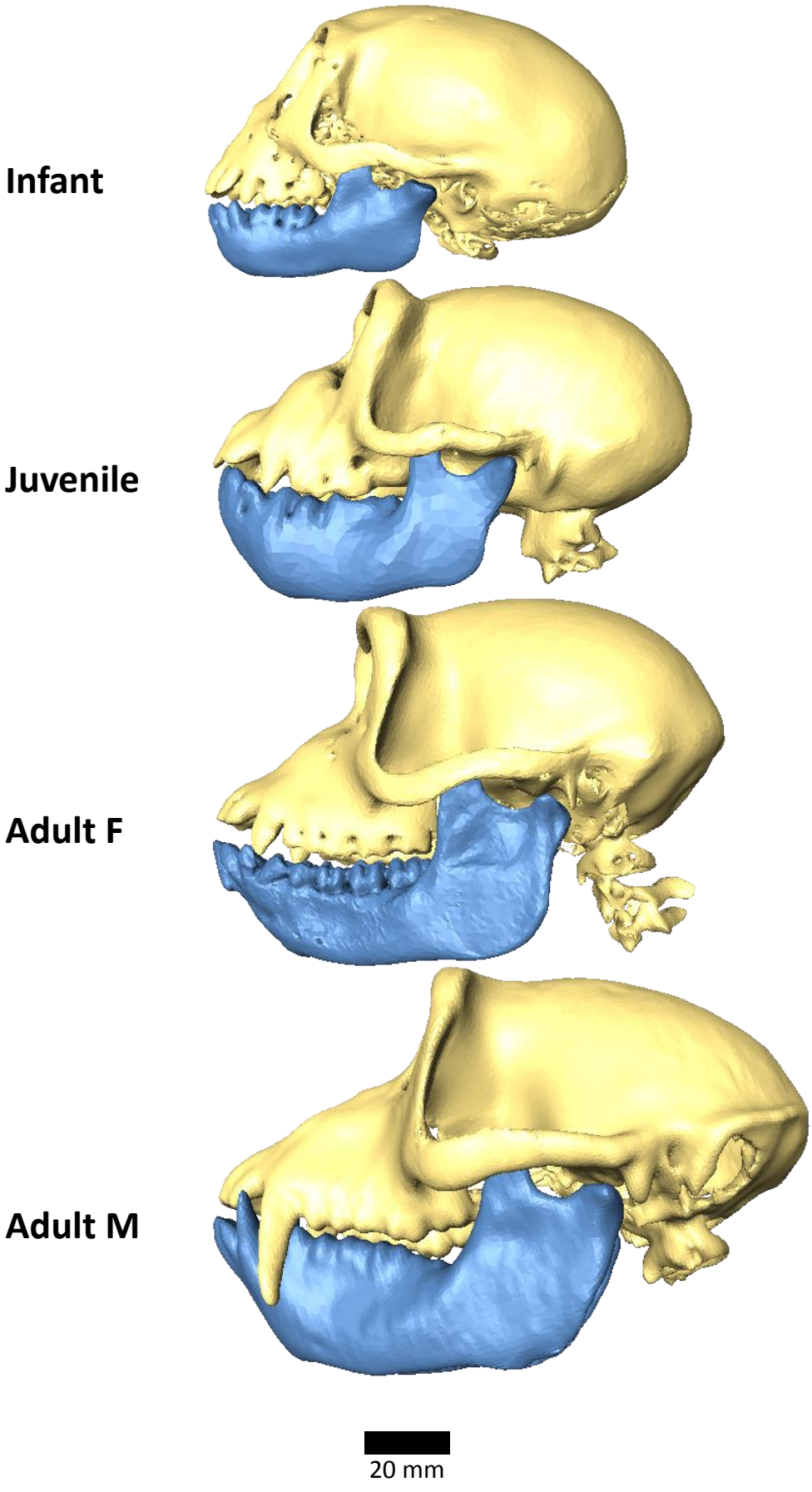

Figure 1. Reconstructed crania and mandibles used for model generation. Scale bar = 20 mm.

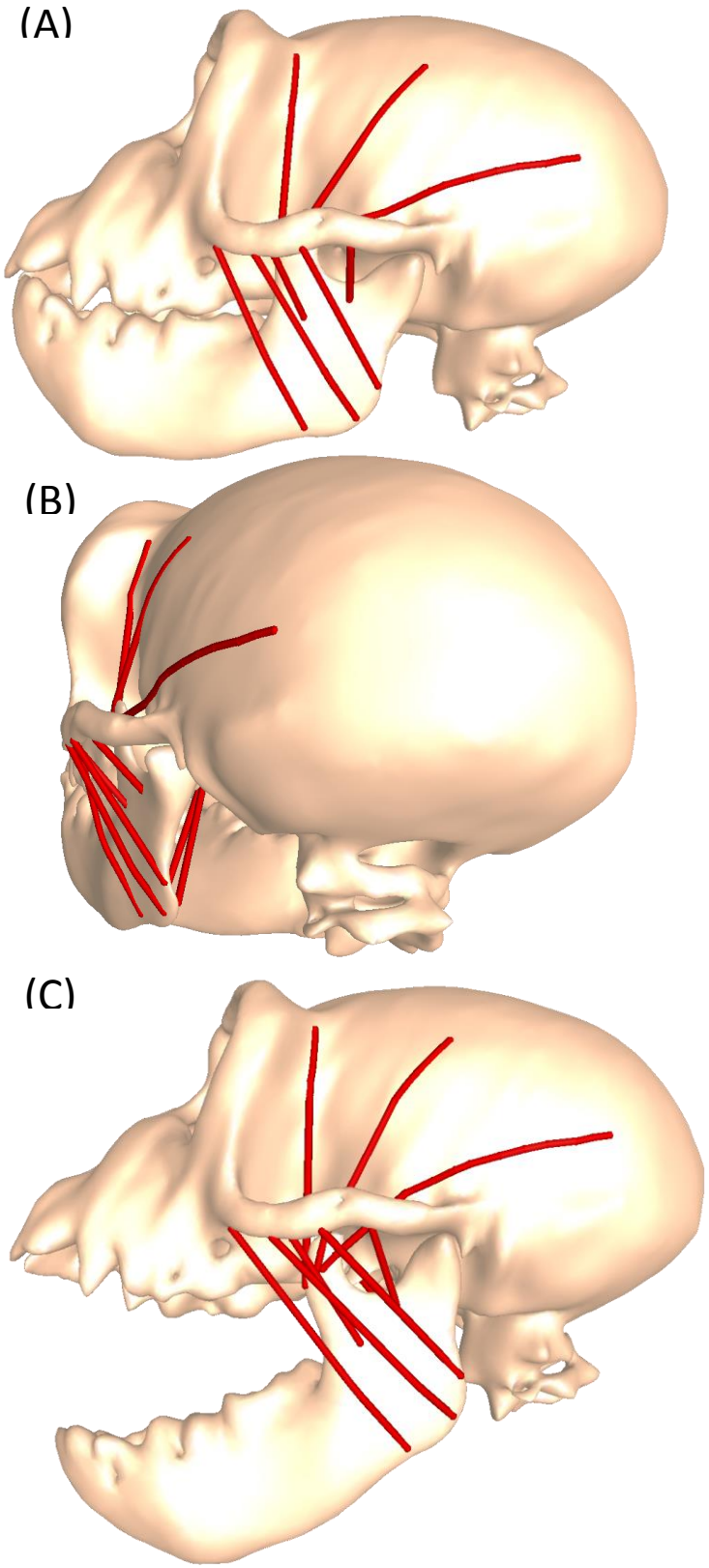

Figure 2. Example model of juvenile *M. fascicularis* specimen, with wrapped muscle strand configuration in place. (A) lateral view of cranium and mandible, showing muscle strands for superficial and deep masseter as well as temporalis; (B) postero-lateral view of cranium and mandible, showing muscle strands of superficial and deep masseter, temporalis, and medial pterygoid; (C) lateral view of cranium and mandible showing the increase in musculotendon lengths as a result of a 25° jaw rotation.

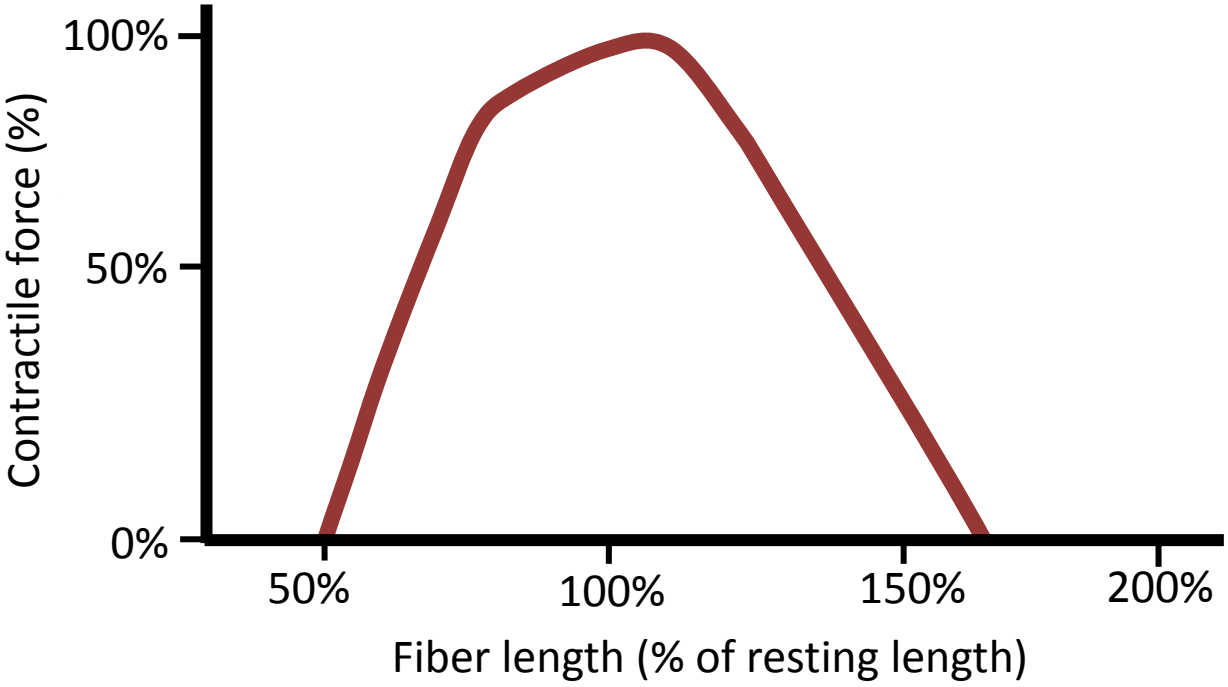

Figure 3. Standardized length-tension curve used to calculate changes in muscle strand forces as a result of jaw rotation.

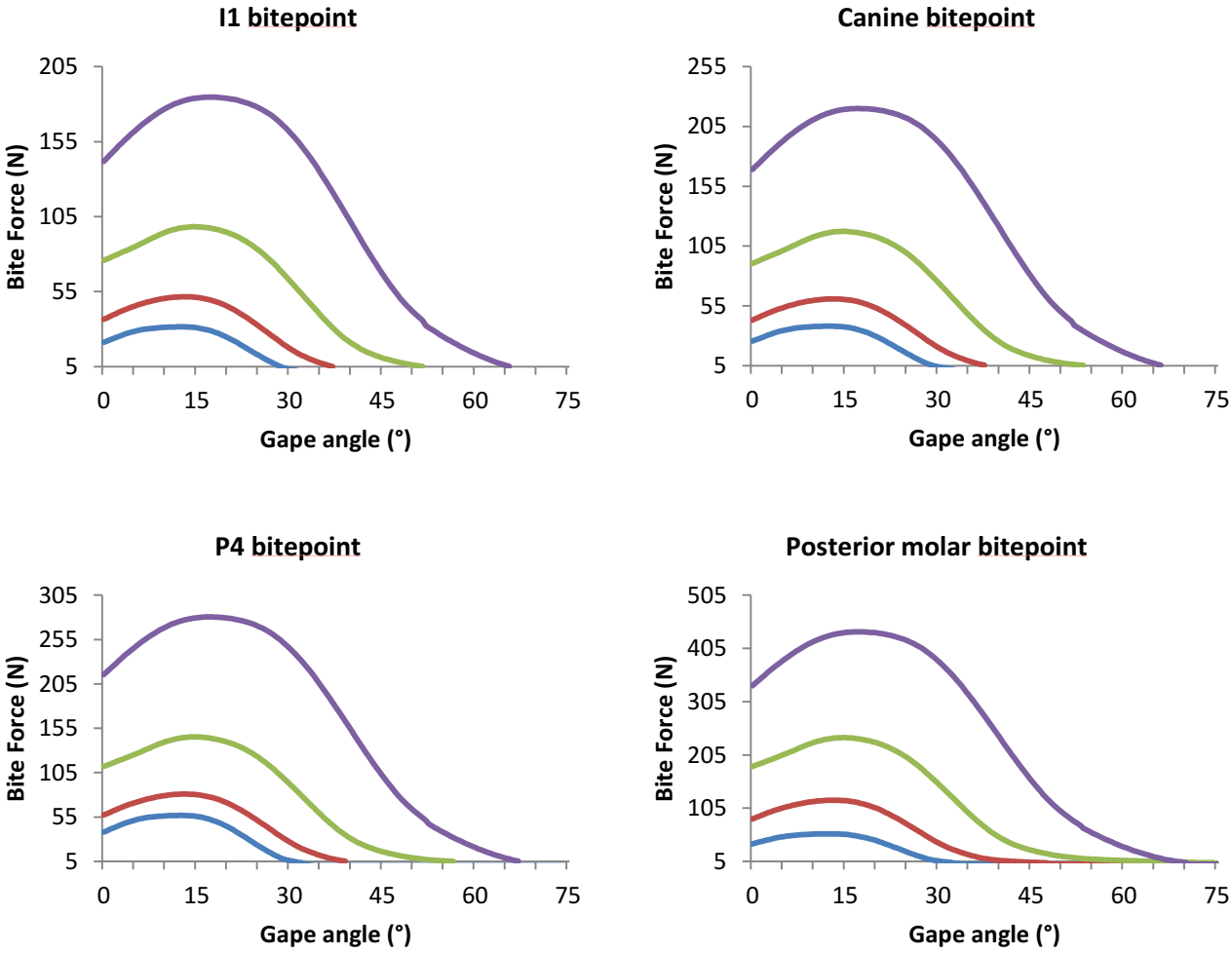

Figure 4. Trajectories of bite force vs. gape angle in *M. fascicularis* during development at four bitepoints (incisor, canine, premolar, and the most posterior molar tooth).

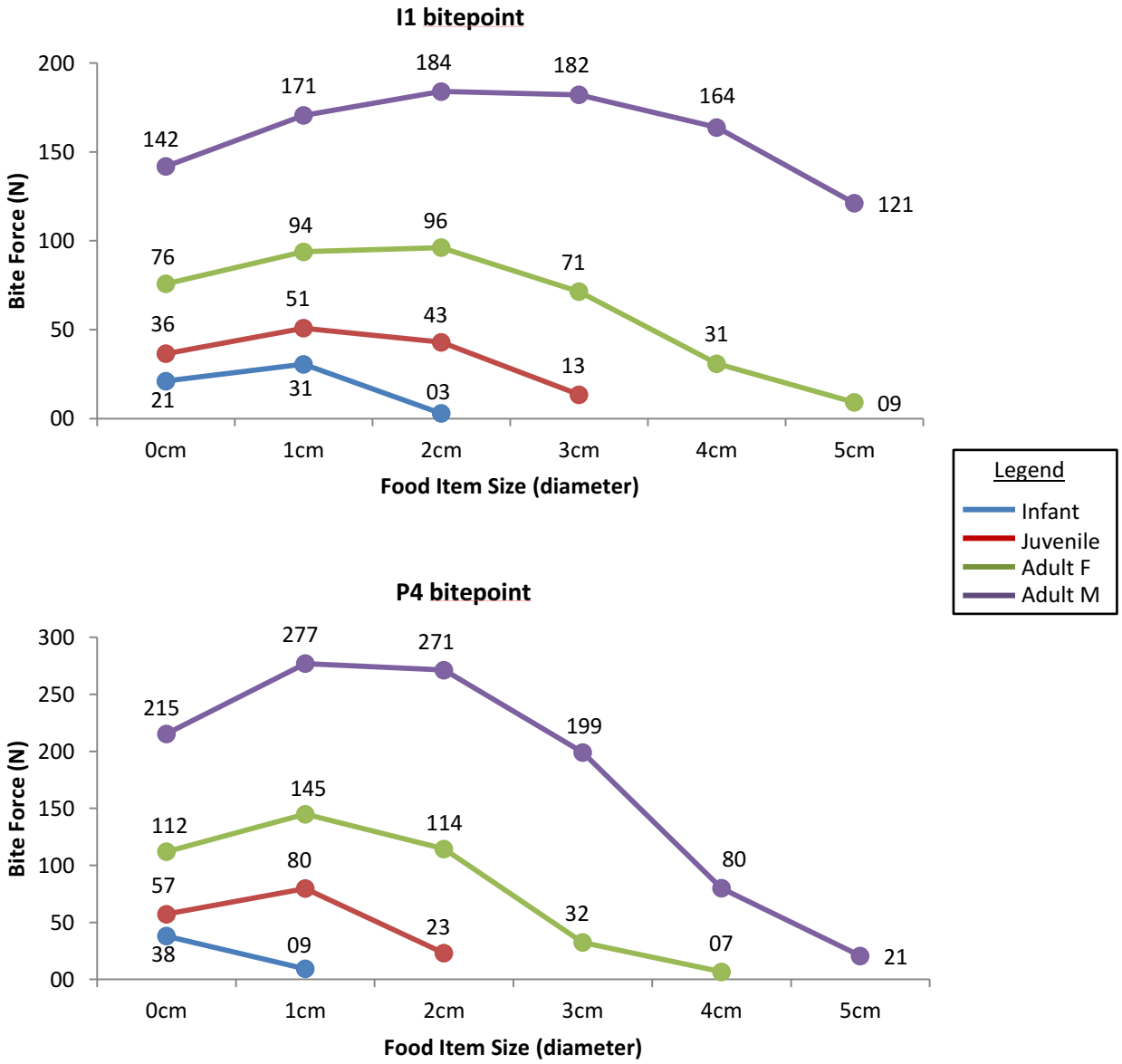

Figure 5. Maximum bite force within *M. fascicularis* during development at a series of controlled gapes (0-5 cm), measured at an anterior (I1) and postcanine (P4) bitepoint.

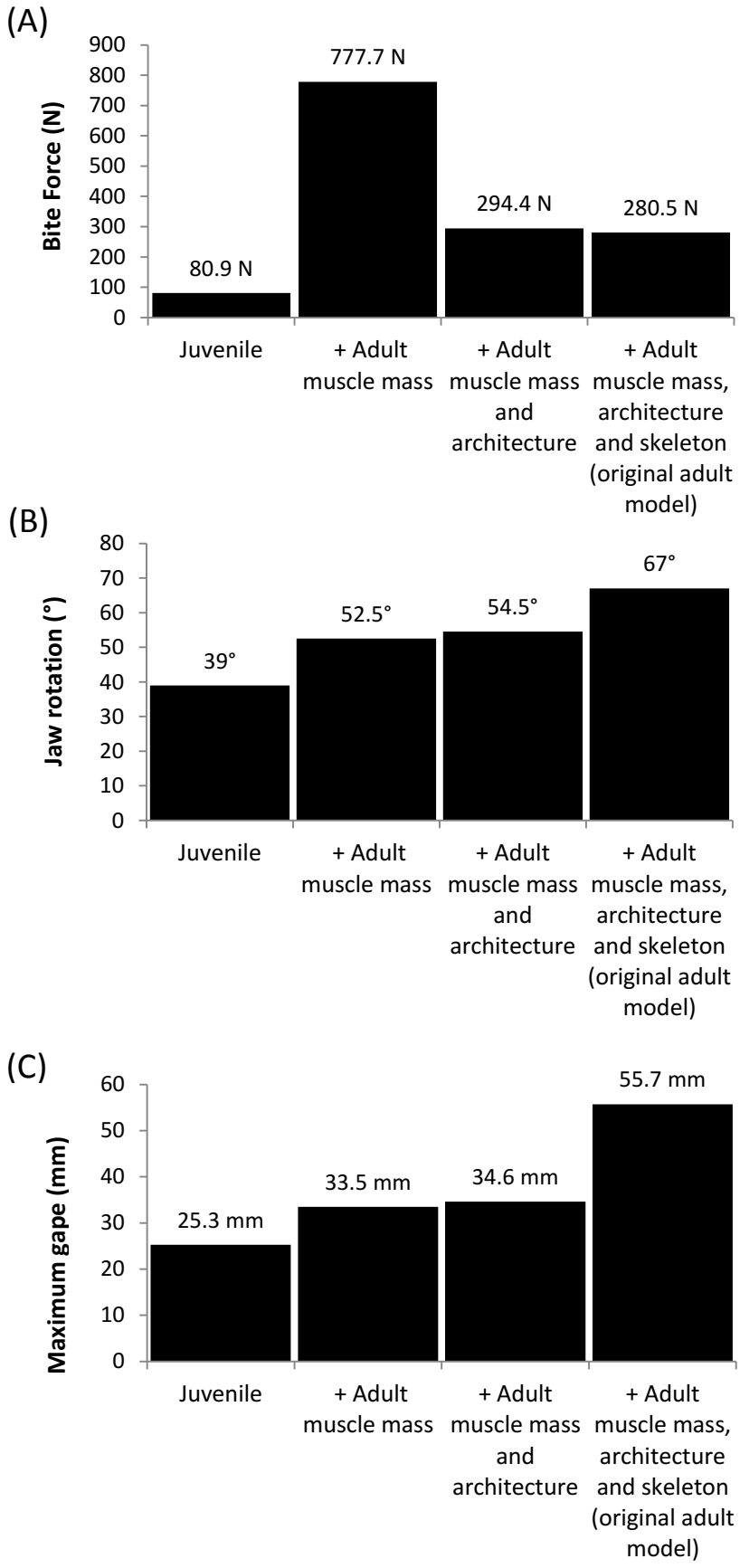

Figure 6. Functional capacity of a juvenile *M. fascicularis* compared to hypothetical models displaying components of adult morphology. (A) Bite force; (B) jaw rotation; (C) maximum gape.

5. DISCUSSION

Developmental changes to the masticatory apparatus

The masticatory apparatus combines an array of soft- and hard-tissue structures which collectively fulfil a range of dietary and social roles. This study explored developmental changes to several key components of this system – including the adductor musculature, craniomandibular form, and the lever-arm mechanics of the masticatory apparatus – within a model primate species (*M. fascicularis*) to provide an insight into ontogenetic scaling patterns within the masticatory system, and how differences in masticatory anatomy within this species during development may be observed to affect measures of overall masticatory function.

Developmental changes to muscle architectural variables within the adductor complex had not previously been quantified and reported within a primate species, yet such data are incredibly valuable to our understanding of masticatory development within primates. Within chapter two, data upon several key variables – muscle mass, fiber lengths, pennation angle, and PCSA – are reported across ontogeny within *M. fascicularis*. We observed that both the size and internal configuration of the adductor musculature exhibit significant shifts during development. Muscle mass increased between each successive age group within all muscles; as a result, average summed adductor muscle mass increased by a factor of two between infants and juveniles and between juveniles and adult females, while a threefold increase in mass was observed between adult female and male individuals. In terms of architectural properties, too, significant increases in both fiber lengths and PCSA were observed in all muscles during development. Such changes highlight the high degree of developmental plasticity that may be observed within the muscles of mastication during development, and support previous studies into developmental trends within the adductor musculature of non-primate taxa, in which significant increases in muscle mass and fiber lengths are also reported (Herring and Wineski, 1986; Weijs et al., 1987).

In addition to absolute increases in muscle size and the length of constituent fibers, soft-tissue variables within the masticatory musculature also scale positively relative to hard-tissue components of the masticatory apparatus during development. Muscle mass, PCSA and fiber length all scale with positive allometry relative to three craniomandibular proxies: jaw length, condyle-molar length and basicranial length. These relationships suggest that the muscles of mastication experience more significant changes to their form and structure during growth than bony elements of the masticatory apparatus.

Looking at these bony structures more closely, both jaw length and condyle-molar length scale with positive allometry relative to basicranial length during development. This finding mirrors previously reported data on the scaling of the primate face during ontogeny, in which mandibular length is reported to scale positively to cranial length during ontogeny within both cercopithecines and colobines (Ravosa, 1991). It also corresponds to broader patterns of craniomandibular growth reported within primates, in which viscerocranial elements experience higher magnitudes of postnatal growth than those of the neurocranium (Schultz, 1960; Freedman, 1962; Cochard, 1985).

These regional differences in craniofacial growth exhibited by *M. fascicularis* result in significant changes to the biomechanical efficiency of the masticatory system during ontogeny. As the length of the jaw increased at a faster rate during development than cranial proxies, load-arm lengths within the masticatory system became relatively elongated compared to lever-arm lengths of the adductor muscles. Consequently, the mechanical advantage of all jaw adductors decreased during development, such that a lower proportion of intrinsic muscle force reaches the jaw within older individuals than younger.

This trend may reflect the differing pressures experienced by the masticatory system at different stages of development. Not surprisingly, infants and juveniles have absolutely smaller muscles (shown also by Cachel, 1984) which generate lower magnitudes of contractile force; as a result, a higher mechanical advantage is therefore important to ensure the availability of sufficient bite force within the jaw during feeding. By contrast, adults present larger muscles and PCSAs, and may subsequently generate such an increase in intrinsic muscle force that a slight decline in mechanical advantage is more than accounted for. As a result, bite force potential increases universally across all bitepoints during development.

The elongation of the adult jaw allows for wider absolute gape generation by enhancing the radius of the rotational arc around the TMJ while the jaw is opened. Additionally, as increases in jaw length exceed corresponding increases to lever-arm (or in-lever) lengths within the masticatory system, the degree of muscle stretch per degree of jaw rotation remains relatively constant during development. This enables adults to exact the full benefit of jaw elongation upon gape without undermining their physiological capacity for maintaining wide-gape jaw postures. Anatomical changes to the masticatory apparatus within *M. fascicularis* during ontogeny therefore function to enable adults to maximize gape potential, while juveniles retain a higher mechanical advantage which enables them to maximize the bite forces generated by their smaller and less powerful adductor musculature.

Masticatory function within an ecological context

These findings correspond well with previously published observational data of behavioural and dietary ecology within this species. Adults of both sexes are reported to consume larger and more mechanically resistant foods than juveniles or infants (van Schaik and Noordwijk, 1986). The ability to consume such foods may be particularly important in diversifying the dietary niche of adults, notably adult males, for whom their larger body sizes likely impose greater caloric demands. Indeed, in *Papio anubis*, which shows a similar level of dimorphism to *M. fascicularis*, resting metabolic rate (RMR) is almost twice as high in adult males (798 kcal/day) than in females (434 kcal/day), while similar patterns are also observed within dimorphic hominoids including *Pongo pygmaeus* and *Pan troglodytes* (Leonard and Robertson, 1992). A broader dietary niche may be particularly critical during periods of resource scarcity – initiated either by the seasonal absence of preferred foods or by broader environmental factors which restrict overall food item availability – by enabling larger adults to 'fall back' on more mechanically challenging food items as a source of energy. The role of fallback foods within the primate dietary repertoire has been discussed within a number of taxa (e.g. *Pan troglodytes* and *Gorilla gorilla* (Furuichi et al., 2001; Yamagiwa and Basabonse, 2009); *Cercopithecus ascanius* and *Lophocebus albigena* (Lambert et al., 2004); *Rhinopithecus bieti* (Grueter et al., 2009); *Presbytis rubicunda* (Hanya and Bernard, 2012); and a number of species within the genus *Cebus* (Wright et al., 2009)). Interestingly, within the cercopithecine clade, fallback foods have been characterized as more mechanically challenging than core subsistence items (Lambert et al., 2004). Further, the increased mechanical resistance of fallback foods has been suggested to be responsible for adaptations within the primate masticatory apparatus towards the consumption of harder food items (Lambert et al., 2004). Adaptations towards maximizing bite force within adult – particularly adult male – *M. fascicularis* may therefore confer seasonal benefits to these individuals through diversifying their range of exploitable food items during times of resource scarcity.

Though developmental changes in masticatory form appear to correspond well to ontogenetic shifts in dietary ecology, social pressures may also be seen to shape the anatomy of the masticatory complex in *M. fascicularis*. Adults, particularly adult males, frequently engage in canine-baring display behaviours as a means of establishing and maintaining social rank (Altmann, 1967; Troisi et al., 1990; Deputte, 1994; Thierry, 2004; Soltis, 2004), with the prevalence of these behaviours increasing fourfold between juvenility and adulthood in both sexes (Deputte, 1994). Elongation of the jaw (and of muscle fibers within the adductor musculature) within adults might therefore also reflect their unique social ecology and its pressures towards gape maximization. Indeed, a growing volume of literature has emphasized the importance of social display as a critical factor driving masticatory form within primates, particularly within adult males (e.g. Hylander, 2013; Terhune et al., 2015; Taylor et al., 2018). Even within strongly durophagous (hard-object feeding) taxa,

adaptations towards maximizing gape appear to supersede those towards the enhancement of bite force potential (Taylor et al., 2018). As a result, it has been argued that the strongest selective pressures experienced by the masticatory apparatus within papionins may be towards maximizing the efficacy of gape display behaviours, even at the cost of mechanical advantage and bite force (Taylor et al., 2018).

Socioecological pressures may consequently best explain differences in both masticatory anatomy (chapter 2) and functional performance (chapter 4) between adult male and female *M. fascicularis*. Though adults of both sexes consume similar proportions of mechanically challenging food items (28% of foods consumed by adult males are considered mechanically challenging, compared to 27% for females; van Schaik and Noordwijk, 1986) and express similar profiles in terms of the sizes of consumed food items (24% of foods consumed by adult males exceed a 20mm diameter, compared to 23% in females; van Schaik and Noordwijk, 1986), males and females exhibit major differences in both bite force and gape potential. Adult males demonstrate a maximum gape of 88.0 mm (65.5°) and maximum bite forces of 436 N, compared to 60.4 mm (51.5°) and 237 N within females. These disparities in masticatory performance reflect dimorphic differences in both craniofacial configuration (with adult males possessing longer jaws than female conspecifics) and soft-tissue structures (with males demonstrating elongated muscle fibers and significantly increased PCSA values across the adductor complex).

From a social perspective, maximizing gape potential enhances the efficacy of canine-baring displays; while an increase in bite force potential may prove critical during direct agonistic encounters with rivals, in which the jaw is used as a weapon. Anatomical specializations observed within the male masticatory apparatus are therefore likely to represent part of a suite of anatomical adaptations towards their highly competitive social environment, in which agonistic displays and physical conflicts play a key role in determining an individual's hierarchical status and, ultimately, reproductive potential.

Both social and dietary pressures therefore appear to shape anatomical structures within the masticatory system, and contribute to differences in masticatory form and function within *M. fascicularis* during development. To understand differences in masticatory anatomy, either within a developmental or an interspecific context, it is therefore pivotal to consider this interplay between dietary and social pressures from an evolutionary perspective. Only by exploring the totality of a species' ecological context can we begin to appropriately interpret anatomical adaptations, and begin to identify the unique pressures driving changes in functional performance.

Broader perspectives and future directions

Suggested datasets for further study

The collected studies presented here quantify developmental changes to the masticatory system of *M. fascicularis* and their functional impact upon masticatory performance at various stages of ontogeny. To contextualize these findings, however, additional data on the scaling of muscle size and architectural variables within other cercopithecine taxa are necessary. Such datasets would provide invaluable insight into the extent to which *M. fascicularis* represents a good model for the masticatory apparatus of papionins, and more broadly of Old World monkeys.

Of particular value would be developmental sequences for species which exhibit differences in dietary and social ecology. As discussed in chapter four, *Cercocebus atys* represents a durophagous feeder which exhibits remarkable consistency in dietary selection during development (McGraw et al., 2011; Daegling et al., 2011; Taylor et al., 2018). A single food item – the nut *Sacoglottis gabonensis* – constitutes over 50% of the diet within both adult and non-adult individuals (McGraw et al., 2011). As *S. gabonensis* rank among the most mechanically challenging foods consumed by this taxon (with a Young's modulus in excess of 200 MPa, and toughness values of 2,000-7,000 Jm-2) and are relatively large (averaging 32 mm along their major axis and 24 mm along their minor axis; Daegling et al., 2011), both adults and juveniles therefore experience high and consistent pressures upon the masticatory apparatus towards attaining and maintaining high bite forces throughout development. However, mangabeys – including *C. atys* – are believed to engage in wide-gape canine display behaviours with similar frequency to the sister genus *Macaca*, which may necessitate adaptations within adult individuals towards gape maximization – even at the cost of bite force potential (Taylor et al., 2018). Analysing the interplay between these two competing pressures within *C. atys* during development may therefore provide uniquely valuable insights into the roles of dietary and social ecology in shaping masticatory form throughout ontogeny.

Similarly, quantifying developmental changes in masticatory form within taxa which display less overt levels of dimorphism and intra-sexual competition may prove useful in better contextualising the respective roles of dietary and social pressures upon the anatomy of the masticatory apparatus. Several platyrrhine species present notably low frequencies and intensities of interspecific aggression, both in terms of male-male and male-female agonistic events (Kay, 1988; Plavcan and van Schaik, 1992). Quantifying developmental trends to the masticatory apparatus within such taxa – which include sakis (genus *Chiropotes*), titi monkeys (genus *Callicebus*) and night monkeys (genus *Aotus*) – may therefore provide interesting comparative datasets to supplement the findings presented here. Of particular interest within this group may be sakis, which frequently consume nuts

with exceptionally hard and tough seed pods and which display several craniodental adaptations towards facilitating the ingestion of such food item (Roosmalen, Mittermeier and Fleagle, 1998).

More generally, analyses of differences in the ontogenetic scaling of muscle architectural variables between catarrhine, platyrrhine, hominoid and strepsirrhine taxa may provide interesting insights into clade-level differences in the growth of the primate jaw, and the extent to which phylogeny may impact upon patterns of postnatal growth within the masticatory apparatus (supplementing analyses on variation in masticatory form within *Carnivora*, which suggest that ecomorphological adaptations supersede phylogenetic signals within the jaw (Meloro et al., 2011)). Data on the developmental scaling of architectural properties of the adductor complex across primates would further supplement several recent interspecific analyses which report distinct differences in the scaling relationships of key architectural variables within adult specimens among these groups. Across the range of adult body sizes found within hominoids, both muscle mass and PCSA are reported to scale with positive allometry relative to jaw length and condyle-M1 (Taylor and Vinyard, 2013). However, within platyrrhines, muscle mass, fiber lengths, and PCSA all scale with negative allometry relative to both jaw length, and condyle-M1 length (Taylor et al., 2015); within strepsirrhines, meanwhile, muscle mass, fiber length, and PCSA scale isometrically relative to the same size proxies (Perry et al., 2011). Quantifying developmental trends within these groups would provide new insights into these reported differences, and improve our understanding of masticatory development across the primate order. A broader understanding of developmental scaling patterns within the primate jaw would also greatly aid reconstructions of social and dietary ecology within fossil primate taxa such as the ancestral cercopithecine *Macaca majori*, which demonstrates a distinct facial form relative to extant macaque taxa (Rook and O'Higgins, 2005), including a reduction in palatal length and lateral flaring of the zygomatic roots.

Digital reconstruction of architectural parameters

While additional data sources are therefore needed to improve our understanding of architectural scaling patterns within the primate jaw, new techniques may offer the opportunity to collect these data in much higher resolution than previously possible. As outlined in chapter three, digital reconstruction of architectural properties through the use of diceCT permits the three-dimensional analysis of fascicle distributions across an entire muscle or muscle portion. In contrast to traditional methods of architectural analysis, which rely on a select number of sampling sites, such methods provide a much more comprehensive overview of fascicular properties within skeletal muscle. A number of potential shortcomings of this technique, however, were also discussed: namely the relatively poor agreement between digital and dissection-derived measurements for muscles with a complex and irregular fascicle orientation (such as the temporalis), and the high investment of time

and computational resources necessary for the implementation of this technique. Two important questions therefore remain, namely: 1) in which circumstances should digital reconstructions be considered for application over traditional gross dissection? And 2) by what means might errors in the registration process be further eliminated, so as to improve the quality of reconstructions within future studies?

Due to the nature of digitally-reconstructed fascicle datasets, the application of this methodology appears particularly well suited to studies investigating questions related to regional specialization and compartmentalization within skeletal muscle. By analysing many more fascicles than could be manually considered during gross dissection, digital fascicle reconstruction makes it possible to explore regional variation in architectural properties at a scale that would previously have been impossible. Further, as demonstrated within chapter 3, the representation of fascicles as digital streamlines makes it straightforward to calculate region-specific data for architectural variables (e.g. pennation angle – see Chapter 3, Figure 6A) and to analyze variation within this variable across a muscle.

The non-destructive nature of iodine staining also renders this technique appropriate for use on specimens that cannot be sacrificed to destructive methods of dissection, allowing architectural data to be collected from otherwise unusable specimens. Indeed, the diceCT toolkit has been demonstrated to produce high-quality results even when applied to museum specimens sourced from long-term ethanol, formaldehyde, and gasoline storage (Mahlow et al., 2016). As specimens may also be destained through the use of a sodium thiosulphate postwash, iodine staining may even be reversed such that the specimen can be returned for display or alternate research purposes following analysis (Gignac et al., 2016; Morhardt and Witmer, 2016).

To minimize registration errors during the generation of digital fascicles, meanwhile, adjustments may also be made to the workflow outlined in chapter 3. While data for superficial and deep masseter corresponded well to the results collected during manual dissection, considerably less agreement was observed between these two techniques for the temporalis. This is interpreted to reflect the more heterogenous distribution of muscle fascicles within the temporalis relative to the masseter complex. To address this issue, muscles displaying irregular fascicular distributions – such as temporalis – may be divided into distinct portions during the segmentation process, following the natural divisions of the muscle (in the case of temporalis, generating distinct deep and superficial portions). This subdivision would serve to reduce variation in fascicle orientation within each volume, and may thus act to reduce the frequency of registration errors during the mapping process.

This technique provides a novel and potentially powerful tool for quantifying the distribution of muscle fascicles on a whole-muscle level. Continuation of the study presented in chapter 3 will involve further investigation into regional differences in muscle architectural properties within primates, alongside additional sensitivity analysis in which the results of digital fascicle reconstruction are compared to manually segmented muscle fascicles measured from diceCT datasets, alongside measurements collected during gross dissection. Such work will serve to better clarify the extent to which digitally-reconstructed architectural variables may be compared to those derived by gross dissection.

Modelling masticatory performance: future goals

The series of multibody dynamics models presented in chapter 5 explore developmental differences in masticatory performance within *M. fascicularis*, demonstrating consistent increases in both bite force and gape potential throughout ontogeny. These models represent a good first approximation of masticatory performance, with both gape and bite force outputs corresponding well to previously published data collected on living macaque specimens, suggesting biological validity. However, the relatively simple nature of these models allows for several advancements within further iterations. To begin, kinematic data on jaw movements within macaques during the gape cycle (e.g. Hylander, et al., 2005) would provide much more finely-tuned data on bite force potential at specific jaw postures. Integrating these data in place of the simple hinge-rotation motions used within the existing models would provide new insights into the scaling of masticatory performance during development.

Biting actions within these models also employ 100% activation of all muscles during each biting motion. Integration of muscle recruitment patterns, either derived from EMG data on the macaque chewing cycle (Hylander, Johnson and Compton, 1987; Hylander, Johnson and Crompton, 1992; Hylander et al., 2005) or estimated using dynamic optimization criteria (e.g. Shi et al., 2012; Gröning et al., 2013) could be used to explore changes in the relative contributions of each muscle towards the generation of bite force at different jaw postures. Similarly, while models currently simulate only unilateral biting by the working-side musculature, balancing-side muscles could be integrated to further enhance the accuracy of masticatory simulation.

Ongoing work also utilizes these models to explore patterns of regional specialization within the masticatory musculature at different stages of developments. By analysing the force generation potential of each muscle strand along the gape cycle, it is possible to map regional patterns of optimization towards different components of the gape cycle within each muscle portion. Analysis of these trends throughout ontogeny also permits assessment of the extent to which patterns of

regional specialization are maintained throughout ontogeny. Preliminary results of these analyses support previous assertions that anterior fibers within the jaw adductors, particularly within superficial masseter, experiences the greatest degrees of stretching during jaw opening (Herring and Herring, 1974; Herring et al., 1984; Taylor and Vinyard, 2004) and suggest that elongated fiber lengths within these regions may enhance the ability of these muscle portions to maintain force production throughout the gape cycle.

Integration of these results with other modes of digital modelling, such as finite element analysis, may also provide broader insights into developmental variation within masticatory performance. By exporting existing data on muscle loading parameters – including muscle forces, joint moments, and bitepoint-specific bite forces – and assigning mechanical properties to the hard-tissue components of the model, it is possible to analyse how forces generated during biting simulations within these models are dissipated throughout the craniofacial skeleton. Combining these modelling techniques would therefore provide the necessary toolkit to explore not just changes in bite force potential during ontogeny, but the extent to which changes in craniofacial morphology during growth function to minimize localized stresses within the face during mastication. Such data would provide a fascinating insight into the relationship between masticatory behaviours and craniofacial form within the developing primate skull.

Expanding analyses of the masticatory apparatus

In addition to increasing the diversity of taxa for which architectural data are reported and the resolution at which such data are collected, future studies should also endeavor to incorporate analyses of other craniofacial components. The masticatory apparatus consists of a myriad of complex structures, and a holistic interpretation of ontogenetic changes in masticatory performance requires consideration of how developmental changes to architectural and biomechanical components of the masticatory apparatus might impact other properties of the masticatory system.

The facial skeleton

Increases in bite force potential during development – resulting from absolute increases in muscle mass across the adductor complex – may contribute towards broad ontogenetic changes in craniofacial form, particularly within the facial skeleton. Within *Macaca*, both the length and width of the mandibular symphysis increase during development, scaling with positive allometry relative to body mass and other dimensions of the jaw (Ravosa, 1991). Such modifications have been shown to reduce stress magnitudes experienced within the symphysis during wishboning (Hylander, 1985). Consequently, patterns of growth in the symphyseal region of the mandible might reflect adaptive responses to developmental increases in bite force potential within *Macaca* (chapter 4), as a means

of withstanding the higher wishboning stresses associated with mastication. Within the cranium, meanwhile, finite element (FE) simulations of the principal stresses associated with postcanine loading in *M. fascicularis* demonstrate peaks of localized stress within the zygomas and the immediate suborbital region (Kupczik et al., 2007, 2009; Curtis et al., 2008). Distributions of von Mises strains within the macaque face also display similar peaks across 10 different loading scenarios (Fitton et al., 2012). As the macaque face undergoes a marked increase in robusticity within these regions during ontogeny (yet more posteriorly-positioned elements of the cranium experience comparatively little change in form) (Richtsmeier et al., 1993), such adaptations could be related to the higher stresses associated with more powerful mastication in adults. Investigating the effects of ontogenetic changes in craniofacial form and bite force magnitudes upon stress/strain distributions in the macaque face during simulated mastication could therefore provide interesting insights into the relationship between masticatory loads and craniofacial form during ontogeny.

Dental form and function

An integrated analysis of masticatory potential during development must also consider ontogenetic changes to the dentition. As the terminal element of the masticatory apparatus, the occlusal morphology of dental elements determines the efficiency of food item breakdown and the necessary forces needed to initiate fracture during ingestion and mastication (Lucas, 2004). Two major features impact upon the morphology of the dentition during development. Principally, the primary deciduous dentition is replaced by their permanent counterparts, extending the postcanine dental row with the iterative eruption of the permanent molar dentition (Hillson, 2005). Secondarily, the occlusal morphology of dental elements undergo changes due to the accumulation of dental wear. As the loss of enamel tissue as a result of macroscopic wear is irreversible, due to the non-regenerative nature of enamel, wear accumulated during life permanently impacts the efficiency of food item breakdown (Lucas and Luke 1984; Lucas, 2004). It is therefore important to consider how changes in occlusal form during ontogeny might alter predicted patterns of masticatory performance during life (e.g. chapter four).

In mechanical terms, the most effective means of inducing food item fracture is to concentrate stresses within a localized area by minimizing the contact surface area, thereby increasing the force per unit area (or pressure) transmitted during the biting action (Lucas, 1982; Lucas, 2004). Sharp dental cusps with a reduced radius of curvature would therefore prove most efficient for this purpose (Lucas, 1982; Evans and Sanson, 1998). As newly-erupted teeth present the sharpest cusps, differences in dental morphology may enable younger individuals to process food items with reduced masticatory forces, allowing juveniles to overcome their relative disadvantage in masticatory force

production relative to adult conspecifics (Popowics and Fortelius, 1997; Evans and Sanson, 1998; Logan and Sanson, 2002; Lucas, 2004).

Recent studies, however, have demonstrated that the relationship between cusp sharpness and food item breakdown may be more complex than initially hypothesized. Dental topographic analyses of changes in occlusal morphology as a result of wear accumulation have demonstrated that while occlusal slope and relief decreases with wear – resulting in a flatter occlusal surface – angularity remains relatively consistent (Ungar and M'Kirera, 2003; Bunn and Ungar, 2009; Cuozzo et al., 2014). Additionally, an increase in cusp sharpness may prove detrimental to overall tooth longevity, as such morphologies produce high localized stresses within the enamel as well as within the target food item (Berthaume et al., 2013). As a result, the 'secondary morphology' achieved by teeth following the accumulation of wear may ultimately provide a more effective morphology. Further studies exploring the effects of dental wear upon food item breakdown (e.g. Swan 2016) and the impact of changes in masticatory force upon potentially detrimental stresses experienced within dental enamel during biting are therefore necessary to fully resolve our understanding of how ontogenetic changes to the masticatory apparatus impact upon the efficiency and safety factor of food item breakdown.

Fiber-type profiles during ontogeny

Finally, future analyses of the developing masticatory apparatus should also consider ontogenetic changes within other properties of the adductor musculature. Just as the architectural properties of the masticatory musculature determine bite force potential and maximum potential gape, changes in muscle fiber phenotype similarly contribute towards the contractile capabilities of the adductor musculature. Slow-twitch, oxidative type-I fibers demonstrate a reduction in both contractile velocity and peak power relative to fast-twitch type-II fibers. However, type-II fibers rely upon glycolytic actions for the rapid generation of ATP, and consequently experience rapid fatigue. An increased frequency of type-II heavy fibers therefore suggests optimization towards peak force production and high contractile velocities, while type-I fibers reflect a greater emphasis upon sustained muscle contraction and repeated loading cycles.

Existing data on fiber-type profiles within the primate masticatory apparatus highlight the potential for high degrees of variation. Sexually dimorphic differences in muscle fiber profile are reported in adult *Papio anubis* by Wall et al., (2013), in which males possess a higher concentration of type-II fibers which enable the production of faster and more powerful bites. This same trend was reported by Maxwell et al., (1979) within *M. mulatta*, while a similar relationship within *M. fascicularis* was predicted by Terhune et al., (2015).

Developmentally, meanwhile, Maxwell et al., (1979) further report that juvenile *M. mulatta* present a fiber-type profile more similar to adult males in having a higher proportion of type-II fibers in both the temporalis and masseter. This contractile profile would enhance the ability of juveniles to generate higher magnitudes of contractile force, and could represent one mechanism by which younger individuals overcome a relative disadvantage in muscle mass (chapter two). However, as fiber phenotypes have been shown to vary drastically as a result of both diet (Ravosa et al., 2010) and ageing (Anapol and Herring, 2000; Korfage *et al.*, 2006) within other mammalian taxa, further quantification of such changes within the primate adductor musculature during development is necessary before reliable interpretations can be made.

6. CONCLUSIONS

Previous data regarding ontogenetic changes to the primate masticatory apparatus are sparse, particularly in terms of changes to muscle architectural properties during development. However, quantifying these changes is crucial to understanding variation in masticatory performance during life, and interpreting ecological shifts between juvenile and adult individuals. Chapter 2 of this thesis reports data on the developmental scaling of architectural and biomechanical variables within the jaw-adductor musculature of a model primate species (*M. fascicularis*).

Significant changes were observed in both architectural and biomechanical properties during development. Fiber lengths increased absolutely within each successive age group, scaling with positive allometry relative to both jaw length and condyle-molar length. Muscle mass and PCSA similarly scaled with positive allometry during development relative to both biomechanical proxies. TMJ height also scaled with positive allometry against both measurements of mandibular length, while jaw length and condyle-molar length were themselves observed to scale with positive allometry relative to basicranial length. Finally, lever arm lengths scaled isometrically relative to jaw length and tended towards positive allometry relative to condyle-molar length. The positive scaling of muscle mass and PCSA indicated an increase in maximum bite force during development; meanwhile, increases to both jaw length and fiber length were interpreted to reflect adaptations towards an increase in maximum gape capacity. These relationships also suggested that the muscles of mastication experience more significant changes to their form and structure during growth than bony elements of the masticatory apparatus.

To quantify the potential impact of these adaptations, these data were used alongside digital reconstructions of the craniofacial complex to estimate changes in functional masticatory performance during ontogeny using a series of simple multibody dynamics models (Chapter 4). Four representative models (infant, juvenile, adult female, and adult male) were constructed to provide datapoints on developmental and dimorphic differences in the functional capacity of the masticatory system. Measures of maximal gape were calculated for each model; additionally, at each degree of jaw opening, bite force was measured at four bitepoints along the dental row. Finally, a series of hypothetical food items (spheres of a controlled diameter) were placed at two bitepoints (I1 and P4) within each model to assess feeding performance upon objects of increasing size. These data provided a comprehensive analysis of masticatory performance at each stage of the gape cycle within each model. Maximum bite force was demonstrated to increase at each bitepoint during development, reaching a peak of 436 N within the adult male model. Maximum gape potential similarly increased during development, from 20.4 mm (with a 28.5° jaw rotation) in the infant model to 88.0 mm (with a 65.5° jaw rotation) in the adult male model. Finally, older models proved more

effective at exploiting food items of a larger diameter. Infants could not bite upon foods above a 2 cm diameter, while juveniles could process a 3 cm but not 4 cm diameter food item. Adult females could process a 5 cm sphere at an I1 bitepoint, but not at the P4; by contrast, the adult male model could accommodate all food items at both bitepoints. Measures of maximum bite force and gape accord strongly with *in vivo* data collected on these parameters in *M. mulatta* and *M. fascicularis* respectively, suggesting biological validity of the model.

A theoretical model was also constructed to test form-function hypotheses related to the craniofacial complex during development. The juvenile model was iteratively warped towards an adult model by successively altering variables, and quantifying the effect of each isolated change upon both gape and bite force potential. Increasing muscle size from a juvenile to an adult magnitude produced a significant (~900%) increase in bite force potential. The application of adult architectural properties, which included longer muscle fibers, reduced this degree of force – though bite force was significantly higher than within the original juvenile model. Further, applying adult architectural properties resulted in an increase in maximum gape potential. Finally, the effect of applying an adult craniofacial configuration resulted in a slight decline in bite force potential (294 N to 281 N), but a significant increase in gape capacity (from 34.6 mm to 55.7 mm) – reflecting the magnitude of adaptations towards gape maximization within the adult skull and jaw.

In addition to analysing changes in masticatory form and function, this thesis also explored new techniques for the digital reconstruction and analysis of muscle architectural properties. Chapter 3 introduces a technique for the non-invasive and non-destructive determination of key architectural variables, including fiber length, pennation angle, muscle volume and PCSA. To assess the accuracy of this process, digitally reconstructed data were compared to dissection-derived findings from the contralateral musculature. Strong agreement between methodologies was observed for both components of the masseter complex; however, temporalis demonstrated significant divergences in the measurement of muscle fiber lengths (and as a result, PCSA). This disagreement is interpreted to reflect errors in the fascicle registration process for this muscle, due to the more complex and heterogeneous distribution of muscle fascicles within the temporalis muscle.

These data suggest that digital reconstruction techniques may be applied to future specimens, enabling architectural data to be collected from specimens which could not be sacrificed to destructive methods of dissection; however, for muscles which represent irregular morphologies, it may prove preferable to separately analyse superficial and deep portions of the muscle. Indeed, ongoing work continues to improve the accuracy of digital fascicle reconstruction, and will provide digital datasets for additional taxa. Reconstructions of the adductor complex within the common marmoset (*Callithrix jacchus*) are underway, and will evaluate the extent to which subdividing

complex muscles – such as the temporalis – into distinct regions may improve the registration process. This work is also supplemented by a new technique focused upon the manual segmentation of muscle fascicles from contrast-enhanced μCT datasets.

Collectively, the data presented within this thesis provide novel insights into the ontogenetic scaling of key architectural and biomechanical properties in the jaw-adductor complex of a primate species. Such data allowed us to observe, for the first time, the effect of growth and development upon key components of the primate masticatory apparatus. To contextualize these studies, however, corresponding data is required for additional primate taxa during development. The analysis of taxa which display a distinct dietary and/or social ecology from *M. fascicularis* may be particularly valuable, making it possible to evaluate the extent to which the scaling of architectural properties during development represents the unique ecology of a primate species.

Using multibody dynamics modelling techniques, it was also possible to quantify the functional effect of ontogenetic changes to soft- and hard-tissue structures upon overall masticatory performance. Such models allow us to observe how changes to individual soft- or hard-tissue components of the craniofacial complex during development affect specific variables of masticatory performance. The resultant data also correspond well to *in vivo* datasets on masticatory performance within the genus *Macaca*, suggesting such models represent highly useful tools as a means of exploring form-function relationships within the musculoskeletal system. Future work will continue to apply these techniques to address critical questions relating to the form and function of the primate jaw. Indeed, ongoing work utilizes the multibody dynamics models introduced in chapter four to explore developmental and dimorphic patterns of regional specialization within the masticatory musculature of primates during mastication. A new series of models exploring the functional impact of architectural and craniofacial differences between *Pan troglodytes* and *Pan paniscus* will also employ a similar modelling protocol.

As a whole, the data presented here strive to improve our understanding of developmental changes within the primate masticatory apparatus, and the extent to which such changes in masticatory form reflect ontogenetic variation in dietary and social ecology. Understanding the relationship between masticatory form and ecology is critical to interpretations of anatomical specializations within the primate face, particularly in the context of fossil primates. Similarly, quantifying the relationship between masticatory form and metrics of masticatory performance such as bite force and gape improves our ability to reconstruct the dietary ecology of fossil taxa. Further studies into form-function relationships within the primate jaw during development are therefore crucial to enhance interpretations of the primate masticatory apparatus from an evolutionary perspective.

7. LITERATURE CITED

Allen V, Elsey RM, Jones N, Wright J, Hutchinson JR. 2010. Functional specialization and ontogenetic scaling of limb anatomy in Alligator mississippiensis. J. Anat 216:423–445.

Altmann S. 1967. The structure of primate social communication. In: Altmann S, editor. Social communication among primates. Chicago: University of Chicago Press. p 3325-3362.

Anapol F, and Barry K. 1996. Fiber architecture of the extensors of the hindlimb in semiterrestrial and arboreal guenons. American Journal of Physical Anthropology 99(3):429-447.

Anapol F, and Herring SW. 2000. Ontogeny of histochemical fiber types and muscle function in the masseter muscle of miniature swine. American journal of physical anthropology 112(4):595-613.

Anapol F, and Lee S. 1994. Morphological adaptation to diet in platyrrhine primates. American Journal of Physical Anthropology 94(2):239-261.

Anapol F, and Jungers WL. 1986. Architectural and histochemical diversity within the quadriceps femoris of the brown lemur (Lemur fulvus). American Journal of Physical Anthropology 69(3):355-375.

Anapol F, Shahnoor N, Ross CF. 2008. Scaling of reduced physiologic cross-sectional area in primate muscles of mastication. In: Primate craniofacial function and biology. Berlin: Springer. p. 201–216.

Anderson CM. 1986. Predation and primate evolution. Primates 27(1):15-39.

Anton SC. 1999. Macaque masseter muscle: Internal architecture, fiber length and cross-sectional area. Int J Primatol 20:441–462.

Anton SC. 2000. Macaque pterygoid muscles: internal architecture,fiber length, and cross-sectional area. Int J Primatol 21:131–156.

Azizi E, and Deslauriers AR. 2014. Regional heterogeneity in muscle fiber strain: the role of fiber architecture. Frontiers in physiology 5:303.

Bang ML, Li X, Littlefield R, Bremner S, Thor A, Knowlton KU, Lieber RL, and Chen J. 2006. Nebulin-deficient mice exhibit shorter thin filament lengths and reduced contractile function in skeletal muscle. J Cell Biol 173(6):905-916.

Bates KT, and Falkingham PL. 2012. Estimating maximum bite performance in Tyrannosaurus rex using multi-body dynamics. Biology Letters:rsbl20120056.

Baur V, Hanggi J, Langer N, Jancke L. 2013. Resting-state functional and structural connectivity within an insula—amygdala route specifically index state and trait anxiety. Biological Psychiatry 73:85–92.

Baverstock H, Jeffery NS, and Cobb SN. 2013. The morphology of the mouse masticatory musculature. Journal of Anatomy 223(1):46-60.

Bodine SC, Roy R, Meadows D, Zernicke R, Sacks R, Fournier M, and Edgerton V. 1982. Architectural, histochemical, and contractile characteristics of a unique biarticular muscle: the cat semitendinosus. Journal of Neurophysiology 48(1):192-201.

Bolter DR, and Zihlman AL. 2003. Morphometric analysis of growth and development in wild-collected vervet monkeys (Cercopithecus aethiops), with implications for growth patterns in Old World monkeys, apes and humans. Journal of Zoology 260(1):99-110.

Bunn JM, and Ungar PS. 2009. Dental topography and diets of four old world monkey species. American Journal of Primatology 71(6):466-477.

Cachel S. 1984. Growth and allometry in primate masticatory muscles. Arch Oral Biol 29(4):287-293.

Carlson KJ. 2006. Muscle architecture of the common chimpanzee (Pan troglodytes): Perspectives for investigating chimpanzee behavior. Primates 47:218–229.

Chalk J, Richmond BG, Ross CF, Strait DS, Wright BW, Spencer MA, Wang Q, Dechow PC. 2011. A finite element analysis of masticatory stress hypotheses. Am J Phys Anthropol 145:1–10.

Cochard LR. 1985. Ontogenetic allometry of the skull and dentition of the rhesus monkey (Macaca mulatta). In: Jungers WL, editor. Size and scaling in primate biology. New York: Plenum Press. p 231-255.

Collard M, and O'Higgins P. 2001. Ontogeny and homoplasy in the papionin monkey face. Evolution & Development 3(5):322-331.

Conroy GC. 1990. Primate Evolution. New York: Norton.

Corlett R, and Lucas P. 1990. Alternative seed-handling strategies in primates: seed-spitting by long-tailed macaques (Macaca fascicularis). Oecologia 82(2):166-171.

Corner BD, and Richtsmeier JT. 1991. Morphometric analysis of craniofacial growth in Cebus apella. American Journal of Physical Anthropology 84(3):323-342.

Cox PG, and Faulkes CG. 2014. Digital dissection of the masticatory muscles of the naked mole-rat, Heterocephalus glaber (Mammalia, Rodentia). PeerJ 2:e448.

Cox PG, and Jeffery N. 2011. Reviewing the morphology of the jaw-closing musculature in squirrels, rats, and guinea pigs with contrast-enhanced microCT. The Anatomical Record 294(6):915-928.

Cox PG, Fagan MJ, Rayfield EJ, Jeffery N. 2011. Finite element modelling of squirrel, guinea pig and rat skulls: Using geometric morphometrics to assess sensitivity. J Anat 219:696–709.

Cox PG, Rayfield EJ, Fagan MJ, Herrel A, Pataky TC, and Jeffery N. 2012. Functional evolution of the feeding system in rodents. PLoS One 7(4):e36299.

Cuozzo FP, Head BR, Sauther ML, Ungar PS, and O'Mara MT. 2014. Sources of tooth wear variation early in life among known-aged wild ring-tailed lemurs (Lemur catta) at the Bezà Mahafaly Special Reserve, Madagascar. American journal of primatology 76(11):1037-1048.

Curtis N. 2011. Craniofacial biomechanics: an overview of recent multibody modelling studies. Journal of anatomy 218(1):16-25.

Curtis N, Jones ME, Evans SE, Shi J, O'Higgins P, and Fagan MJ. 2010. Predicting muscle activation patterns from motion and anatomy: modelling the skull of Sphenodon (Diapsida: Rhynchocephalia). Journal of the Royal Society Interface 7(42):153-160.

Curtis N, Kupczik K, O'higgins P, Moazen M, and Fagan M. 2008. Predicting skull loading: applying multibody dynamics analysis to a macaque skull. The Anatomical Record 291(5):491-501.

Daegling DJ, McGraw WS, Ungar PS, Pampush JD, Vick AE, and Bitty EA. 2011. Hard-object feeding in sooty mangabeys (Cercocebus atys) and interpretation of early hominin feeding ecology. PLoS One 6(8):e23095.

Damon BM, Ding Z, Anderson AW, Freyer AS, and Gore JC. 2002. Validation of diffusion tensor MRI-based muscle fiber tracking. Magnetic resonance in medicine 48(1):97-104.

Dechow PC, and Carlson DS. 1990. Occlusal force and craniofacial biomechanics during growth in rhesus monkeys. American Journal of Physical Anthropology 83(2):219-237.

Delp SL, and Loan JP. 1995. A graphics-based software system to develop and analyze models of musculoskeletal structures. Computers in biology and medicine 25(1):21-34.

Dennis JC, Ungar PS, Teaford MF, and Glander KE. 2004. Dental topography and molar wear in Alouatta palliata from Costa Rica. American Journal of Physical Anthropology 125(2):152-161.

Deputte BL. 1994. Ethological study of yawning in primates. I. Quantitative analysis and study of causation in two species of Old World monkeys (Cercocebus albigena and Macaca fascicularis). Ethology 98(3-4):221-245.

Descamps E, Sochacka A, D, Kegel B, Van Loo D, Van Hoorebeke L, Adriaens D. 2014. Soft tissue discrimination with contrast agents using micro-CT scanning. Belg J Zool 144:20–40.

Dickinson E, Stark H, and Kupczik K. 2018. Non-Destructive Determination of Muscle Architectural Variables Through the Use of DiceCT. The Anatomical Record 301(2):363-377.

Dumont ER, Samadevam K, Grosse I, Warsi OM, Baird B, and Davalos LM. 2014. Selection for mechanical advantage underlies multiple cranial optima in new world leaf-nosed bats. Evolution 68(5):1436-1449.

Eng CM, Ward SR, Vinyard CJ, and Taylor AB. 2009. The morphology of the masticatory apparatus facilitates muscle force production at wide jaw gapes in tree-gouging common marmosets (Callithrix jacchus). J Exp Biol 212(Pt 24):4040-4055.

Evans A, and Sanson G. 1998. The effect of tooth shape on the breakdown of insects. Journal of Zoology 246(4):391-400.

Fa JE. 1989. The genus Macaca: a review of taxonomy and evolution. Mammal Review 19(2):45-81.

Felder A, Ward SR, Lieber RL. 2005. Sarcomere length measurement permits high resolution normalization of muscle fiber length in architectural studies. J Exp Biol 208:3275–3279.

Fitton LC, Dickinson E, Swan K, and Cobb S. 2015. Functional Integration During Development Within The Masticatory Apparatus. The FASEB Journal 29(1 Supplement):865.815.

Fitton LC, Shi J, Fagan M, and O'Higgins P. 2012. Masticatory loadings and cranial deformation in Macaca fascicularis: a finite element analysis sensitivity study. Journal of Anatomy 221(1):55-68.

Fleagle JG. 1998. Primate adaptation and Evolution, 2nd Ed. New York: Academic Press.

Friederich JA, and Brand RA. 1990. Muscle fiber architecture in the human lower limb. Journal of biomechanics 23(1):91-95.

Furuichi T, Hashimoto C, and Tashiro Y. 2001. Fruit availability and habitat use by chimpanzees in the Kalinzu Forest, Uganda: examination of fallback foods. International Journal of Primatology 22(6):929-945.

Furuuchi K, Koyabu D, Mori K, Endo H. 2013. Physiological crosssectional area of the masticatory muscles in the giraffe (Giraffa camelopardalis). Mammal Study 38:67–71.

Gans C. 1982. Fiber architecture and muscle function. Exercise and sport sciences reviews 10(1):160-207.

Gans C, and Bock WJ. 1965. The functional significance of muscle architecture--a theoretical analysis. Ergebnisse der Anatomie und Entwicklungsgeschichte 38:115.

Gantt, DG. 1979. Patterns of dental wear and the role of the canine in Cercopithecinae. Am J Phys Anthropol 51(3):353-359.

Gignac PM, and Kley NJ. 2014. Iodine-enhanced micro-CT imaging: Methodological refinements for the study of the soft-tissue anatomy of post-embryonic vertebrates. Journal of Experimental Zoology Part B: Molecular and Developmental Evolution 322(3):166-176.

Gignac PM, Kley NJ, Clarke JA, Colbert MW, Morhardt AC, Cerio D, Cost IN, Cox PG, Daza JD, and Early CM. 2016. Diffusible iodine-based contrast-enhanced computed tomography (diceCT): an emerging tool for rapid, high-resolution, 3-D imaging of metazoan soft tissues. Journal of anatomy 228(6):889-909.

Gokhin DS, Bang ML, Zhang J, Chen J, and Lieber RL. 2009. Reduced thin filament length in nebulin-knockout skeletal muscle alters isometric contractile properties. Am J Physiol Cell Physiol 296(5):C1123-1132.

Gordon AM, Huxley AF, Julian FJ. 1966a. Tension development in highly stretched vertebrate muscle fibres. J Physiol 184:143.

Gordon A, Huxley AF, and Julian F. 1966b. The variation in isometric tension with sarcomere length in vertebrate muscle fibres. J Physiol 184:170.

Gossl C, Fahrmeir L, P€utz B, Auer LM, Auer DP. 2002. Fiber tracking from DTI using linear state space models: Detectability of the pyramidal tract. Neuroimage 16:378–388.

Greaves WS. 1978. The jaw lever system in ungulates: a new model. Journal of Zoology 184(2):271-285.

Greaves WS. 1983. A functional analysis of carnassial biting. Biol J Linn Soc 20: 353–363.

Greaves WS. 1985. The mammalian postorbital bar as a torsion-resisting helical strut. J Zool 207: 125–136.

Greaves WS. 2012. The Mammalian Jaw: A Mechanical Analysis. Cambridge: Cambridge University Press.

Gröning F, Jones ME, Curtis N, Herrel A, O'Higgins P, Evans SE, and Fagan MJ. 2013. The importance of accurate muscle modelling for biomechanical analyses: a case study with a lizard skull. Journal of The Royal Society Interface 10(84):20130216.

Hartstone-Rose A, Perry JM, and Morrow CJ. 2012. Bite force estimation and the fiber architecture of felid masticatory muscles. Anat Rec (Hoboken) 295(8):1336-1351.

Harvey PH, and Clutton-Brock TH. 1985. Life history variation in primates. Evolution 39(3):559-581.

Hautier L, Lebrun R, and Cox PG. 2012. Patterns of covariation in the masticatory apparatus of hystricognathous rodents: implications for evolution and diversification. Journal of Morphology 273(12):1319-1337.

Heemskerk AM, Strijkers GJ, Vilanova A, Drost MR, and Nicolay K. 2005. Determination of mouse skeletal muscle architecture using three-dimensional diffusion tensor imaging. Magnetic resonance in medicine 53(6):1333-1340.

Herring SW, Grimm AF, and Grimm BR. 1979. Functional heterogeneity in a multipinnate muscle. Developmental Dynamics 154(4):563-575.

Herring SW, and Herring SE. 1974. The superficial masseter and gape in mammals. The American Naturalist 108(962):561-576.

Herring SW, and Wineski LE. 1986. Development of the masseter muscle and oral behavior in the pig. Journal of Experimental Zoology Part A: Ecological Genetics and Physiology 237(2):191-207.

Hiiemae K. 1984. Functional aspects of primate jaw morphology. Food acquisition and processing in primates: Springer. p 257-281.

Hillson S. 2005. Teeth. Cambridge: Cambridge university press.

Holliday CM, Tsai HP, Skiljan RJ, George ID, and Pathan S. 2013. A 3D interactive model and atlas of the jaw musculature of Alligator mississippiensis. PLoS One 8(6):e62806.

Hylander WL. 1985. Mandibular function and biomechanical stress and scaling. American Zoologist 25(2):315-330.

Hylander WL. 2009. The functional significance of canine height reduction in early hominins. Am J Phys Anthropol Suppl 48:154.

Hylander WL. 2013. Functional links between canine height and jaw gape in catarrhines with special reference to early hominins. Am J Phys Anthropol 150(2):247-259.

Hylander WL, and Vinyard CJ. 2006. The evolutionary significance of canine reduction in hominins: functional links between jaw mechanics and canine size. Am J Phys Anthropol Suppl 42:107.

Ito K, and Endo H. 2016. Compartive Study of Physiological Cross-Sectional Area of Masticatory Muscles among Species of Carnivora. Mammal Study 41(4):181-190.

Jeffery NS, Stephenson RS, Gallagher JA, Jarvis JC, and Cox PG. 2011. Micro-computed tomography with iodine staining resolves the arrangement of muscle fibres. Journal of biomechanics 44(1):189-192.

Kaplan E, Naeser MA, Martin PI, Ho M, Wang Y, Baker E, Pascual-Leone A. 2010. Horizontal portion of arcuate fasciculus fibers track to pars opercularis, not pars triangularis, in right and left hemispheres: a DTI study. Neuroimage 52:436–444.

Kawakami Y, Akima H, Kubo K, Muraoka Y, Hasegawa H, Kouzaki M, Imai M, Suzuki Y, Gunji A, Kanehisa H, etal. 2001. Changes in muscle size, architecture, and neural activation after 20 days of bed rest with and without resistance exercise. Eur J Appl Physiol 84:7–12.

Kikuchi Y. 2010. Comparative analysis of muscle architecture in primate arm and forearm. Anat Histol Embryol 39:93–106.

Klose U, Erb M, Saur R, Seeger U, Grodd W. 2005. Segmentierung der weißen Hirnsubstanz auf der Grundlage von MR-DTI-Vorzugsrichtungen. Z Med Phys 15:247–255.

Koolstra J, and Van Eijden T. 2005. Combined finite-element and rigid-body analysis of human jaw joint dynamics. Journal of biomechanics 38(12):2431-2439.

Korfage J, Van Wessel T, Langenbach G, Ay F, and Van Eijden T. 2006. Postnatal transitions in myosin heavy chain isoforms of the rabbit superficial masseter and digastric muscle. Journal of anatomy 208(6):743-751.

Koyabu DB, and Endo H. 2010. Craniodental mechanics and diet in Asian colobines: morphological evidence of mature seed predation and sclerocarpy. Am J Phys Anthropol 142(1): 137-48.

Kupczik K, Dobson C, Crompton R, Phillips R, Oxnard CE, Fagan M, and O'Higgins P. 2009. Masticatory loading and bone adaptation in the supraorbital torus of developing macaques. American Journal of Physical Anthropology 139(2):193-203.

Kupczik K, Dobson C, Fagan M, Crompton R, Oxnard C, and O'Higgins P. 2007. Assessing mechanical function of the zygomatic region in macaques: validation and sensitivity testing of finite element models. Journal of Anatomy 210(1):41-53.

Kupczik K, Stark H, Mundry R, Neininger FT, Heidlauf T, and Röhrle O. 2015. Reconstruction of muscle fascicle architecture from iodine-enhanced microCT images: A combined texture mapping and streamline approach. Journal of theoretical biology 382:34-43.

La Croix S, Zelditch M, Shivik J, Lundrigan B, and Holekamp K. 2011. Ontogeny of feeding performance and biomechanics in coyotes. Journal of Zoology 285(4):301-315.

Lamas LP, Main RP, and Hutchinson JR. 2014. Ontogenetic scaling patterns and functional anatomy of the pelvic limb musculature in emus (Dromaius novaehollandiae). PeerJ 2:e716.

Langenbach G, Zhang F, Herring S, and Hannam A. 2002. Modelling the masticatory biomechanics of a pig. Journal of Anatomy 201(5):383-393.

Leonard WR, and Robertson ML. 1992. Nutritional Requirements and Human Evolution: A Bioenergetics Model. American Journal of Human Biology 4:179-195.

Lieber RL. 1986. Skeletal muscle adaptability. I: Review of basic properties. Developmental Medicine & Child Neurology 28(3):390-397.

Lieber RL. 2002. Skeletal muscle structure, function, and plasticity: Lippincott Williams & Wilkins.

Lieber RL, and Blevins FT. 1989. Skeletal muscle architecture of the rabbit hindlimb: functional implications of muscle design. Journal of morphology 199(1):93-101.

Lieber RL, and Friden J. 2000. Functional and clinical significance of skeletal muscle architecture. Muscle & nerve 23(11):1647-1666.

Lieber RL, and Ward SR. 2011. Skeletal muscle design to meet functional demands. Philosophical Transactions of the Royal Society B: Biological Sciences 366(1570):1466-1476.

Lieber RL, Jacobson MD, Fazeli BM, Abrams RA, Botte MJ. 1992. Architecture of selected muscles of the arm and forearm: Anatomy and implications for tendon transfer. J Hand Surg Am 17:787–798.

Logan M, and Sanson GD. 2002. The effect of tooth wear on the feeding behaviour of free-ranging koalas (Phascolarctos cinereus, Goldfuss). Journal of Zoology 256(1):63-69.

Lucas P, and Corlett R. 1991. Relationship between the diet of Macaca fascicularis and forest phenology. Folia Primatologica 57(4):201-215.

Lucas PW. 2004. Dental functional morphology: how teeth work: Cambridge University Press.

Lucas PW, and Luke DA. 1984. Chewing it over: basic principles of food breakdown. In: Chivers DJ WB, Bilsborough A., editor. Food acquisition and processing in primates. New York: Plenum Press. p 283-302.

Manal K, and Buchanan TS. 2004. Subject-specific estimates of tendon slack length: a numerical method. Journal of Applied Biomechanics 20(2):195-203.

Mathewson MA, Kwan A, Eng CM, Lieber RL, Ward SR. 2014. Comparison of rotator cuff muscle architecture between humans and other selected vertebrate species. J Exp Biol 217:261–273.

Maxwell LC, Carlson DS, McNamara JA, and Faulkner JA. 1979. Histochemical characteristics of the masseter and temporalis muscles of the rhesus monkey (Macaca mulatta). The Anatomical Record 193(3):389-401.

McGraw WS, Vick AE, and Daegling DJ. 2011. Sex and age differences in the diet and ingestive behaviors of sooty mangabeys (Cercocebus atys) in the Tai Forest, Ivory Coast. Am J Phys Anthropol 144(1):140-153.

McMillan AB, Shi D, Pratt SJ, and Lovering RM. 2011. Diffusion tensor MRI to assess damage in healthy and dystrophic skeletal muscle after lengthening contractions. BioMed Research International 2011.

Meloro C, Raia P, Carotenuto F, and Cobb SN. 2011. Phylogenetic signal, function and integration in the subunits of the carnivoran mandible. Evolutionary Biology 38(4):465-475.

Metscher BD. 2009. MicroCT for comparative morphology: Simple staining methods allow high-contrast 3D imaging of diverse nonmineralized animal tissues. BMC Physiol 9:11.

Michilsens F, Vereecke EE, D'août K, and Aerts P. 2009. Functional anatomy of the gibbon forelimb: adaptations to a brachiating lifestyle. Journal of Anatomy 215(3):335-354.

Mitteroecker P, Gunz P, Bernhard M, Schaefer K, and Bookstein FL. 2004. Comparison of cranial ontogenetic trajectories among great apes and humans. Journal of Human Evolution 46(6):679-698.

Morhardt AR, RC; Witmer, LM. 2016. ABSTRACT: Diffusible iodine-based contrast enhancement of large, post-embryonic, intact vertebrates for CT scanning: staining, destaining, and long-term storage. International Congress of Vertebrate Morphology. Washington, D.C.

Morris CB. 1948. The measurement of the strength of muscle relative to the cross section. Res Quarterly Am Assoc Heal Phys Educ Recreat 19:295–303.

Murray WM, Buchanan TS, and Delp SL. 2000. The isometric functional capacity of muscles that cross the elbow. Journal of biomechanics 33(8):943-952.

Napadow VJ, Chen Q, Mai V, So PTC, Gilbert RJ. 2001. Quantitative analysis of three-dimensional-resolved fiber architecture in heterogeneous skeletal muscle tissue using NMR and optical imaging methods. Biophys J 80:2968–2975.

Ogihara N, Oishi M, Kanai R, Shimada H, Kondo T, Yoshino-Saito K, Ushiba J, and Okano H. 2017. Muscle architectural properties in the common marmoset (Callithrix jacchus). Primates:1-12.

O'Higgins P, and Jones N. 1998. Facial growth in Cercocebus torquatus: an application of three-dimensional geometric morphometric techniques to the study of morphological variation. Journal of Anatomy 193(2):251-272.

Oishi M, Ogihara N, Endo H, and Asari M. 2008. Muscle architecture of the upper limb in the orangutan. Primates 49(3):204-209.

Organ JM, Teaford MF, and Taylor AB. 2009. Functional correlates of fiber architecture of the lateral caudal musculature in prehensile and nonprehensile tails of the Platyrrhini (Primates) and Procyonidae (Carnivora). The Anatomical Record 292(6):827-841.

Otten E. 1988. Concepts and models of functional architecture in skeletal muscle. Exercise and sport sciences reviews 16(1):89-138.

Pauwels E, Van Loo D, Cornillie P, Brabant L, Van Hoorebeke L. 2013. An exploratory study of contrast agents for soft tissue visualization by means of high resolution X-ray computed tomography imaging. J Microsc 250:21–31.

Payne RC, Crompton RH, Isler K, Savage R, Vereecke EE, Günther MM, Thorpe S, and D'Août K. 2006. Morphological analysis of the hindlimb in apes and humans. I. Muscle architecture. Journal of anatomy 208(6):709-724.

Pearson AM. 1990. Muscle growth and exercise. Critical Reviews in Food Science and Nutrition 29(3):167-196.

Perry JM, Hartstone-Rose A, and Wall CE. 2011. The jaw adductors of strepsirrhines in relation to body size, diet, and ingested food size. Anat Rec (Hoboken) 294(4):712-728.

Perry JM, Macneill KE, Heckler AL, Rakotoarisoa G, and Hartstone-Rose A. 2014. Anatomy and Adaptations of the Chewing Muscles in Daubentonia (Lemuriformes). The Anatomical Record 297(2):308-316.

Perry JM, and Wall CE. 2008. Scaling of the chewing muscles in prosimians. Primate craniofacial function and biology: Springer. p 217-240.

Pfaller JB, Gignac PM, Erickson GM. 2011. Ontogenetic changes in jaw-muscle architecture facilitate durophagy in the turtle Sternotherus minor. J Exp Biol 214:1655–1667.

Plavcan JM. 2001. Sexual dimorphism in primate evolution. American Journal of Physical Anthropology 116(S33):25-53.

Plavcan JM, and van Schaik CP. 1992. Intrasexual competition and canine dimorphism in anthropoid primates. American Journal of Physical Anthropology 87(4):461-477.

Plavcan JM, van Schaik CP. 1997 Interpreting hominid behavior on the basis of sexual dimorphism. J Hum Evol 32:345–374.

Plavcan JM, van Schaik CP, Kappeler PM. 1995. Competition, coalitions and canine size in primates. J Hum Evol 28:245–276.

Popowics TE, and Fortelius M. 1997. On the cutting edge: tooth blade sharpness in herbivorous and faunivorous mammals. Annales Zoologici Fennici: JSTOR. p 73-88.

Powell PL, Roy RR, Kanim P, Bello MA, and Edgerton VR. 1984. Predictability of skeletal muscle tension from architectural determinations in guinea pig hindlimbs. Journal of Applied Physiology 57(6):1715-1721.

Radinsky LB. 1981. Evolution of skull shape in carnivores I: Representative modern carnivores. Biol J Linn Soc 15:369–388.

Ravosa MJ. 1991. The ontogeny of cranial sexual dimorphism in two Old World monkeys: Macaca fascicularis (Cercopithecinae) andNasalis larvatus (Colobinae). International Journal of Primatology 12(4):403.

Ravosa MJ. 1996. Jaw morphology and function in living and fossil Old World monkeys. International Journal of Primatology 17(6):909-932.

Ravosa MJ, Ning J, Costley D, Daniel A, Stock S, and Stack M. 2010. Masticatory biomechanics and masseter fiber-type plasticity. Journal of Musculoskeletal Neuronal Interactions 10(1):46-55.

Rayne J, and Crawford G. 1975. Increase in fibre numbers of the rat pterygoid muscles during postnatal growth. Journal of anatomy 119(2):347.

Reese TG, Weisskoff RM, Smith RN, Rosen BR, Dinsmore RE, Wedeen VJ. 1995. Imaging myocardial fiber architecture in vivo with magnetic resonance. Magn Reson Med 34:786–791.

Richmond BG, Wright BW, Grosse I, Dechow PC, Ross CF, Spencer MA, and Strait DS. 2005. Finite element analysis in functional morphology. The Anatomical Record 283(2):259-274.

Richtsmeier JT, Cheverud J, Danahey S, Corner B, and Lele S. 1993. Sexual dimorphism of ontogeny in the crab-eating macaque (*Macaca fascicularis*). Journal of Human Evolution 25(1):1-30.

Rook L, and O'Higgins P. 2005. A comparative study of adult facial morphology and its ontogeny in the fossil macaque *Macaca majori* from Capo Figari, Sardinia, Italy. Folia Primatologica 76(3):151-171.

Ross CF. 1995. Muscular and osseous anatomy of the primate anterior temporal fossa and the functions of the postorbital septum. Am J Phys Anthropol 98(3):275-306.

Ross CF, Iriarte-Diaz J, and Nunn CL. 2012. Innovative Approaches to the Relationship Between Diet and Mandibular Morphology in Primates. International Journal of Primatology 33(3):632-660.

Roy RR, Bello MA, Powell PL, Simpson DR. 1984. Architectural design and fiber-type distribution of the major elbow flexors and extensors of the monkey (cynomolgus). Am J Anat 171:285–293.

Roy RR, Powell PL, Kanim P, Simpson DR. 1984. Architectural and histochemical analysis of the semitendinousus muscle in mice, rats, guinea pigs, and rabbits. J Morphol 181:155–160.

Sacks RD, and Roy RR. 1982. Architecture of the hind limb muscles of cats: functional significance. Journal of Morphology 173(2):185-195.

Santana SE, Dumont ER, and Davis JL. 2010. Mechanics of bite force production and its relationship to diet in bats. Functional Ecology 24(4):776-784.

Santana SE, Grosse IR, and Dumont ER. 2012. Dietary hardness, loading behavior, and the evolution of skull form in bats. Evolution 66(8):2587-2598.

Schenk P, Siebert T, Hiepe P, Güllmar D, Reichenbach J, Wick C, Blickhan R, and Böl M. 2013. Determination of three-dimensional muscle architectures: validation of the DTI-based fiber tractography method by manual digitization. Journal of Anatomy 223(1):61-68.

Schultz AH. 1960. Age changes and variability in the skulls and teeth of the Central American monkeys Alouatta, Cebus and Ateles. Journal of Zoology 133(3):337-390.

Schumacher GH. 1961. Funktionelle morphologie der kaumuskulatur. Jena: G. Fischer.

Schwartz DJ, and Huelke DF. 1963. Morphology of the head and neck of the macaque monkey: the muscles of mastication and the mandibular division of the trigeminal nerve. Journal of Dental Research 42(5):1222-1233.

Sellers WI, and Crompton RH. 2004. Using sensitivity analysis to validate the predictions of a biomechanical model of bite forces. Annals of Anatomy-Anatomischer Anzeiger 186(1):89-95.

Shi J, Curtis N, Fitton LC, O'Higgins P, and Fagan MJ. 2012. Developing a musculoskeletal model of the primate skull: predicting muscle activations, bite force, and joint reaction forces using multibody dynamics analysis and advanced optimisation methods. Journal of theoretical biology 310:21-30.

Singleton M. 2005. Functional shape variation in the cercopithecine masticatory complex. In: Slice DE, editor. Modern Morphometrics in Physical Anthropology. New York: Plenum Press. p 319-348.

Singleton M. 2015. Functional geometric morphometric analysis of masticatory system ontogeny in papionin primates. Anat Rec (Hoboken) 298(1):48-63.

Sinha S, Sinha U, and Edgerton VR. 2006. In vivo diffusion tensor imaging of the human calf muscle. Journal of Magnetic Resonance Imaging 24(1):182-190.

Smith AL, Benazzi S, Ledogar JA, Tamvada K, Smith LCP, Weber GW, Spencer MA, Dechow PC, Grosse IR, Ross CF. 2015. Biomechanical implications of intraspecific shape variation in chimpanzee crania: Moving towards an integration of geometric morphometrics and finite element analysis. Anat Rec 298:122.

Smith K, and Beighton D. 1986. The effects of the availability of diet on the levels of exoglycosidases in the supragingival plaque of macaque monkeys. Journal of Dental Research 65(11):1349-1352.

Smith K, and Beighton D. 1987. Proteolytic activities in the supragingival plaque of monkeys (Macaca fascicularis). Archives of Oral Biology 32(7):473-476.

Smith R. 1984. Comparative functional morphology of maximum mandibular opening (gape) in primates. In: Chivers DJ, Wood B, Bilsborough A, editors. Food acquisition and processing in primates. New York: Plenum Press. p 231-255.

Smith R and Jungers WL. 1997. Body mass in comparative primatology. J Hum Evol 32(6):523-559.

Sokal R, and Rohlf F. 1995. Biometry. New York: WH Freeman.

Soltis J. 2004. Mating Systems. In: Thierry B, Singh M, and Kaumanns W, editors. Macaque societies: a model for the study of social organization. Cambridge: Cambridge University Press. p 135-155.

Son VD. 2003. Diet of Macaca fascicularis in a mangrove forest, Vietnam. Laboratory Primate Newsletter 42(4):1-5.

Spencer MA. 1999. Constraints on masticatory system evolution in anthropoid primates. American Journal of Physical Anthropology 108(4):483-506.

Stewart S, and German R. 1999. Sexual dimorphism and ontogenetic allometry of soft tissues in Rattus norvegicus. Journal of Morphology 242(1):57-66.

Tanner JB, Zelditch ML, Lundrigan BL, and Holekamp KE. 2010. Ontogenetic change in skull morphology and mechanical advantage in the spotted hyena (Crocuta crocuta).

Taylor AB. 2002. Masticatory form and function in the African apes. American Journal of Physical Anthropology 117(2):133-156.

Taylor AB, Eng CM, Anapol FC, and Vinyard CJ. 2009. The functional correlates of jaw-muscle fiber architecture in tree-gouging and nongouging callitrichid monkeys. Am J Phys Anthropol 139(3):353-367.

Taylor AB, Terhune C.E., Hylander, W.L., Vinyard, C.J. 2014. In vitro sarcomere-length operating range of the masseter and temporalis muscles in Macaca fascicularis. Am J Phys Anthropol 153(S58):252.

Taylor AB, Terhune CE, Toler M, Holmes M, Ross CF, and Vinyard CJ. 2018. Jaw-Muscle Fiber Architecture and Leverage in the Hard-Object Feeding Sooty Mangabey are not Structured to Facilitate Relatively Large Bite Forces Compared to Other Papionins. Anat Rec (Hoboken) 301(2):325-342.

Taylor AB, and Vinyard CJ. 2004. Comparative analysis of masseter fiber architecture in tree-gouging (Callithrix jacchus) and nongouging (Saguinus oedipus) callitrichids. J Morphol 261(3):276-285.

Taylor AB, and Vinyard CJ. 2009. Jaw-muscle fiber architecture in tufted capuchins favors generating relatively large muscle forces without compromising jaw gape. J Hum Evol 57(6):710-720.

Taylor AB, and Vinyard CJ. 2013. The relationships among jaw-muscle fiber architecture, jaw morphology, and feeding behavior in extant apes and modern humans. Am J Phys Anthropol 151(1):120-134.

Taylor AB, Yuan T, Ross CF, and Vinyard CJ. 2013. The scaling of jaw-muscle fiber architecture in anthropoid primates. Am J Phys Anthropol 150 Suppl 56: 269.

Taylor AB, Yuan T, Ross CF, and Vinyard CJ. 2015. Jaw-muscle force and excursion scale with negative allometry in platyrrhine primates. Am J Phys Anthropol 158(2):242-256.

Terhune CE, Hylander WL, Vinyard CJ, and Taylor AB. 2015. Jaw-muscle architecture and mandibular morphology influence relative maximum jaw gapes in the sexually dimorphic Macaca fascicularis. J Hum Evol 82:145-158.

Thierry, B. 2000. Covariation of conflict management patterns across macaque species. In: Aureli F, de Waal FBM (Eds.), Natural Conflict Resolution . Berkeley: University of California Press.

Thierry B. 2004. Social Epigenesis. In: Thierry B, Singh M, and Kaumanns W, editors. Macaque societies: a model for the study of social organization. Cambridge: Cambridge University Press. p 267-295.

Thierry B, Iwaniuk AN, and Pellis SM. 2000. The influence of phylogeny on the social behaviour of macaques (Primates: Cercopithecidae, genus Macaca). Ethology 106(8):713-728.

Troisi A, Aureli F, Schino G, Rinaldi F, and Angelis N. 1990. The influence of age, sex, and rank on yawning behavior in two species of macaques (Macaca fascicularis and M. fuscata). Ethology 86(4):303-310.

Tsai HP, and Holliday CM. 2011. Ontogeny of the Alligator cartilago transiliens and its significance for sauropsid jaw muscle evolution. PLoS One 6(9):e24935.

Tseng ZJ, Mcnitt-Gray JL, Flashner H, Wang X, Enciso R. 2011. Model sensitivity and use of the comparative finite element method in mammalian jaw mechanics: Mandible performance in the gray wolf. PLoS One 6:e19171.

Turnbull WD. 1970. Mammalian masticatory apparatus. Fieldiana Geol 18:149-356.

Ungar PS, and M'Kirera F. 2003. A solution to the worn tooth conundrum in primate functional anatomy. Proceedings of the National Academy of Sciences 100(7):3874-3877.

van Eijden T, Korfage J, and Brugman P. 1997. Architecture of the human jaw-closing and jaw-opening muscles. Anat Rec 248(3):464-474.

van Minh N, Mouri T, Hamada Y. 2015. Aging-related changes in the skulls of Japanese macaques (Macaca fuscata). Anthropological Science 123(2): 107-119.

van Schaik CP, and van Noordwijk M, A. 1986. The hidden costs of sociality: intra-group variation in feeding strategies in Sumatran long-tailed macaques (Macaca fascicularis). Behaviour 99(3):296-314.

Vickerton P, Jarvis J, and Jeffery N. 2013. Concentration-dependent specimen shrinkage in iodine-enhanced microCT. Journal of anatomy 223(2):185-193.

Vinyard CJ, Wall CE, Williams SH, and Hylander WL. 2003. Comparative functional analysis of skull morphology of tree-gouging primates. Am J Phys Anthropol 120(2):153-170.

Vinyard CJ, Wall CE, Williams SH, Hylander WL. 2008. Patterns of variation across primates in jaw-muscle electromyography during mastication. Integr Comp Biol 48:294–311.

Wainwright PC, Alfaro ME, Bolnick DI, and Hulsey CD. 2005. Many-to-one mapping of form to function: a general principle in organismal design? Integrative and Comparative Biology 45(2):256-262.

Wall CE, Briggs MM, Huq E, Hylander WL, and Schachat F. 2013. Regional variation in IIM myosin heavy chain expression in the temporalis muscle of female and male baboons (Papio anubis). Arch Oral Biol 58(4):435-443.

Wang Q, Smith AL, Strait DS, Wright BW, Richmond BG, Grosse IR, Byron CD, Zapata U. 2010. The global impact of sutures assessed in a finite element model of a macaque cranium. Anat Rec 293:1477–1491.

Ward SR, and Lieber RL. 2005. Density and hydration of fresh and fixed human skeletal muscle. J Biomech 38(11):2317-2320.

Watson PJ, Gröning F, Curtis N, Fitton LC, Herrel A, McCormack SW, and Fagan MJ. 2014. Masticatory biomechanics in the rabbit: a multi-body dynamics analysis. Journal of The Royal Society Interface 11(99):20140564.

Weber E. 1846. Wagner's Handworterbuche der Physiologie. Braunschweig: Vieweg.

Weijs W, Brugman P, and Klok E. 1987. The growth of the skull and jaw muscles and its functional consequences in the New Zealand rabbit (Oryctolagus cuniculus). Journal of Morphology 194(2):143-161.

Wheatley B. 1980. Feeding and ranging of East Bornean Macaca fascicularis. In: Lindburg D, editor. The macaques: studies in ecology, behavior, and evolution. New York: Van Nostrand Reinhold. p 215-246.

Williams SH, Peiffer E, and Ford S. 2009. Gape and bite force in the rodents Onychomys leucogaster and Peromyscus maniculatus: does jaw-muscle anatomy predict performance? J Morphol 270(11):1338-1347.

Winters TM, Takahashi M, Lieber RL, Ward SR. 2011. Whole muscle length-tension relationships are accurately modeled as scaled sarcomeres in rabbit hindlimb muscles. J Biomech 44:109–115.

Wright BW. 2005. Craniodental biomechanics and dietary toughness in the genus Cebus. Journal of Human Evolution 48(5):473-492.

Yeager CP. 1996. Feeding ecology of the long-tailed macaque (Macaca fascicularis) in Kalimantan Tengah, Indonesia. International Journal of Primatology 17(1):51-62.

Yeager CP, and Kirkpatrick RC. 1998. Asian colobine social structure: ecological and evolutionary constraints. Primates 39(2):147.

Zielinski DE. 1965. A study of the normal anatomy of the masticatory apparatus of Macaca mulatta. Chicaco: Loyal University Chicago (Masters Thesis).

SUPPLEMENTARY MATERIAL

Table S1, Part 1. Raw biomechanical, architectural and dental eruption sequence data for each individual within the sample. Abbreviations DM, SM and Temp denote deep masseter, superficial masseter, and temporalis respectively. For the purposes of age determination, only the mandibular molar row was considered. Dental elements were required to be found in occlusion on only one side of the jaw to be scored as such for the purposes of classification. Mac# refers to the unique identification number of each specimen within the archives of Hull York Medical School, the source of this material.

Mac #	Jaw length (mm)	Condyle-Molar length (mm)	Basicranial length (mm)	TMJ Height (mm)	SM Fiber Length (mm)	DM Fiber Length (mm)	Temp. Fiber Length (mm)	Dental eruption state (molar row)	Age classification
21	47.710	26.912	37.05	6.21	7.01	4.08	5.90	Deciduous only	Infant
20	48.657	27.511	36.74	6.47	5.56	4.34	5.50	Deciduous only	Infant
45	56.691	32.722	39.4	9.57	6.64	5.30	8.39	Deciduous only	Infant
24	50.393	28.846	38.36	8.45	8.62	7.50	8.79	Deciduous only	Infant
68	51.893	30.153	43.82	9.99	7.08	6.07	8.58	Deciduous only	Infant
9	42.114	23.493	32.33	3.01	5.64	5.20	6.12	Deciduous only	Infant
91	55.690	28.180	40.70	9.79	8.63	6.31	10.02	M1 in occlusion	Juvenile
35	57.097	27.685	48.11	12.39	8.48	5.70	6.83	M1 in occlusion	Juvenile
99	55.684	28.653	44.04	10.30	8.59	7.13	9.84	M1 in occlusion	Juvenile
57	59.995	24.435	39.98	11.58	9.81	5.90	8.10	M1 in occlusion; M2 erupted and approaching occlusion	Juvenile
103	60.996	31.176	49.99	12.29	10.15	7.78	11.42	M1 in occlusion	Juvenile
48	56.788	27.869	51.15	10.55	7.57	6.44	8.27	M1 in occlusion	Juvenile
30	68.251	32.162	48.49	9.56	10.50	6.38	11.99	M2 in occlusion	Juvenile
46	64.599	29.880	34.74	9.97	9.57	6.42	7.86	M2 in occlusion	Juvenile
44	62.519	29.161	45.41	12.06	10.43	5.84	9.74	M2 in occlusion	Juvenile
88	64.681	23.003	35.64	13.40	9.35	7.16	11.81	M2 in occlusion; M3 erupted and approaching occlusion	Juvenile
71	57.971	24.175	32.51	12.12	7.49	6.46	9.32	M2 in occlusion	Juvenile
38	59.412	26.649	37.61	9.44	7.89	7.03	8.15	M2 in occlusion	Juvenile
90	69.272	27.105	46.89	14.90	12.13	7.64	14.50	M3 in occlusion	Adult F
76	72.998	31.197	51.53	14.07	9.14	6.33	12.93	M3 in occlusion	Adult F
89	70.562	28.820	45.91	9.97	10.93	7.56	13.98	M3 in occlusion	Adult F
41	71.025	28.069	45.84	15.38	10.17	7.41	11.10	M3 in occlusion	Adult F
150	83.092	34.340	50.53	15.48	14.82	10.74	20.04	M3 in occlusion	Adult M
151	76.111	31.482	39.20	15.31	13.33	7.03	21.62	M3 in occlusion	Adult M
162	82.685	36.762	48.56	16.30	14.96	8.90	25.35	M3 in occlusion	Adult M
165	93.029	40.216	51.76	21.95	19.80	10.77	31.66	M3 in occlusion	Adult M

Table S1, Part 2. Raw biomechanical, architectural and dental eruption sequence data for each individual within the sample. Abbreviations DM, SM and Temp denote deep masseter, superficial masseter, and temporalis respectively. For the purposes of age determination, only the mandibular molar row was considered. Dental elements were required to be found in occlusion on only one side of the jaw to be scored as such for the purposes of classification. Mac# refers to the unique identification number of each specimen within the archives of Hull York Medical School, the source of this material.

Mac #	SM Pennation Angle (°)	DM Pennation Angle (°)	Temp. Pennation Angle (°)	SM Weight (g)	DM Weight (g)	Temp. Weight (g)	SM PCSA (cm^2)	DM PCSA (cm^2)	TEMP PCSA (cm^2)	Dental eruption state (molar row)	Age classification
21	11.0	0.0	21.4	0.403	0.101	1.081	0.541	0.239	1.694	Deciduous only	Infant
20	18.4	0.0	26.5	0.546	0.127	1.331	0.914	0.276	2.212	Deciduous only	Infant
45	18.4	0.0	25.0	0.711	0.249	2.193	0.996	0.445	2.397	Deciduous only	Infant
24	17.6	0.0	24.3	0.516	0.194	1.743	0.558	0.241	1.822	Deciduous only	Infant
68	17.7	0.0	24.1	0.447	0.179	1.787	0.589	0.279	1.914	Deciduous only	Infant
9	18.7	0.0	25.9	0.293	0.123	0.982	0.484	0.223	1.468	Deciduous only	Infant
91	19.2	0.0	12.4	0.825	0.238	2.314	0.888	0.356	2.174	M1 in occlusion	Juvenile
35	10.9	0.0	25.8	0.492	0.173	1.537	0.546	0.288	2.059	M1 in occlusion	Juvenile
99	19.0	0.0	24.4	1.174	0.301	3.349	1.271	0.400	3.125	M1 in occlusion	Juvenile
57	11.6	15.5	25.2	0.659	0.151	2.393	0.632	0.240	2.709	M1 in occlusion; M2 erupted and approaching occlusion	Juvenile
103	16.0	16.3	21.6	1.402	0.442	3.620	1.291	0.471	2.932	M1 in occlusion	Juvenile
48	24.3	0.0	33.2	0.928	0.338	2.749	1.127	0.497	2.976	M1 in occlusion	Juvenile
30	18.3	15.5	13.3	1.196	0.410	3.493	1.060	0.602	2.343	M2 in occlusion	Juvenile
46	12.9	16.2	21.7	0.554	0.176	1.701	0.543	0.256	2.002	M2 in occlusion	Juvenile
44	11.2	27.3	14.9	0.838	0.329	2.150	0.756	0.513	2.066	M2 in occlusion	Juvenile
88	13.5	0.0	19.3	1.105	0.374	3.171	1.108	0.495	2.494	M2 in occlusion; M3 erupted and approaching occlusion	Juvenile
71	21.9	17.9	25.0	0.666	0.320	2.862	0.821	0.462	2.817	M2 in occlusion	Juvenile
38	20.9	0.0	28.1	0.867	0.338	2.959	1.017	0.455	3.301	M2 in occlusion	Juvenile
90	20.7	16.8	22.7	1.719	0.456	5.313	1.313	0.556	3.381	M3 in occlusion	Adult F
76	26.2	33.8	21.0	1.400	0.600	3.900	1.400	0.847	2.558	M3 in occlusion	Adult F
89	18.8	21.0	23.2	1.686	0.793	6.941	1.435	0.972	4.575	M3 in occlusion	Adult F
41	16.4	19.9	33.5	1.450	0.597	4.602	1.331	0.747	3.705	M3 in occlusion	Adult F
150	34.7	25.6	35.0	5.852	1.285	23.311	3.516	1.096	10.342	M3 in occlusion	Adult M
151	16.7	18.1	25.4	4.649	1.305	20.474	3.211	1.663	8.505	M3 in occlusion	Adult M
162	16.8	16.9	15.3	3.805	1.126	20.058	2.346	1.165	7.356	M3 in occlusion	Adult M
165	11.2	12.7	16.2	6.040	1.867	28.572	2.852	1.615	8.365	M3 in occlusion	Adult M

DECLARATION OF HONOUR

I hereby declare that this dissertation “Structural and functional integration within the primate masticatory system during development” represents my own work. Any sections of text derived from a third party have been appropriately cited as such throughout this thesis. I have acknowledged all relevant assistance and personal communications from third-party sources within this work. The contributions of my coauthors on the included manuscripts – Kornelius Kupczik (MPI-EVA, Leipzig), Heiko Stark (FSU, Jena) and Laura Fitton (Hull York Medical School, York, UK) – have been appropriately recognised. I confirm that I have not enlisted the assistance of a doctoral consultant (Promotionsberater) during the production of this dissertation, and that no third parties have received either direct or indirect monetary benefits for work connected to this dissertation. I confirm that this dissertation has not previously been submitted to another University or Scientific Institution at any point. Finally, I acknowledge the current doctoral degree regulations of the Biologisch-Pharmazeutische Fakultät at the Friedrich-Schiller-Universität Jena and have followed these regulations to the best of my ability.

Leipzig, 23.05.2018

CURRICULUM VITAE

Working Address: *Max Planck Institute for Evolutionary Anthropology, Deutscher Platz 6, Leipzig 04103.*

Contact Information: *Telephone: +49 (0)341 3550 875 | Email: edwin_dickinson@eva.mpg.de*

Education

February 2015 – June 2018	**Max Planck Institute for Evolutionary Anthropology**
	PhD program
September 2013 – September 2014	**Hull York Medical School**
	MSc Human Evolution
September 2010 – May 2013	**University of Southampton**
	BSc Archaeology

Scientific Publications

Dickinson, E., Stark, H., & Kupczik, K. 2018. Non-destructive determination of muscle architectural variables through the use of DiceCT. The Anatomical Record. 301: 363-377.

Dickinson , E., Fitton, L., & Kupczik, K. (accepted). Ontogenetic changes to muscle architectural properties within the jaw-adductor musculature of Macaca fascicularis. American Journal of Physical Anthropology.

Conference Presentations

Dickinson, E., Fitton, L., & Kupczik, K. (2017). Scaling relationships within architectural properties of the jaw adductor musculature in Macaca fascicularis. Poster presentation – AAPA 2017. Abstract in American Journal of Physical Anthropology 162 (S64).

Leipzig, 23.05.2018